APPLICATIONS OF ELECTROKINETICS FOR DISEASE DIAGNOSTICS

A Thesis

Presented in Partial Fulfillment of the Requirement for the

Degree of Master of Science

with a

Major in Chemical Engineering

in the

College of Graduate Studies

University of Idaho

by

Ezekiel Olusola Adekanmbi

Major Professor: Soumya Srivastava, PhD.

Committee Members: James Moberly, PhD.; Wudneh Admassu, PhD.

Department Chair: D. Eric Aston, PhD.

April 2016

AUTHORIZATION TO SUBMIT THESIS

This thesis of Ezekiel Olusola Adekanmbi, submitted for the degree of Master of Science with a major in Chemical Engineering and titled: 'APPLICATIONS OF ELECTROKINETICS FOR DISEASE DIAGNOSTICS,' has been reviewed in final form. Permission, as indicated by the signatures and dates given below, is now granted to submit final copies to the College of Graduate Studies for approval.

Major Professor: _____   Date: _____

                              Soumya K. Srivastava, PhD

Committee Members: _____   Date: _____

                              James Moberly, PhD

                              _____   Date: _____

                              Wudneh Admassu, PhD

Department Chair: _____   Date: _____

                              D. Eric Aston, PhD

ABSTRACT

Disease diagnostics is an important subset of medical diagnosis. Before the advent of microfluidics, diagnostic activities were largely in specified, confined spaces and often require large sample volumes. They also require substantial time-frame to generate results and the probability of human errors is considerably high. Miniaturizing these diagnostic components solves the aforementioned problems and thus improves the entire diagnostic process. A viable electro-kinetic technique employed in microfluidic devices is insulator-based dielectrophoresis. Dielectrophoresis has been used to manipulate various diseased cells. Applications of this technique are reported here for malaria, human African trypanosomiasis, dengue, anthrax, and myriads of cancerous conditions. This same technique was utilized to sort and concentrate red blood cells infected with Babesia pathogen: the intra-erythrocytic apicomplexan etiologic agent for the dreaded disease called Babesiosis. The separation of infected red blood cells from their homogeneous mixture with healthy red blood cells requires both numerical and experimental commitments. In the numerical analysis, no cell separation was observed below and above the operating voltage of 6.2V. This numerical value compares favorably with the experimental operating voltage, which was found to be 6.0V. Validation of the dielectrophoretic separation was carried out in two phases: microscopy and numerical quantifications. Both fluorescence and bright-field microscopic examinations underscore the separation. Quantitative analysis revealed the micro-device's capability to concentrate infected red blood cells from an average of 7% to 70%. These results represent the first step needed in building a portable, accurate, quick and easy-to-use diagnostic device for Babesiosis. The pathogen can also be extracted from the concentrated cells and attenuated for preliminary works on Babesiosis vaccine formulation.

ACKNOWLEDGEMENTS

DEDICATION

I dedicate this work to my mother, who always deny herself of immeasurable pleasure in order to see me fulfill my education desire.

TABLE OF CONTENTS

LIST OF FIGURES

LIST OF TABLES

CHAPTER 1

INTRODUCTION

1.1   Background of the research

Human body embodies various systems that naturally work together for maintaining the overall health and wellbeing. At the body's optimal internal and external environmental conditions, these systems thrive so well that the need for troubleshooting the etiology of diseases do not necessarily arise. Appropriate nutrition, hygiene, and other paraphernalia of good living are the thriving factors that ensure the operational perfectness of these systems. However, a switch from good health occurs when either or both internal and external body conditions become adverse. While illness may attend this adverse condition, diseases may also result. In certain cases, both illness and disease can characterize an adverse health condition[1]. There is, therefore, a need to know the cause(s) of both illness and diseases. This is where the concept of medical diagnosis comes in.

Medical diagnosis is the identification of a condition, disease, disorder, or problem by systematic analysis of the background or history of the human being, examination of the signs or symptoms, evaluation of the research or test results, and investigation of the assumed or probable causes[2]. Hippocrates, the father of western medicine, documented the value of objectively evaluating all aspects of the patient's symptoms, diet, sleep patterns, and habits. He termed this as a medical interview: the process of gathering data that will lead to an understanding of the disease and the underlying physiological process. No finding was considered insignificant and he encouraged physicians to employ all their senses (i.e. sight, hearing, smell, taste, and touch in making a diagnosis[3]).

A subset of diagnosis is called diagnostics (medical tests). Diagnostics literally represents the theory and science of discovering the nature of an adverse or diseased condition. Various techniques are utilized in diagnostic testing and it has been reported that between 60 and 70 % of medical decisions draw upon diagnostic test results[4]. This establishes the importance of diagnostics in the medical arena. Long before now, diagnostic activities were carried out solely in pre-defined spaces. In fact, patients do travel miles for one form of medical test or the other. However, as time passes and technology advances, some of the bottlenecks bedeviling diagnostics started fading away with the introduction of mobile diagnostic devices.

Some of these devices are being used not only for accurate diagnoses but also to screen large numbers of apparently healthy individuals.

Historically, diagnostic devices have been offering major help to humanity since the invention of magnifying glass by Roger Bacon in 1250[5]. Roger employed the principles of optical physics, which had been in existence since the development of theories of light and vision by ancient Greek and Indian philosophers, to develop the first convex lens for scientific purposes. Since then, the medical diagnostic world has been characterized with myriads of advancement.

In the early 20th century, most highly important diagnostic tools were really bulky. Some could occupy volumes as large as 180 cubic feet. Besides, they were mostly immobile and diagnostic tests were carried out in confined spaces. However, technological advancement in electronic industry coupled with the seminar / talk presented by Richard Feynman[6] on the possibilities of miniaturizing medical devices revolutionized medical diagnostics.

Current observations in the miniaturization of medical device do not come without the integrated field of micro- nano- fluidics. Microfluidics is a multidisciplinary field intersecting engineering, physics, chemistry, and nanotechnology, with practical applications to the design of systems in which very low volumes of samples are processed to achieve multiplexing, automation, and high-throughput screening collectively known as lab-on-a-chip (LOC)[7]. Since the dawn of microfluidics, various attempts have been made to transform the usual immobile laboratory setting into various carry-on easy-to-use devices known broadly as point-of-care (POC) devices. The first analytical laboratory miniaturization was achieved at Stanford University in 1979 by Terry *et al*., who fabricated a gas chromatograph system on a silicon chip[8]. This brought microfluidics into frontline in the early 80s and advances made in molecular analysis, biodefense, molecular biology, and microelectronics have substantially improved the relevance of microfluidics to disease diagnostics.

There are techniques used in microfluidics to manipulate the particles flowing within the microfluidic channels. One such technique involves the utilization of electric field (uniform or non-uniform) to direct particles according to their intrinsic electric characteristics. Usually, the electric field is set up with platinum (Pt) or gold (Au) electrodes[7]. Microfluidic devices that utilize uniform electric field are said to be electrophoretic (EP) in nature while those that

employ non-uniform electric field are dielectrophoretic (DEP)[7]. This thesis primarily focuses on the dielectrophoretic aspect of microfluidics as applicable to disease diagnostics.

1.2   Thesis Layout

This thesis is divided into five (5) chapters. The first chapter introduces medical diagnosis and how microfluidics has sprung up to assist accurate diagnosis. Chapter 2 discusses hydrodynamics and its importance to microfluidics. Electro-osmosis (EO), electrophoresis (EP) as well as dielectrophoresis (DEP) are fully discussed. Chapter 3 presents dielectro-phoresis as applicable to biological cells. Model analyses for biological cells as well as the microelectrode configurations of dielectrophoretic devices are fully explained. The chapter also gives a detailed report on the dielectrophoretic applications to disease diagnostics, which include malaria, human African trypanosomiasis, dengue, anthrax, and various types of cancer. In chapter 4, proof-of concept analyses on the isolation of Babesia-infected red blood cells (RBCs) from healthy population of RBCs are presented. The, simulation and fabrication of the microfluidic device, experimentation using the microdevice, and validation of the results i.e. sorting efficiency are discussed in detail. The relevant inferences drawn from this as well as the future directions of this research presented in 4 are discussed in Chapter 5.

References

1.   A. Wikman, S. Marklund, K. Alexanderson, *J Epidemiol Community Health*, 2005, **59**, 450-454.

2.   S. Baron, *Medical Microbiology*, University of texas Medical Branch at Galveston, 4th edn., 1996.

3.   R. Jutte, *A history of the senses: From Antiquity to Cyberspace*, Polity Press, cambridge, UK, 2005.

4.   L. Carey, Marion Long, *Canada Health Infoway*, 2014.

5.   A. Saldarriage, S. Azemoon, 2015, 1-12.

6.   R. P. Feynman, presented in part at the American Physical Society, Pasadena, 1959

7.   S. Srivastava, A. Gencoglu and A. Minerick, Anal. Bioanal. Chem., 2011, 399, 301-321.

8.   S. Vyawahare, , A. D. Griffiths, C. A. Merten, , Chemistry and Biology, 2010, 17, 1052-1065.

CHAPTER 2

THEORY OF ELECTROKINETICS

Electrokinetics is the science that governs the flow of fluid in a microfluidic channel under the influence of electric field. Electrokinetics is basically the combination of electrostatics and hydrodynamics. R. J. Hunter in his book: 'Foundation of Colloid Science' defines electrokinetics as "those processes in which the boundary layer between one charge phase and another is forced to undergo some sort of shearing process. The charge attached to one phase will move in one direction and that associated with the adjoining phase will move in the opposite direction"[1]. Before this technique is discussed vis-a-vis its operability, it is important to give detailed explanations of various phenomenological concepts that come into play prior to the effective orientation of bioparticles with respect to their trajectories.

This chapter, therefore, starts with the concept of electrostatics: the principle behind charge-environment interrelation for statics. The static charge analysis is then extended to moving-charge scenario through the principle of electrodynamics. The technique of electro-osmosis (EO) as a driving force for fluid is then discussed in two folds with respect to what is happening at the bulk of the medium and the happenings at channel wall regions. Electrophoresis (EP), the study of motion of suspended charged particles under uniform electric field is also discussed. The chapter further gives adequate attention to the principles behind dielectrophoresis (the manipulation of particles through non-uniform electric field) and how these electrokinetic forces (EO and EP) are regulated for maximum dielectrophoretic impact on the particles.

2.1   The origin of charges and their effects

Every matter is made up of particles and each particle contains protons, neutrons, and electrons. While protons and electrons are positively and negatively charged respectively, neutrons have no charge. Whenever the number of protons (positive charges) in a particle equals that of the electrons (negative charges), the particle is said to be electrically neutral. When such a neutral atom gains an electron, it becomes negatively charged and positively charged when it loses an electron. The negatively charged particle is referred to as anion while the positively charged particle is called cation. Both protons and electrons of a neutral particle

are termed bound charges unlike a charged particle, which has free charges. Hence, electrically charged particles could be represented by both free charges and bound charges.

In microfluidics, it is cumbersome to keep track of the details in bound charges because of the enormous associated equations[2]. Hence, all effects of the bound charges are usually accounted for by a term called electrical permittivity. This, therefore, allows enough focus on the free charges, which are the charges that contribute to the effects the particle would have on its environment or vice versa[2].

Point-charge particles have been known to have convergent or divergent electric field lines of force depending on their polarity. Therefore, when a charged particle is brought near another charged particle, an interaction between the fields of these particles occurs. This non-contact influence - known as an electric force - occurs at certain range of distance between these two charges. Suffice it to say that any charged particle can exert this force upon other particles - both charged and uncharged particles.

When a charged particle is introduced into a medium, it creates an electric displacement[2]. This electric displacement, D, is partially described by the electric field. It also involves the polarization of the medium[2]. In other words, when a charged particle is introduced into a liquid medium, it creates both electric field and polarization of the medium. Usually, the electric field component of displacement is so small that only the polarization part becomes dominant[2]. Therefore, considerable attention is given to the polarization effects caused by the introduction of a charged particle into a medium.

If the charged particle is placed in free space, it induces an electric field but there is no polarization since no medium is present in free space. But if the charged particle is in a liquid, say water, it creates electric field and as well causes water to polarize. This is because, in water, the hydrogen ion (H^+) or hydroxonium ion (H_3O^+) has partial positive charge while the oxygen ion (O^{2-}) has partial negative charge. This molecule possesses an inherent dipole, which is organized with some amount of hydrogen bonding. Statistically speaking, its orientation in space is random. Therefore, if a negatively charged particle, for instance, is introduced into water, all the water atoms will rotate so as to make the H^+ or H_3O^+ in water closer to the introduced charge. The two components of displacement can be represented in three (3) different forms.

$$\vec{D} = \vec{E} + \vec{P} \tag{2.1}$$

where,   E =Electric Field and P=Polarization

$$\vec{D}= \varepsilon_o \, \vec{E} \, (1+X_e)$$ (2.2)

where, X_e is called electric susceptibility of the medium and ε_o is the permittivity of the vacuum

$$\vec{D}=\varepsilon\vec{E}$$ (2.3)

where, ε is the electrical permittivity of the medium. While Eq. 2.1 describes the physics of the problem, Eq. 2.2 allows the description of the part played by both free space and the medium i.e. D=$\varepsilon_o \vec{E}$ (for free space) and $\varepsilon_o \vec{E}X_e$ (for the medium). In free space, there is no medium. So, the electric susceptibility is zero. Eq. 2.3 basically states that the displacement (what describes the effects of the charge on its environment) is linearly dependent on the electric field $\vec{E}$ (which describes how the environment acts back on the charge). If the electric permittivity is assumed constant, then it implies that the medium responds instantaneously to the charge and the response is linear.

Eq. 2.3 is the most commonly used relation for displacement and electric field. For the expression of displacement in Eq. 2.3, two key equations are usually applied:

1) Gauss' Law for electricity

$$\nabla . \vec{D} = \rho_E$$ (2.4)

where ρ_E is the net charge density

2) Volumetric force on a charge fluid

$$f= \rho_E\vec{E}$$ (2.5)

Gauss law is one of the four Maxwell equations used in electromagnetism. Usually in microfluidics, magnetic effect is always neglected since its effect is very infinitesimal. Magnetic effect is always neglected because charges in electrolyte solution in microfluidic devices are carried by the moving ions, which are way slow than electrons moving in metals. An attempt to create a magnetic field by ions moving in water has been found to be highly negligible[2].

If the particle is not charged, there would be a need to make it charged so as to create the displacement effects discussed above. This induced-charge generation process can be accomplished by using an extrinsic electric field (This is discussed in section 2.4). Particles that can be polarized by an applied electric field are referred to as dielectric particles and

they (as well as charged particles) are usually employed in dielectrophoretic separation.

2.2   Electro-osmosis

Having known that a charged particle (or dielectric particles under the influence of electric field) placed in a medium can cause the medium to polarize, it is then necessary to give the details of how the bulk of the medium travels along the microchannel when electric fields are applied across the channel. This section describes the details of what happens at the boundary between the medium and the channel walls and how this wall-medium interrelation plays an important role in the bulk motion of the medium as well as particle transport. The utilization of the boundary conditions in obtaining the velocity profile of the flowing fluid is also discussed. The transport of the bulk fluid medium along the microchannel under the influence of electric field is called electro-osmosis.

2.2.1   Fluid flow generation in microfluidic devices

In order to make fluid flow in microfluidic channel, two methods are usually employed. One such method involves the use of an external pumping device called micropump. This makes the fluid flow under pressure and the velocity profile associated with such pressure-driven flow is parabolic. Other technique is the use of electro-osmosis, which is usually referred to as electro-osmotic pumping. This electro-osmotic-driven flow stems from what is happening at the interface of the medium and the material used in constructing the microchannel. It is important to know what is happening at the boundary of the microchannel because the information obtained from these boundary conditions will help in solving the Navier-Stokes equation: the equation governing the fluid flow.
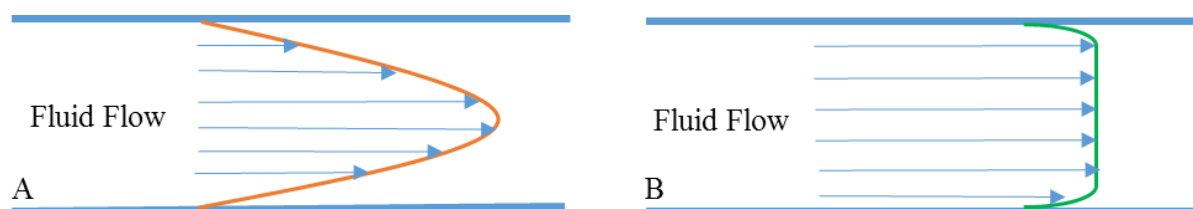
Figure 2.1   The velocity profile of fluid flow in microchannel. (A) Flow profile for pressure-driven flow. (B) The flow profile for electro-osmotic flow.

If the voltage at the wall and the voltage of the bulk solution of electrolyte flowing in a microfluidic channel are measured, a potential difference will be observed. This is because, for a system at equilibrium, the electrochemical potential has to be the same everywhere. Since

the chemical potential of the ions at the wall and the bulk are different, it means the potential must be different if the system must remain at equilibrium. This potential difference has been found to decay exponentially from the wall to the bulk solution or the mid-point of the microchannel and this is responsible for the shape of the velocity profile observed at some distance from the channel walls as seen in Figure 2.1B.

Microfluidic channels are usually made of glass or polymers like polydimethylsiloxane (PDMS). Each of these materials consists of component structures which offer them some form of surface charge when placed in contact with a liquid medium (or electrolyte). Glass, for instance, has surface terminal that is dominated by the silanol (SiOH) group.
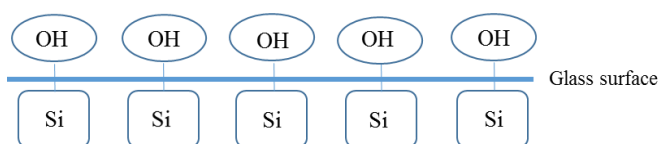
Figure 2.2   The structural representation of the glass surface

If a pH-7 (neutral) electrolyte solution is placed in contact with glass, the SiOH group behaves like a weak acid and thus ionizes and releases H^+ or H_3O^+ into the electrolyte solution leaving SiO^- group at the glass surface. This SiO^- group at the glass surface makes the glass wall negatively charged. Hence, a negative charge density exists at the wall and this is associated with a relatively lower electric potential at the wall.
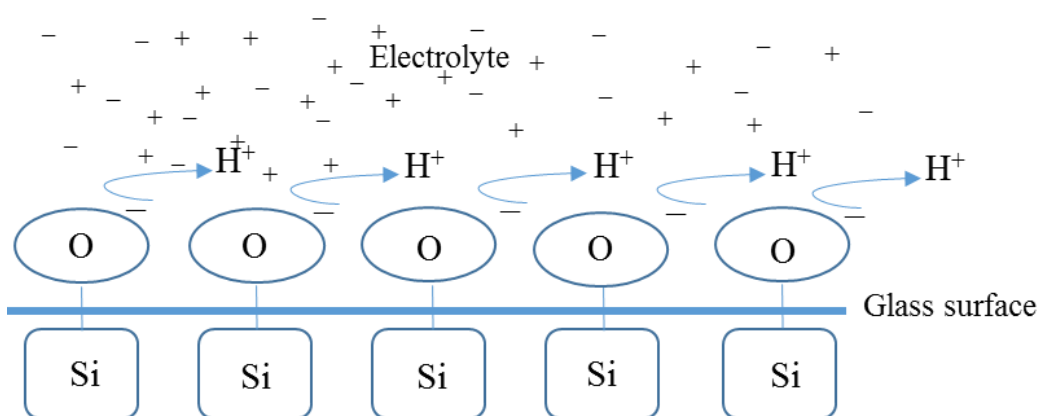
Figure 2.3   The behavior of silanol group on contact with a neutral electrolyte

This lower potential at the wall is caused by the re-orientation of the dipole molecules in the polar electrolyte (polar electrolytes are usually used in microfluidic channel). A good observation is that if a magical voltmeter is used to measure the voltage at the wall and in the bulk, the voltage difference decays in a very short length scale (~10 nm). In order words, at

about 10 nm from the wall, the intrinsic electric potential in the whole microchannel becomes uniform. This distance (10 nm) away from the glass surface at which the electrical potential becomes uniform is called Debye length. For any wide microchannel (> 25µm), the details of the wall region can be neglected and intrinsic potential difference ignored.

Since the glass surface is negatively charged as a result of the ionization process, positive charges from the polar electrolytes become tightly adsorbed on the glass surface and form stable layer with the SiO- group. This layer is termed stern layer. The remaining negative charges in the polar electrolyte become attracted to the positive charges on the stern layer by electrostatically-induced Coulomb force, thus creating a second layer of ions (called the diffuse layer) on the glass surface. However, owing to the fact that the bond on the stern layer (i.e. between SiO^- and the positive charges of the polar medium) is stronger that the Coulomb force tending to create a bond between the positive surface of the stern layer and the diffuse layer, the negative ions on the positive surface of the stern layer are swept away by other negative charges in the medium. This creates the motion of the fluid near the walls and transfers via viscous forces into convective motion of the bulk fluid. This is the process by which bulk motion of the fluid is achieved in a microchannel.
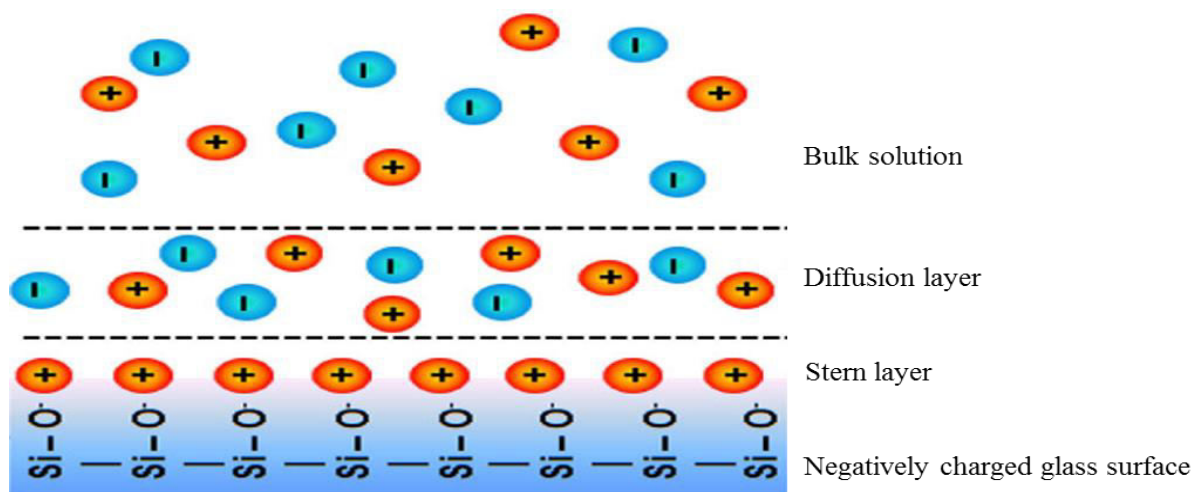
Figure 2.4   Formation of stern and diffusion layer through silanol ionization and Columbic interaction

The combination of both stern and diffuse layer generates the electric double layer (EDL) at the glass surface and this is the underpinning principle that governs the electrokinetic transportation of materials within any microchannel[3]. Suffice it to say that a potential does exist between the stern layer and the diffuse layer. This potential is called the Zeta potential

and is again a function of the properties of the materials used in constructing the microchannel[2].
If the suspended particles in the medium are negatively charged, some of them will be attracted
by the weak Coulomb force and they will be seen moving along the surface of the channel wall
while the bulk of the electrolyte is moving. This phenomenon is referred to as electro-osmotic
pumping.

2.2.2 Integration of electric field into electro-osmotic flow profile

In any microfluidic device, fluid flow and electric field analyses are usually integrated.
Fluid flow analysis is usually made through Navier-Stokes equation in conjunction with the
continuity equation. This fluid flow, as given in section 2.2.1 can be electro-osmotically driven.
Mathematically, electro-osmotic fluid flow in microfluidic channel can be analyzed. Figure
2.5 shows a representation of an elemental volume of fluid (very close to the channel wall)
flowing parallel to a no-slip wall of a microchannel such that $\phi=0$ is the electric potential of
the bulk of the solution, and $\phi= \phi_o$ is the specified potential at the wall. Distance h is so small
that $\phi=0$ at level B.
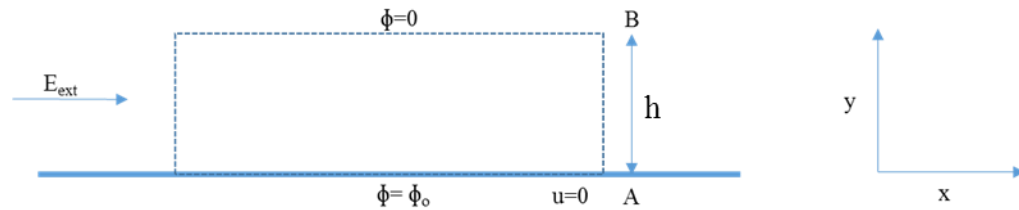
Figure 2.5 Demonstration of potential change between the fluid-glass interface and the bulk
solution

For electroneutral fluid, the fluid flow equation: Navier-Stoke's can be written as

$$\rho\frac{\delta u}{\delta t} + \rho u.\nabla u + \nabla.P = \mu\nabla^2 u \qquad (2.6)$$

where, ρ is the density of the fluid, P is the associated pressure, u and μ are the velocity and
viscosity of the flowing fluid respectively.

Assuming there is no pressure gradient and that the flow is unidirectional at steady
state, then Navier-Stoke's equation turns to

$$\mu\nabla^2 u = 0 \qquad (2.7)$$

If an electric field potential difference occurs as intrinsic potential difference (in y-
direction) and extrinsic potential difference (in x-direction), then, electro neutrality of the fluid
cannot be assumed[2], hence, Eq. 2.7 becomes

$$\mu \nabla^2 u + \rho_E E_{ext} = 0 \tag{2.8}$$

where, ρ_E is the net charge density.

Eq. 2.8 means that in any local control volume of fluid, there is an electric field that is pushing on it and it is being counterbalanced by net flux of viscous momentum.

One critical observation that comes out of electrostatics is the relation between charge density and electric field (Eq. 2.5). But in the figure above (Figure 2.5), there is no ρ_E in the boundary condition. Hence, there is need to relate Eq. 2.8 to the parameters in the boundary condition of Figure 2.5. This is done by invoking the Gauss Law, which states that the divergence of the electric displacement is given by the charge density i.e. Eq. 2.4.

Since Eq. 2.3 and electric field is given as the negative of the gradient of the electric potential, i.e.

$$E = -\nabla \phi \tag{2.9a}$$

then, substituting Eq. 2.3 and Eq. 2.9 into Eq. 2.4 gives

$$-\varepsilon \nabla^2 \phi = \rho_E \tag{2.9b}$$

provided that ε is spatially uniform. Using Eq. 2.9b, Eq. 2.8 can be written as

$$\mu \nabla^2 u = \varepsilon E_{ext} \nabla^2 \phi \tag{2.10}$$

The electro-osmotic velocity profile of the of the moving fluid is then obtained by solving Eq. 2.10 in any desired coordinate system.

2.3   Electrophoresis

In section 2.2, detailed exposition was given regarding the bulk motion of electrolyte solution (medium) within a microchannel under the influence of electric field. This phenomenon was termed electro-osmosis. In this section, attention will be devoted to the basic mechanisms that govern the transport of charged particles within the microchannel under the influence of the electric field. This is a term called electrophoresis.

2.3.1   Basic principle of electrophoresis

Electrophoresis is the movement of charged particles (suspended in a medium) along a microchannel under the influence of a uniform electric field[4]. When a charged (say, negative) particle is introduced into a polar electrolyte solution in a microchannel, two things will happen. First, the surface charge on the channel wall becomes ionized and the electrolyte solution is affected with reference to its orientation, thus, generating an electro-osmotic force

that pushes forward the bulk of the electrolyte solution in the direction of an applied external electric field (section 2.2). Second, the negatively charged particle causes the polarization of the medium such that the positive charges from the medium re-orientate themselves around the particle generating the stokes frictional force (the force acting on the interface between the fluid and the particle).

Anode (+ve)   Electric Field direction   Cathode (-ve)

Electrophoretic force

Electrostatic force

Frictional force
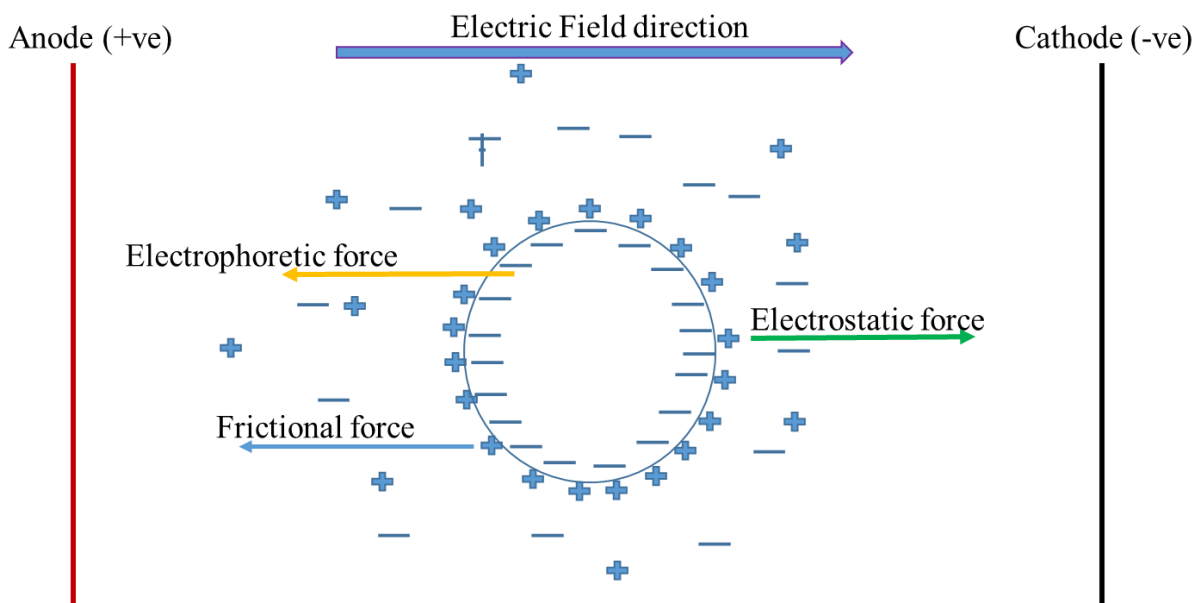
Figure 2.6   The schematic diagram showing the forces acting on a negatively charged particle flowing under a uniform electric field within a microchannel.

When an electric field is applied, the negatively charged particle moves towards the anode of the electric field source through electrophoresis. However, the positive charges that surround the negatively charged particle tend to move the particle towards the cathode (through electro-osmosis). This electro-osmotic process, which tends to force the particle to move forward along the direction of the external electric field, creates a drag force on the charged particle and thus move it forward (in a direction that is opposite to electrophoretic line of action). It is therefore evident that under the influence of electric field, a charged particle will move forward by the combine effects of both electro-osmosis and electrophoresis. These combined effects are referred to as electrokinetics.

2.4   Dielectrophoresis

So far, it has been shown that the electrokinetics forces (EO and EP) are important forces in a microchannel that aid fluid transport. It has also been demonstrated how the

application of electric field causes particle motion along the length of a microchannel. The applied electricity mentioned in these demonstrations is usually uniform. In this section, focus will be on the examination of what is happening to both the medium and the particle when the applied electric field is non-uniform. The utilization of non-uniform electric field in a microchannel for manipulating the trajectories of the dielectric particles flowing within the channel is what is referred to as dielectrophoresis. This technique relies on the electrical property differences between the particles and the medium and also the electrophysiological properties of the particle itself.

2.4.1 The concept of dielectrophoresis (DEP)

When a polarizable particle is subjected to non-uniform electric field, the force exerted on the particle causes it to move towards high or low field density regions; this behavior is known as dielectrophoresis [5, 6]. The motion of the particle is quantified by the polarity of charges in addition to the magnitude of the DEP force generated by the applied electric field and this phenomenon is often referred to as 'classical DEP' [7].

DEP is observed only when non-uniform electric field is exerted on the cells because the coulomb forces generated on both sides of the particle are different, thus facilitating the movement of the particle towards the region of electric field maxima or minima. If a uniform field exists, the coulomb forces generated are equal but opposite in charge. This, combined with the alternating orientation of the electric field, makes the net force on the particle over time equal to zero [7]. Both AC and DC electric fields can be applied to nonlinear field geometries and both will generate non-uniform columbic forces across a particle thus yielding DEP behavior.

Dielectrophoretic phenomena have traditionally been associated with the application of AC voltage and frequency in conjunction with spatially non-uniform electrode geometries to create novel electric field gradients essential for manipulating particles of interest [8]. However, in a new area of research, DC voltage has also been applied to achieve dielectrophoretic separation. Dielectrophoresis depends on a wide range of properties in both the medium and the particle. Due to differences in physical and chemical properties, one of two phenomenological DEP effects first explained by H.A. Pohl [9] are usually observed: positive DEP and negative DEP. In the next two subsections, these phenomena are discussed in concert with a discussion on classical dielectrophoresis (AC-DEP) or electrode DEP and

the newly explored direct current dielectrophoresis (DC-DEP) or electrodeless DEP.

2.4.2. Alternating Current Dielectrophoresis (AC-DEP):

This is the classical DEP technique employing AC voltage and frequency to manipulate particles of interest. Embedded microelectrodes positioned in a spatially non-uniform manner are used to achieve particle separation, trapping, and focusing by applying AC electric fields from kHz-GHz range [10]. The use of high-frequency (>100 kHz) AC field has some advantages: 1) no electrophoretic movement is observed due to the cell membrane being statically charged and 2) electrochemical reactions such as those producing gas (i.e. bubble generation) are reduced [10]. When a microparticle is suspended in a highly conductive medium, the particle experiences less polarization compared to the medium. In such case, the particle / cell exhibits negative dielectrophoresis (nDEP), wherein the particle moves away from the high field density regions. In case of positive dielectrophoresis (pDEP), the particle is attracted towards the high field density regions by a translational force due to the greater polarizability of the particle as compared to the medium's. [5, 8]
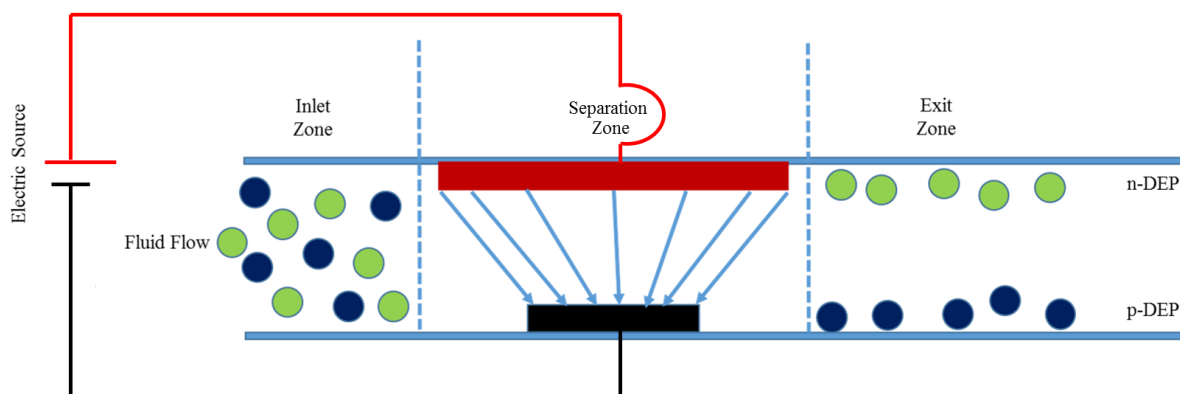
Figure 2.7   A typical representation of particle separation through AC-DEP. Electrodes are embedded within the microchannel.

The transition between negative DEP and positive DEP as one moves up in AC frequency is known as the crossover frequency. At this frequency the force experienced by the particle is zero [11]. Crossover frequency depends on the dielectric properties of the particle as well as the properties of the suspending medium. It is different for each particle or cell and this information can be used to optimize trapping or separation schemes. Some complex cells exhibit multiple crossover frequencies. Most biomolecules exhibit nDEP but mixed responses

might also be possible due to the complex make-up of their structures, compositions, and charge distributions [12, 13] The net dielectric force, $\vec{F}_{DEP}$ resulting from transient polarization of cells[9] and the electric field[14] is given by

$$\vec{F}_{DEP} = 2\pi r^3 \epsilon_m \alpha \nabla \overrightarrow{E^2},$$ (2.11)

where the particle radius is 'r', 'ε_m' is the medium permittivity, '$\vec{E}$' is the applied electric field, and 'α' is the real part of the Clausius-Mossotti factor, which is the effective polarizability of the particle relative to the suspending medium and is frequency dependent.

$$\alpha = Re[K(\omega)]$$ (2.12)

$$K(\omega) = \frac{\varepsilon_p^* - \varepsilon_m^*}{\varepsilon_p^* + 2\varepsilon_m^*}$$ (2.13)

$$\varepsilon^* = \varepsilon - \left(\frac{i\sigma}{\omega}\right)$$ (2.14)

where, ε^* denotes complex permittivity and the subscript 'p' refers to a lossless dielectric sphere particle suspended in a medium 'm'. The complex permittivity ε^* given by Eq. 2.14, which is a function of permittivity, ε, medium electrical conductivity, σ, and the angular frequency, ω[9, 14].

The transient polarization of particles results in their movement in the electric field that scales between two extremes depending on the exciting AC frequency. Herbert Pohl, in his seminal text "*Dielectrophoresis: The behavior of neutral matter in nonuniform electric fields*" defined these two phenomenological extremes as positive dielectrophoresis and negative dielectrophoresis[9]. These two cases arise because of the polarizability of a uniform composition particle being greater or lesser than the polarizability of the medium in which it is suspended. If the real part of the effective polarizability, Re[α] of the particle is greater than that of the medium, then the electric field lines pass through the particle causing a polarization, which is slightly skewed due to the spatially varying electric field lines. A resultant force directs the particle to high field density regions and this observed movement is known as 'positive dielectrophoresis' (pDEP). If the effective polarizability, Re[α] of the particle is less than that of the medium in which it is suspended, spatially non-uniform electric field lines divert around

the outside of the particle causing ion depletion at the particle poles and subsequent polarization. The resulting force directs the particle to the low field density regions and this is termed 'negative dielectrophoresis' (nDEP) [9, 15].

2.4.3   Direct Current Dielectrophoresis (DC-DEP):

Direct current dielectrophoresis is a novel technique developed in the last decade. It employs insulating objects or hurdles, fabricated by a variety of microfabrication methods, within the channel to create spatial field non-uniformities [6, 16] (Figure 2.8). It is also known as insulator-based dielectrophoresis (iDEP) or electrodeless dielectrophoresis (eDEP) owing to the fact that the electrodes are placed far outside the channel in inlet and outlet ports. The electrodes are immersed in the suspending media, but are not in direct contact with the particles being observed. This is a huge advantage over the traditional AC dielectrophoretic technique [17]. In DC-DEP, there is no frequency dependency involved so spatial electric field non-uniformities are solely responsible for the DEP forces experienced by the polarizable particles.
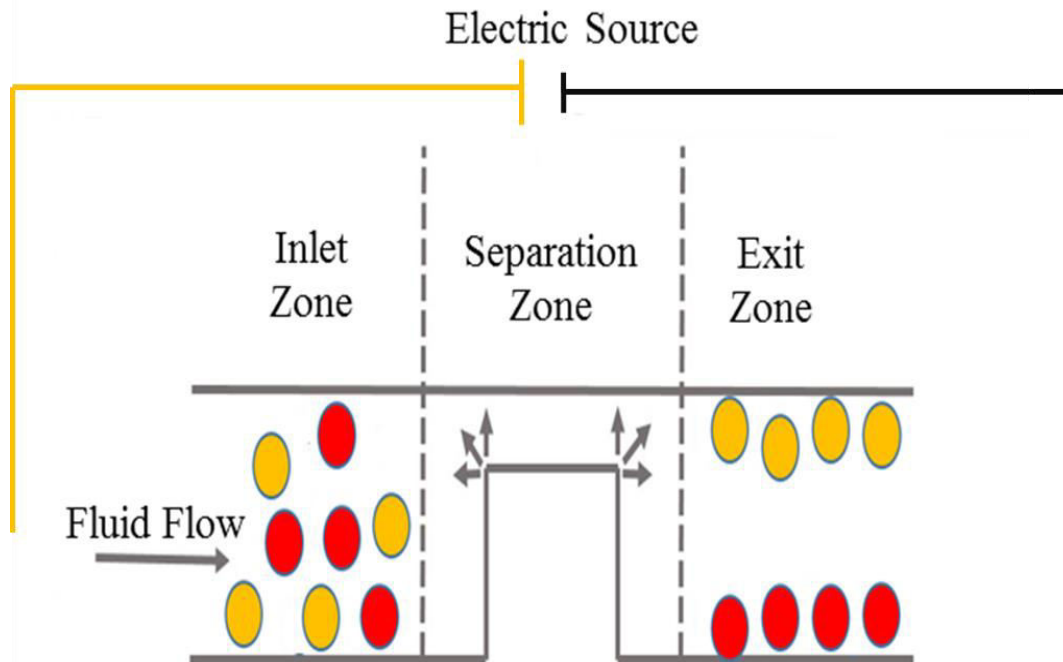
Figure 2.8   The basic idea behind DC-DEP particle separation: An insulating hurdle is being used to generate electric field non-uniformity at the separation zone.

The force exerted on the particle impels the particle to move away from the insulating obstacle region thus undergoing nDEP phenomena. In case of pDEP, the particles get trapped at sharp points or constrictions in the insulating region, which is the region of high field

maxima in DC-iDEP devices. A particle in the insulating obstacle region experiences dielectrophoretic and electro-osmotic forces; the relative magnitude of each determines whether the particle is trapped or flows through the constriction in a specific fluid flow streamline.

The observed cell motion in iDEP devices depends on two forces: electrokinetics (EK) and dielectrophoresis (DEP).

$$\vec{j} \propto \vec{u}_{EK} + \vec{u}_{DEP} \tag{2.15}$$

where $\vec{j}$ is the particle flux, $\vec{u}_{EK}$ the electrokinetic velocity (expressed as the sum of electrophoretic $\vec{u}_{EP}$ and electro-osmotic $\vec{u}_{EO}$ velocities) and $\vec{u}_{DEP}$ the dielectrophoretic velocity of the particle. Electrokinetic velocity can be expressed as the sum of electro-osmotic and electrophoretic mobilities:

$$\vec{u}_{EK} = \mu_{EK}\vec{E} = (\mu_{EP} + \mu_{EO})\vec{E} \tag{2.16}$$

where μ_{EK} is the electrokinetic mobility, μ_{EP} electrophoretic mobility, μ_{EO} electro-osmotic mobility and $\vec{E}$ applied electric field to create non-uniformities in the channel. Neglecting the frequency component for strict DC-iDEP, the CM factor in Eq. 2.13 is modified to:

$$\alpha = \frac{\sigma_p - \sigma_m}{\sigma_p + 2\sigma_m} \tag{2.17}$$

where σ_p is the conductivity of the particle, σ_m the conductivity of the medium. This simplification is substituted into Eq. 2.11 yielding[6, 18]

$$\vec{F}_{DEP} = \frac{1}{2}V\frac{\sigma_p - \sigma_m}{\sigma_p + 2\sigma_m}\varepsilon_m\nabla\vec{E}^2 \tag{2.18}$$

where V the volume of the particle, ε_m permittivity of the medium, and $\vec{E}$ the magnitude of the applied DC electric field.

From Eq. 2.17, if the conductivity of the particle is greater than the medium, the CM factor gives positive values and the dielectrophoretic force on the particle pushes the particle towards high field density regions thus trapping them i.e. the particle gets attracted towards insulating obstacle region whereas, if the conductivity of the particle is less than that of the medium, the particles are repelled from the high field density regions thus yielding in negative values of CM factor and movement of particles in the fluid streamlines i.e. particles are repelled from the insulating obstacle regions. The conductivity of the particle (σ_p) is given as a function of surface conductivity and bulk conductivity[19]:

$$\sigma_p = \sigma_b + \frac{2K_s}{r}$$

$$(2.19)$$

where σ_b, the bulk conductivity, K_s is the surface conductance and 'r' the radius of the particle.

Due to the electrodes placed in the large reservoirs at the channel inlet and outlet ports, they often cause re-dilution of the concentrated samples with some Joule heating and bubble formation[20]. To mitigate these effects, a simple, robust device was designed where in the electrodes are not in direct contact with the sample. This technique is referred to as contactless dielectrophoresis (cDEP) wherein the electric field is generated by placing the electrodes in two conductive microchambers separated by thin insulating barriers from the main channel[21]. cDEP is particularly well-suited for manipulating sensitive biological particles such as red blood cells and circulating tumor cells[22] .

2.4.4   DC-biased AC dielectrophoresis (AC-iDEP):

Compared to classical DEP (AC DEP), where only AC fields are employed to focus / sort / trap cells, iDEP could be operated utilizing either only DC (DC-iDEP) or with both AC and DC field components (DC-biased AC fields; AC-iDEP)[23].

From Eq. 2.18, the DEP force $\vec{F}_{DEP}$ on a spherical particle under DC-biased AC field (AC-iDEP) conditions is given by:

$$\vec{F}_{DEP} = 2(\alpha^2 + 1)\pi\varepsilon_m r^3 \, \Re[f_{CM}]\nabla\left|\vec{E}_{DC}\right|^2$$

$$(2.20)$$

where 'r' is the radius of the RBC, the real component $\Re[f_{CM}]$ is the particle's induced dipole in a DEP field and the effective polarizability of the cell.

AC-iDEP is operated under the combination of AC and DC voltage defined by α (the ratio of AC to DC electric field amplitudes.

$$\alpha = \frac{\left|\vec{E}_{AC}\right|}{\left|\vec{E}_{DC}\right|}$$

$$(2.21)$$

The Clausius-Mossotti (CM) factor (f_{CM}) depends on both permittivity of the medium (m) and the particle (p), which contain both real and imaginary terms due to the DC / AC component as given by Eq. 2.13.

From Eq. 2.20, *Clausius-Mossotti (CM)* could be positive or negative thus, reflecting the direction of the resulting DEP force on the cell. At higher frequencies, the field penetrates

the plasma membrane into the cell interior, which is more conductive than the suspending medium[23]. The DEP force is now positive (pDEP), and cells are attracted to the strong electric field regions, thus trapping near the insulating obstacle region (in case of AC-iDEP) or electrode surface (classical DEP). At low frequencies, the field penetration is small and the entire applied field appears across the poorly conducting membrane and does not penetrate the cell interior. Thus, cells are less polarizable than the suspending medium and tend to be repelled from strong electrical field regions by negative DEP forces (nDEP)[23].

References

1. R. J. Hunter, Foundations of Colloid Science, Oxford Press University, 2nd edn., 2002.

2. B. J. Kirby, *Micro-and nanoscale fluid mechanics: transport in microfluidics*, Cambridge University Press, 1st edn., 2010.

3. K. Ohno, K. Tachikawa and A. Manz, *Electrophoresis*, 2008, **29**, 4443-4453.

4. R. Pethig, *Biomicrofluidics*, 2010, **4**, 1-35.

5. S. K. Srivastava, P. R. Daggolu, S. Burgess and A. R. Minerick, *Electrophoresis*, 2008, **29**, 5033-5046.

6. S. K. Srivastava, K. M. Leonard, S. C. Burgess and A. R. Minerick, Boston, MA, 2008.

7. C. Zhang, K. Khoshmanesh, A. Mitchell and K. Kalantar-zadeh, *Anal Bioanal Chem*, 2010, **396**, 401-420.

8. F. Yang, X. Yang, H. Jiang, P. Bulkhaults, P. Wood, W. Hrushesky and G. Wang, *Biomicrofluidics*, 2010, **4**, 1-13.

9. H. A. Pohl, *Dielectrophoresis the behavior of neutral matter in nonuniform electric fields*, Cambridge University Press, Cambridge, 1978.

10. P. C. H. Li, *Microfluidic Lab-on-a-Chip for Chemical and Biological Analysis and Discovery*, CRC press, Boca Raton, FL, 2006.

11. M. P. Hughes, *Electrophoresis*, 2002, **23**, 2569-2582.

12. M. D. Pysher and M. A. Hayes, *Anal. Chem.*, 2007, **79**, 4552-4557.

13. B. H. Lapizco-Encinas, B. A. Simmons, E. B. Cummings and Y. Fintschenko, *Anal. Chem.*, 2004, **76**, 1571-1579.

14. R. Pethig, *Critical Reviews in Biotechnology*, 1996, **16**, 331-348.

15. M. Sancho, G. Martínez and C. Martín, *Journal of Electrostatics*, 2003, **57**, 143-156.

16. E. B. Cummings and A. K. Singh, *Anal. Chem.*, 2003, **75**, 4724-4731.

17. K. H. Kang, Y. Kang, X. Xuan and D. Li, *J. Appl. Phys.*, 2006, **99**, 064702-064708.

18. S. K. Srivastava, A. Srivastava, A. Minerick and N. Schulz, presented in part at the American Society of Engineering Education, Pittsburgh, PA, 2008.

19. S. Ozuna-Chacón, B. H. Lapizco-Encinas, M. Rito-Palomares, S. O. Martínez-Chapa and C. Reyes-Betanzo, *Electrophoresis*, 2008, **29**, 3115-3122.

20. H. Shafiee, J. L. Caldwell, M. B. Sano and R. V. Davalos, *Biomed. Microdevices*, 2009, **11**, 997-1006.

21. H. Shafiee, M. B. Sano, E. A. Henslee, J. L. Caldwell and R. V. Davalos, *Lab Chip*, 2010, **10**, 438-445.

22. A. S. Elizabeth S. Elvington, Mark A. Stremier, Fafael V. Davalos, *Journal of Visualized Experiments*, 2013, **79**.

23. S. Srivastava, A. Gencoglu and A. Minerick, *Anal. Bioanal. Chem.*, 2011, **399**, 301-321.

CHAPTER 3

DIELECTROPHORESIS IN DISEASE DIAGNOSTICS

In Chapter 2, the details of fluid flow in a microchannel under the influence of electric field were given. Section 2.4 particularly elucidates the principle behind particle manipulation using non-uniform electric field. Chapter 3 will focus on the utilization of this novel dielectrophoretic technique for the manipulation of biological particles. The chapter is mainly divided into three sections. Section 3.1 gives the details of various models that have been used to depict biological cells. Section 3.2, on the other hand, discusses various ways of generating non-uniform electric field within the dielectrophoretic channel. In Section 3.3, a review of diseases that have been tackled using dielectrophoresis is given.

3.1   Introduction

There is an ever rising need in the area of medical diagnostics for early detection, high quality medical care and new technologies[1, 2]. The driving force beyond this biomedical diagnostic application is the emphasis placed on accuracy, preventive care and least invasive procedures[2]. National Institute of Health (NIH) and Bill and Melinda Gates foundation have prioritized the development of technologies geared towards identifying disease conditions at point-of-care[1]. Current disease diagnostics rely heavily on patients' perception and doctors' interpretations of the symptoms before further analytical tests are conducted. Most of the diagnostic techniques require expensive reagents and laboratory settings, which often are time consuming, cumbersome and invasive. Apart from the time delay, logistic errors such as missing samples and mislabeling may hamper timely diagnosis[3].

Recent technological advances in microfluidics and lab-on-a-chip (LOC) technology have yielded integrated medical microdevices that perform necessary cell manipulation activities on raw samples: cell pre-filtering, cell fractionation, target cell isolation, cell concentration or focusing, cell lysis, and marker molecule trapping and detection[4]. This lab-on-a-chip technology, involving miniaturization of analytical techniques, is implanted to enable highly complex laboratory tests move from the central laboratory into non-laboratory settings. Novel electrical devices assembled by using microfluidics are still subject to technological advancement.

With an increasing impact on health, miniaturized devices are becoming very attractive for detecting diseases[3]. For clinical applications, making point-of-care (POC) devices portable has the potential to reshape the healthcare industry[5]. POC devices for use at homes or in practitioners' offices will aid the accurate and rapid detection of infectious diseases, cancers, inherited diseases and other forms of anomalies within the human systems. In fact, there is a proclivity that the use of these POCs would ensure effective prescription of drugs thereby reducing any unwarranted side effects and ultimately ensuring improved healing rate. Minute sample amounts, reproducibility, and minimizing invasive ways of sample drawing from the body are some advantages of using LOC devices.

They are cost effective, have reduced sampling times and require low man power[3]. Small sample volumes provide an added advantage of effective temperature control within the system. It also minimizes the bulk use of biohazardous and precious samples resulting in reduced operating costs, improved efficiency, increased resolution and sensitivity[6, 7]. However, small sample volumes can easily clog the microdevice and this often calls for regular device maintenance and calibration[8]. Despite this setback, the detection or quantification of cells are much more reproducible, accurate and sensitive in small sample volumes as the local concentration of cells of interest is usually high[9]. Some of the most common LOC devices used in daily-life are the alcohol detecting breath analyzers, glucose monitors for the diabetics, and pregnancy test kits for hormone level detection[3, 9].

There is an increasing level of interest in developing techniques that can physically manipulate cells[10, 11]. Some of them include optical tweezers, acoustic forces, electrical forces, and surface modifications[10]. Manipulating cells by electric forces has been the most common technique and can be classified according the action of the electrical forces (i.e. whether the electrical forces act on the particle's fixed or induced charge). Dielectrophoresis, is one such electrical techniques which acts on the particle's induced charge and can be used to translate, rotate, stretch and manipulate the particles[10].

Dielectrophoresis (DEP), an electrokinetic effect, was first described experimentally by Herbert A. Pohl, who, in 1979, published a book titled "*Dielectrophoresis the behavior of neutral matter in non-uniform electric fields*"[12, 13]. Even though experimental and theoretical foundations for understanding DEP were established about a century ago and extended in the 1920s and 1930s, real experimentations with biological cells started in 1939[14]. However, the

increasing availability of micro-fabricated devices for silicon-based integrated systems has brought rapid advancement in this field since late 1980s[13, 14]. The DEP force exerted on a cell is dependent on: 1) cell's characteristics such as dielectric properties, shape, and size, 2) suspending medium properties like permittivity, conductivity, and 3) applied electric field, which creates the field gradient.

In cases involving biological cells (bacteria, virus, mammalian cell), DEP force experienced by the cells is dependent on permittivity of the membrane and the pathological condition of cells in addition to the other dependencies stated above[15]. DEP has been a commonly used technique for separation, trapping, pre-concentration, and manipulation of cells including diseased[16-20] and healthy cells[21, 22], bacteria[23-26], inert microspheres[27, 28], DNA[29-31], virus[32-34], and proteins[35, 36]. It has also been used to monitor changes in the cells' states associated with activation and clonal expansion, apoptosis, necrosis, and responses to both chemical and physical agents[37].

In this review, the use of DEP for the manipulation of diseased cells (i.e. sorting, trapping, and pre-concentration) is discussed. Section 3.2 reviews the shell models for cells and section 3.3 elucidates the electrode configurations commonly used to manipulate cells in these DEP devices. Various works on the application of dielectrophoresis in research involving malaria, human African trypanosomiasis, dengue, anthrax and diverse forms of cancer are then reported in section 3.4.

3.2   Shell models for cells

The main polarization mechanism at frequencies up to 10^7 Hz is the Maxwell-Wagner polarization[38]. This polarization occurs due to the differences between the electric properties of the cell and the suspending medium[38]. Eq. 2.11 is a generalized equation for spherical, homogenous particles, but is only a precise relation of the DEP force on cells because cells are non-homogenous complex biochemical entities with non-uniform distribution of insulating and conducting components.

The properties of biological species can be characterized by three major dispersions: α (low frequency), β (radio frequency) and γ (microwave frequency)[39]. Due to the Maxwell-Wagner effect at the interface between the cell membrane and the suspending medium, biological cells typically exhibit β dispersion at radio frequency range[39].

Analytical dielectric modeling has been conducted to interpret the movement of biological cells in electric fields using either sphere or ellipse as an approximation for their shapes, but remain approximations[40]. Further, it was shown that correct cell geometrical parameters are critical for understanding permittivity of cell suspensions[41-43]. There are many models available to obtain dielectrophoretic forces and trans-membrane potentials. Some of these models fail to describe the phenomena experienced by a biological cell having a complex inner structure. The theories used to model the dielectric behavior of biological cells are based on Maxwell-Wagner and single-multiple particle shell models[44].

Different mixture models are used to obtain dielectric properties of cells depending on the concentration, shape and conductivity of the cell and the suspending medium[39]. In the next few sections, a review covering the most common models for biological cells is made. Figure 3.1, briefs the structures of the different shell models and its layers.

3.2.1 Maxwell-Wagner theory:

The original theory of mixture formula was developed by Maxwell, which was later extended by Wagner. This Maxwell-Wagner theory is applicable for dilute system of homogenous spherical particles[44]. The dielectric behaviors of homogenous particles arise from the charge build-up at the particle surface. The magnitude of the charge accumulation depends on the field frequency i.e. the rate at which the field changes its sign[44]. Thus, the electric polarization depends inversely on the frequency of the applied field. It is described as a function of dielectric properties of cell and the suspending medium as given by Eq. 3.1[39, 44, 45].

$$\varepsilon_{mix}^{*} = \varepsilon_{m}^{*} \frac{(2\varepsilon_{m}^{*} + \varepsilon_{cell}^{*}) - 2p(\varepsilon_{m}^{*} - \varepsilon_{cell}^{*})}{(2\varepsilon_{m}^{*} + \varepsilon_{cell}^{*}) + p(\varepsilon_{m}^{*} - \varepsilon_{cell}^{*})} \tag{3.1}$$

where p is the cell's volume fraction, and ε^{*} is the complex dielectric permittivity defined by Eq. 2.14. The indices *mix, cell,* and *m* refer to the whole mixture, cell, and the suspending medium. Eq. 3.1 holds good until the particle is not perturbed by the neighboring particles[44]. This theory is very sensitive to cell membrane permittivity and conductivity[45].
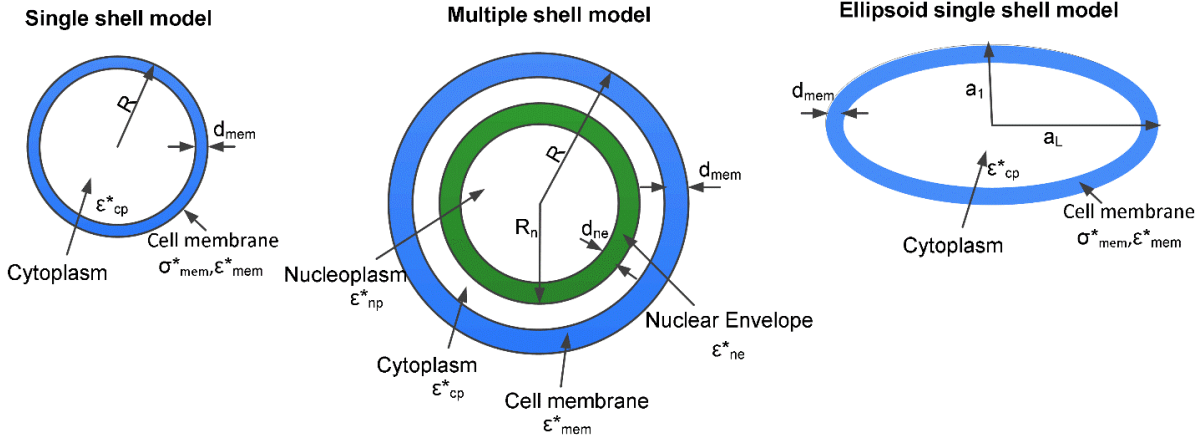
Figure 3.1   Shell models for biological cells

3.2.2   Single-shell model:

Biological cells are considered heterogeneous complex layered particle compared to the homogenous particles. The cell membrane is known to have a high electrical resistance and is usually represented by a very thin layer with dielectric constant between 2 and 10 and low conductivity, with values that range between 0 and 10^{-2} S/m[46].

In a single-shell model, the biological cell is considered a homogenous conducting particle of complex permittivity ε_{cp}^{*} enclosed in a poorly conducting shell of complex permittivity ε_{mem}^{*}. The dielectric constant ε_{p}^{*} can be obtained by[39, 47],

$$\varepsilon_p^* = \varepsilon_{mem}^* \frac{(1 + 2V_m)\varepsilon_{cp}^* + 2(1 - V_m)\varepsilon_{mem}^*}{(1 - V_m)\varepsilon_{cp}^* + (2 + V_m)\varepsilon_{mem}^*} \tag{3.2}$$

where $V_m = (1-d_{mem}/R)^3$, R the outer cell radius and d_{mem} the shell thickness. This equation allows calculating frequency dependency on conductivity and permittivity of cell from its phase parameters[47]. Each cell and its components (cell membrane, cytoplasm, and nucleoplasm) are described by permittivity and conductivity. Thus, in a single-shell model, a cell can be described by four dielectric phase parameters. Single-shell models are suitable for characterizing dielectric properties of mammalian erythrocytes since it does not include nucleus or cytoplasm[47].

3.2.3   Multi-shell (double) model:

Another popular model for estimating dielectric properties of cell is the multi-shell model. Many researchers have explored this model with some modifications[38, 44, 46, 48]. For cells

of complex internal structure, a gross model including the lipid bilayer enclosing conductive cytosol with nucleus has been defined by Irimajiri et al[48]. For simplicity, here we discuss the two-shell model. Double-shell models are appropriate for cells like lymphocytes because of their morphology i.e., these cells have a nucleus occupying >50% of the total cell volume[47].

In the double-shell model, a smaller sphere with a shell is encapsulated in a big sphere. The effective complex permittivity of the whole cell is expressed as a function of phase parameters.

$$\varepsilon_p^* = \varepsilon_{mem}^* \frac{2(1-V_1)+(1+2V_1)E_1}{(2+V_1)+(1-V_1)E_1}$$

(3.3)

where $V_1=(1-d_{mem}/R)^3$, R the outer cell radius and d_{mem} is the plasma membrane thickness and E_1 is given by

where

$V_2=(R_n/(R-d_{mem}))^3$, R_n

$$E_1 = \frac{\varepsilon_{cp}^*}{\varepsilon_{mem}^*}\frac{2(1-V_2)+(1+2V_2)E_2}{(2+V_2)+(1-V_2)E_2}$$

(3.4)

the outer radius of nucleus, indices cp and mem refers to cytoplasm and cell membrane respectively, and E_3 is given by

$$E_2 = \frac{\varepsilon_{ne}^*}{\varepsilon_{cp}^*}\frac{2(1-V_3)+(1+2V_3)E_3}{(2+V_3)+(1-V_3)E_3}$$

(3.5)

where $V_3=(1-d_{ne}/R_n)^3$, d_{ne} is the nuclear envelope thickness, index ne refers to nuclear envelope, and $E_3 = \varepsilon_{np}^*/\varepsilon_{ne}^*$ the ratio of complex permittivities of nucleoplasm and nuclear envelope[39, 44].

3.2.4   DEP of ellipsoid cells:

Different theories have been developed to characterize dielectric properties of biological cells involving sphere encapsulated in a single or multiple shells. All these theories demand the cell to be spherical. The shape of the cell influences the electric field created. For e.g. for characterizing dielectric properties of erythrocytes, the erythrocytes have to be swollen by osmotic pressure to change its shape to spherical, so that single-shell model could be applied[45].

Consider an ellipsoidal cell with a major axis a_L and minor axis a_l having their own Clausius-Mossotti factor[49, 50]:

$$f_{CM,i} = \frac{\varepsilon_p^* - \varepsilon_m^*}{3\left[\varepsilon_m^* + \left(\varepsilon_p^* - \varepsilon_m^*\right)L_i\right]} \tag{3.6}$$

where ε_p^* the complex permittivity of the particle and L_i the depolarization factor are given by,

$$\varepsilon_p^* = \frac{\varepsilon_{mem}^* \varepsilon_{cp}^*}{d_m/_R \varepsilon_{mem}^* \varepsilon_{cp}^*} \tag{3.7}$$

$$L_i = \frac{a_1 a_L^2}{2} \int_0^\infty \frac{1}{(l+R^2)(\sqrt{(l+a_L^2)}(l+a_1^2)^2} dl \tag{3.8}$$

where l is the integration variable and R represents either the major axis a_L or minor axis, a_1.

These ellipsoidal models could be applied to erythrocytes due to their biconcave shape as a lossy dielectric ellipsoid encapsulated in a thin insulating shell[51]. They could be modified depending on the major and minor axes to oblate and prolate ellipsoids. Human erythrocytes could be approximated as oblate ellipsoids[51] whereas dielectric characterization of rod-shaped bacteria could be approximated based on prolate ellipsoid model.

3.3   Micro-electrode configurations of DEP devices

Conventional electrodes were metal sheets, machined blocks, wires, rods or needles for generating non-uniformity in the electric field, but thanks to the advances in soft lithography techniques, microelectrode fabrication is possible and capable of creating precise electrode shapes and thus specific field gradients[27]. Adapting microelectrode has a number of advantages. One such advantage is the rise in DEP forces experienced by the particle. Dielectrophoretic force depends on gradient of the square of electric field (V^2m^{-3}) and direct dimensional analysis demonstrates the substantial increase in force achieved with micron-sized electrodes. Another advantage is the use of low amplitude electric fields for manipulating cells if microelectrodes are used once again because a smaller voltage applied over a micron-sized gap can achieve the same force as large voltages over large gaps. The miniaturization substantially reduces joule heating effects and electrode decay thus retaining viability of biosamples[52]. Apart from metal-based electrodes, other materials have also been used to create non-uniform electric fields[53].

Dielectrophoretic trapping, sorting, electro-rotation and traveling wave DEP

effects could be accomplished by changing the electrode shape and orientation in addition to modulating the frequency and phase applied to achieve DEP[49].

3.3.1 Metal-based:

Metal electrodes have been used extensively to manipulate cells for several decades. They are often positioned inside the microchannel and are always in contact with the sample and the suspending medium[10]. The potential major limitation of using metal electrodes is fouling and electrolysis at high frequencies[54]. The net result could be gas generation or dissolution of electrodes, which would potentially harm the biological sample that is manipulated.

Some of the popular configurations used to achieve DEP effects using AC field are: trapezoidal electrode array[55], interdigitated microelectrodes[56, 57], pyramidal arrangement[58], checker board arrangement, polynomial geometry and multiphase electrodes[59].

The interdigitated electrode array is the most commonly used configuration to achieve field non-uniformity as they are easy to model and create large arrays. They consist of two sets of electrode array; one of the set is grounded[49]. They alternate spatially and have used to trap human leukemia cells and leukocytes[56, 60, 61]. Castellated electrodes are similar to interdigitated electrodes but they consist of square-wave-shaped electrodes. They are placed parallel to each other and regions of field maxima and minima are created[62].

Electrode-based traps are used to observe the activity of a single cell closely. Some of the popular configurations are the micro-well[63], quadrapole electrodes, octopole electrodes, point-and-lid, and ring-dot geometry[10]. The traps could be configured for achieving pDEP or nDEP effects on the cell. Creating nDEP traps are difficult compared to pDEP traps because, it is always easier to hold onto a cell by attraction than repulsion[10].

Recently, the use of circular or spiral array of electrodes has become popular to enrich or trap cells of interest[64, 65]. The applied electric field is switched to the adjacent electrode pair by using relays thus generating a stepping electric field[64].

3.3.2 Insulator-based:

An alternative approach to internal electrodes is to use external electrodes. Here electrodes are not used to create non-uniformity in the electric field, instead an insulating hurdle in the channel is used[53]. There are several advantages in using external electrodes, but

the major advantage is the electrodes need not be fabricated along with the device thus reducing the cost. The electrodes are placed in the outlet ports and the shape of the insulating hurdle defines the electric field generation.

These insulating hurdles can be single or multiple in numbers and sometimes the channel itself could be shaped into any required geometry. Some of the common geometries explored include insulating posts[34, 66], rectangle[67-69], spiral[70], triangle[69], oil droplet[71], saw tooth channel[72], and serpentine microchannel[73, 74]. A variety of particles have been trapped and sorted with these geometries: live vs. dead cells[26], microbes in water[75], yeast cells, bacteria[23], protein[36], DNA[76], virus[34], and inert microspheres[67, 71].

A spatially dense non-uniform field is created as the field lines diverge around the insulating obstacle. Due to the insulating obstacle, a high electric field density region is produced within narrow channel regions created by the obstacle. Fluid flow drives the particle through this narrow constriction, while the field gradient shape aids in particle motion. Since DEP forces push the particle towards or away from the high field density, the particle experiences an attractive or repulsive force as it flows around the corner of the obstacle, thus facilitating particle motion according to its polarizability.

3.4 Dielectrophoretic manipulation of diseased cells

Diseased cells could be trapped using pDEP and sorted or focused using nDEP by applying AC or DC electric fields dielectrophoretically. Dielectrophoresis utilizes the dielectric properties of the cells which typically depend on the cell's structure and composition, thus enabling enhanced particle discrimination accessing multiple properties of the cells[4].

Cells are involved in pathogenesis of many diseases including hematological malignancies, immune disorders, inflammation-associated diseases, and cancer[77, 78]. So they have been widely used to study disease prognosis. It is assumed that the membrane capacitance of the cell varies depending on the size, and cell membrane composition[79]. Also, distinguishable differences at selective frequencies exist among many different types of diseased cells[17]. Extensive and validated studies have shown that different cell types, cells at various stages of maturation or proliferation, and diseased cells, exhibit characteristic DEP signatures associated with their morphology, cellular structures and cell state[80]. Another important dielectric parameter reflected in DEP behavior is the cell membrane capacitance determined by the effective membrane surface area. Morphological changes associated with

membrane folding and ruffling, or the appearance of microvilli, can produce greater changes in the effective membrane capacitance. Such morphological changes often accompany changes in the physiological state and external environment of a cell and are events readily monitored by DEP[80].

The passive electrical conductivity of the membrane is also an important dielectric parameter that can be sensitively monitored by DEP. This conductivity is negligibly small for normal healthy cells, but can increase for diseased or dying cells[80]. Ions present in the aqueous phase of the cells move under electric field until they are obstructed. As the build-up of ions on the cell membranes increases, a process called interfacial polarization occurs which dominates the dielectric properties up to 200 MHz. Thus, the dielectric properties of the cells are dominated by polarization at the frequency range of 5 kHz-200 MHz[4].

The crossover frequency is another important parameter defined as the frequency at which trapping of cells stops and repulsions begin. The DEP cross-over frequency for normal healthy cells is estimated to be in the range of 40-100 kHz whereas for most of the diseased cells it is in the range of 10-30 kHz[4]. A novel dielectrophoretic based method was developed to study the dielectric properties of cells based on the capture voltage spectrum[81].

DEP offers many distinct advantages as a tool for biomedical diagnostic applications: (i) monitor cell viability changes, (ii) isolate viable cells with minimal / no damage, (iii) monitor changes in the surface morphology or internal structure of cells, (iv) sort cells to high specificity for their identification, (v) sort cells without any biochemical labeling or modification, (vi) sort rare target cells from heterogeneous samples, avoiding cell loss with one single process (namely DEP), (vii) process samples at high cell-sorting rates comparable to fluorescence activated cell sorting (FACS)[37].

DEP has successfully been used to trap and sort malaria-infected cells, carcinoma cells like breast cancer, leukemia, melanoma, colorectal cancer cells, oral cancer cells, circulating tumor cells, dengue and anthrax. In the next couple of sections, we review the different parameters and conditions used to manipulate (sort or trap) these diseased cells via DEP.

3.4.1 Malaria

Malaria is the most widespread parasitic disease affecting more than 500 million people each year[82]. About 3.2 billion people-almost half of the world population are also at risk of malaria[83]. In 2015, there were 214 million new cases of malaria and 438,000 deaths[83]. Sub-

Saharan Africa accounted for 89% of the new cases and 91% of the reported deaths. A larger proportion of these deaths were caused by infections due to *P. falciparum* [82]. These parasites are intraerythrocytic in nature. They internalize and accelerate glucose synthesis within the red blood cells and this process releases large portion of energy, which the parasites utilize in breaking down hemoglobin proteins-the important oxygen transport agents[84]. The internalization also results in the disruption of the microscopic network of protein filaments and tubules in the cytoplasm of the red blood cells (RBCs) and the associated de-polymerization impairs the morphology (especially size) and other mechanical[85], adhesive[86] and functional properties of the RBCs[87]. The internalization of the RBCs induce membrane and cellular changes[84], which invariably will affect their DEP response.

As of now, the most common method of diagnosis, often treated as the "gold-standard" test, is the microscopic method wherein a skilled technician analyzes as few as 4 parasites/μL of blood. However, the method is laden with various challenges which can include, lack of portability, difficulty in detecting mixed infections and the need for trained microscopists[88] With a view to improving the diagnosis of malaria, researchers have initiated some dielectrophoretic steps by leveraging the peculiarities stated in the previous paragraph.

Gascoyne *et al*. were the first to attempt DEP methodology for the detection of changes in *Plasmodium*-infected erythrocytes[19]. They used the single-shell oblate spheroid dielectric model to describe the normal erythrocytes. This model enabled the estimation of specific capacitance for the plasma membrane, cytoplasmic permittivity, and conductivity of the normal erythrocytes but reliable electrical peculiarities for the parasitized erythrocytes could not be estimated. As a result, dielectrophoretic crossover frequency measurements were made for both healthy and parasitized erythrocytes. These measurements (Figure 3.2), which were dependent on the conductivities of the cell and the suspending medium, generated the desired specific membrane capacitances for both normal and parasitized erythrocytes to be 12 ± 1.2 mF/m^2 and 9 ± 2 mF/m^2 respectively.
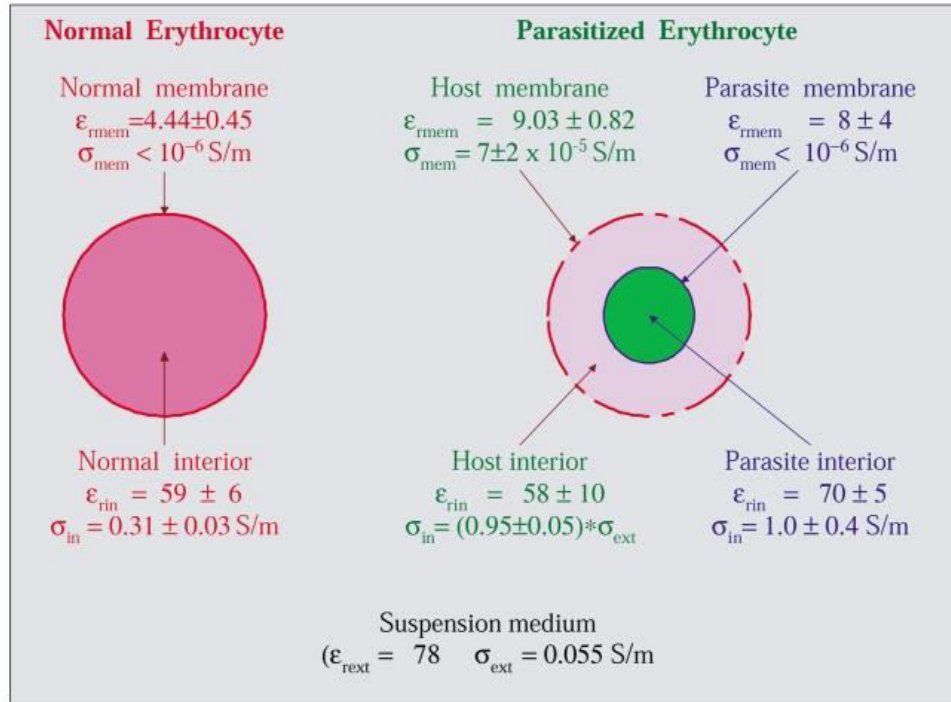
Figure 3.2   Mean dielectric parameters for normal and parasitized cells derived from iterative fitting of shell models as described in the text. Parasitized cells had a very low internal conductivity compared with normal erythrocytes, an indication they had suffered almost complete loss of ions to the low-conductivity suspending medium. The much higher membrane conductivity of parasitized cells compared with normal cells reflects the lowering of membrane barrier function that accounted for this loss. Despite the ion leakage out of their host cells, the parasites retained their internal ions as reflected by their high internal conductivity[89]. (Reproduced with permission from US National Library of Medicine, National Institutes of Health)

For both healthy and parasitized erythrocytes, the membrane conductance were 271 S/m^2 and 1130 S/m^2 respectively[19]. The basis for cell separation was predominantly membrane capacitance: a function of the changes in membrane morphology.

Further work by the same group used spiral as well as interdigitated electrode configurations to isolate *Plasmodium*-parasitized RBCs from healthy cells[89]. The parasitized cells were isolated based on the dielectric differences using the traveling-wave electric fields generated by two microelectrode arrays. The difference in the dielectric properties was based mainly on the ability of the cells to retain cytoplasmic ions[89]. When both healthy and parasitized cells were suspended in a low conductivity medium, the healthy cells were able to

maintain high cytoplasmic conductivity unlike the parasitized cells wherein the membrane conductivity dropped to the low conductivity of the medium within 10 mins. This implied that ion loss was the basis for cell separation. In the experiment, the healthy cells were trapped by pDEP at 5 V_{pp}, and 200 kHz between electrode tips in the interdigitated electrode, whereas in the spiral electrode configuration, healthy cells were trapped at 3 V_{pp} and 2 MHz. Higher trapping efficiencies were achieved using spiral electrode configuration because the cells were subjected to both attractive and travelling-wave properties of the DEP force[89].

3.4.2   Human African Trypanosomiasis (HAT)

HAT, also known as sleeping sickness, is a deadly parasitic disease endemic in sub-Saharan Africa. The disease is caused by single-celled protozoan parasites called trypanosomes, which invade the central nervous system causing neurological disorders[65]. The World Health Organization has set 2020 as a deadline to eliminate this deadly disease. However, there are challenges associated with the early diagnosis of HAT. Apart from the fact that the early-infection symptoms shown by most patients are intersects of other diseases, the low-parasitemia and chronic nature of the disease are some integral contributions to the challenges associated with diagnosis. Moreover, available diagnostic methodologies lack adequate speed and accuracies. These bottlenecks necessitate the search for improved diagnostic methods.

Menachery *et al*. started an alternative diagnostic technique by using dielectrophoresis to enrich trypanosomes in human blood. In their work[65], trypanosome-erythrocyte mixture was introduced into a spiral electrode array containing four arms (Figure 3.3), which generated the required traveling-wave electric field after the application of a quadrature-phase voltage of 2 V_{pp}.
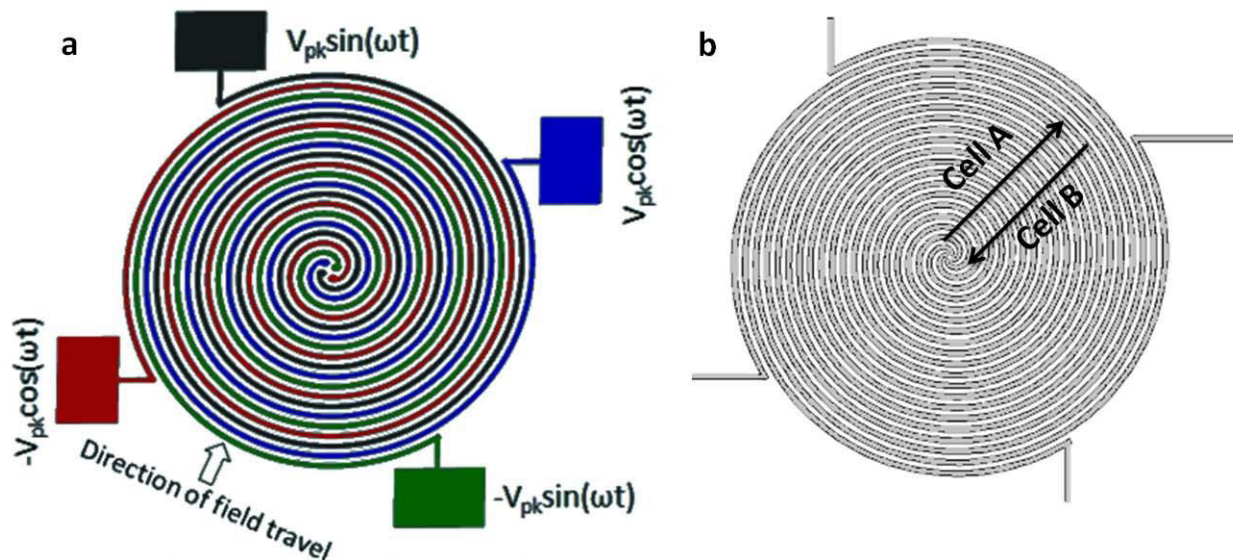
Figure 3.3   Electrode array used in this work. (A)Schematic of the four arm spiral microelectrode array comprising four parallel spiral elements of 30 mm in width and spacing. The electrodes are energized with a 90° phase shift respective to each other. (B)Working principle of the chip. While cell type A (e.g. red blood cells) is expelled from the electrode array, cell type B (e.g. trypanosomes) is concentrated into the center of the array. Both processes take place simultaneously[65]. (Reprinted with permission from nature)

The application of the voltage induced levitation and translational anti-field motion of the RBCs. At the same electric conditions, the trypanosomes were attracted towards the center of the spiral array. In effect, the RBCs were pushed upwards and outwards from the center, whilst the trypanosomes were pulled downwards and inwards making the spiral electrode rich in trypanosomes. The magnitude of the push-pull force on the RBC-trypanosome particles was larger at the plane of the electrodes and decreased rapidly with increase in electrode height. A net force associated with this push-pull phenomenon experienced by the RBCs and the parasites caused the opposite movement, which inadvertently led to their substantial separation. An important point to note here is that the differential movement of the cells were not only influenced by the intrinsic properties but were also dependent on the biophysical differences of the cells. In order to capture these enriched trypanosomes in the spiral array, an AC voltage shift (opposing two-phase AC field) was applied after 10 mins[65].
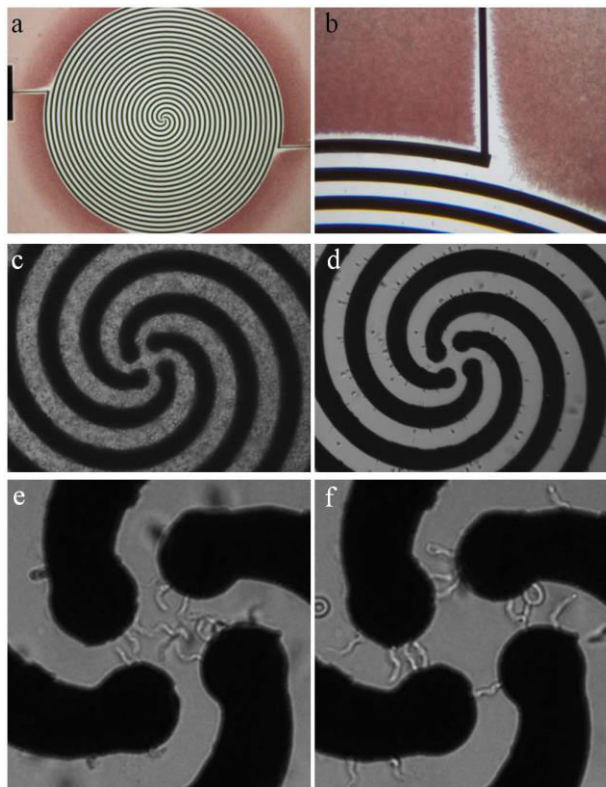
Figure 3.4   Enrichment of trypanosomes from infected blood. Total width of the spiral array is 2.9 mm, electrode width and spacing is 30 mm. (A, B). Micrograph following a separation process, with the RBCs having been pushed away from the electrode array. (C) Parasitized blood on the spiral electrode array. (D) Mouse RBCs are levitated and carried to the outer edges of the spiral. (E) Trypanosomes accumulate in the center of the spiral and undergo circular translational motion. (F) Trypanosomes are trapped along the electrode edges in the center of the spiral upon switching the AC voltage from quadrature-phase to an opposing two-phase[65] (Reproduced with permission from nature)

It is important to note that the pDEP phenomenon used in trapping the trypanosomes would not have come into play if the crossover frequencies of the trypanosomes and the erythrocytes had not been explored. The crossover frequency value was lower for a trypanosome parasite when compared to the RBC's. The observed difference in frequencies was mostly due to the size and shape. It was necessary to identify the electric conditions that would protect the integrity of the parasites at the center of the spiral array and as well ensure optimal enrichment (Figure 3.4). These conditions were found to be 2 V_{pp} and 140 kHz. The limit of detection using a single spiral electrode was found to be $1.2*10^5$ trypanosomes / ml in whole blood. By increasing the number of spiral arrays and sampling volume, the limit could

be improved[65]. This dielectrophoretic technique could be further applied to bacteria and spermatozoa cells.

3.4.3   Cancer

Normal cells possess the ability to communicate information inside themselves and between other cells. The coordination of information by the cells of the body is involved in the regulation and integration of cellular functions and cell growth[90]   They maintain, inside of themselves, a high concentration of potassium and a low concentration of sodium. Cell membranes, however, are composed of a bilayer of highly mobile lipid molecules that electrically act as an insulator (dielectric). The insulating properties of the cell membrane lipids also act to restrict the movement of charged ions and electrons across the membrane except through specialized membrane spanning protein ion channels[91] and membrane spanning protein semiconductors[92] respectively. Because the cell membrane is selectively permeable to sodium and potassium ions a different concentration of these and other charged mineral ions would build up on either side of the membrane. The different concentrations of these charged molecules cause the outer membrane surface to have a relatively higher positive charge than the inner membrane surface thus creating an electrical potential (membrane potential) across the membrane [93] as well as a strong electrical field around the membrane[94]. This membrane potential creates an electrochemical force across the cell membrane[95].

However, when cells are infected or cancerous, sodium and water flows in to the cells and potassium, magnesium, calcium and zinc are lost from the cell interior and the cell membrane potential decreases[96-99]. This causes loss of anchorage of critical mitochondrial enzymes, and that the mitochondria in cancer cells degenerate and are reduced in number[100]. The self-assembling cytoskeletal proteins, which are the dynamic structures that create a fully integrated electronic continuum linking and integrating the proteins of the extracellular matrix with the cell organelles are altered[101],[102]. This disruption in the normal signaling pathways produces cells that exhibit significant growth advantage compared to the other neighboring cells. The growth advantages are due to the genetic or epigenetic changes resulting in the inactivation of tumor suppressor genes[103]. Hence, the membrane structure, membrane function, membrane potential, cell concentration, electrical connections within the cells and between cells are all altered[100].

The result of these mineral movements, membrane composition changes,

energy abnormalities, and membrane charge distribution abnormalities decreases the normal membrane potential and membrane capacitance. Morphological changes associated with membrane folding and ruffling, or the appearance of microvilli, can produce great changes in effective membrane capacitance[104]. The movement of ions also has some effects on the conductivity of the cell. This conductivity is negligibly small for healthy cells, but can increase for diseased cells[104]. Given that capacitance and conductivity are both independent functions of the polarizability of the cells, it is evident that the DEP response of any cancerous cell would differ from the healthy ones. In the next few sub-sections, a review on diagnostics of some of the different types of cancer that has been explored using DEP are presented.

3.4.3.1 Circulating tumor cells

A typical cancerous tumor contains numerous cells harboring genetic mutations that drives them to grow, divide and invade the local tissue in which they are embedded[105]. As these cells proliferate, some of them slough off the edges of a tumor and are swept away by the bloodstream or lymphatic system forming the circulating tumor cells[105]. Circulating tumor cells (CTCs) released into the bloodstream from primary or metastatic tumors have high potential in cancer diagnostics[106]. However, the isolation of CTCs is a challenging task owing to the fact that CTCs can be very rare within the bloodstream and where they are always present, their low concentration is a big issue. Therefore, large volumes of fluids are usually required for analysis. Moreover, CTCs have to be kept viable and pure[107] in order not to hinder the use of CTCs for further biochemical or cell-based assays after isolation but this is a very herculean task. The viability and purity of the CTCs are essential Large variability in morphology and molecular functionalities is another bottleneck associated with CTCs isolation[106].

Despite these challenges, some researchers have attempted to isolate CTCs. Their methods utilized magnetic-labeled antibodies, quadruple magnetism, fluorescence activation, automated scanning fluorescence and PCR[108]. Unfortunately, these methods do not provide the unaltered, viable cells required for molecular analysis[108] hence, the application of dielectrophoresis is novel. Dielectrophoretic isolation of circulating tumor cells from peripheral blood was first demonstrated by Gascoyne et al.[109]. Their work synergized DEP, hydrodynamic lift and sedimentation forces to achieve cell segregation. Electric fields at or below 60 kHz were used to pull tumor cells, which were experiencing steric retardation

towards the interdigitated microelectrodes. CTCs are dependent on the stage of tumor but they are always present in very low concentrations. The isolated CTCs were viable and intact making it suitable for every type of post-separation analysis without the need for antibody or other labeling procedures[109]. Isolation efficiencies were >90% for small samples and decreased to 10% with increase in cell loading concentrations of 23×10^6 peripheral blood cells. It remains an important task to identify the clinically relevant number of cells that would be sufficient in isolating CTCs for a wide range of metastatic tumors.

3.4.3.2 Breast cancer

Breast cancer is one of the most common forms of cancer, with an incidence of about 1.1 million new cases and over 45,000 women dying from the disease each year[110]. One in eight women in the U.S. develop breast cancer in her lifetime[111]. Breast cancer originates in the epithelial cells of the breast organ. Most of the breast cancers begin in the cells that line the ducts (*ductal* cancers); some begin in the cells that line the lobules (*lobular* cancers), and the rest in other tissues. The lymph system is one of the ways in which breast cancers can spread. The lumps, called tumors are a massive erratic proliferation of the breast tissue cell growth[112]. Breast cancer produces malignant tumors[105, 107, 109]. Most common screening methods used are self and clinical breast exams, x-ray mammography, and breast magnetic resonance imaging (MRI).

Several researchers have explored dielectrophoretic characterization of biopsy samples from breast cancer patients on a lab-on-a-chip platform in the past[79, 113-115]. It is assumed that the capacitance of the cell membrane varies according to its size and compositions (such as cell surface proteins (antigens))[79]. Also, distinguishable differences at selective frequencies exist among many different types of cancer cells[17]. Extensive and validated studies have shown that different cell types, cells at various stages of maturation or proliferation, and diseased cells, exhibit characteristic DEP signatures associated with their morphology, cellular structures, and cell state[80]. Morphological alterations associated with membrane folding and ruffling, or the appearance of microvilli, can produce greater changes in the effective membrane capacitance. Such morphological changes often accompany changes in the physiological state and external environment of a cell and are events readily monitored by DEP[80]. The passive electrical conductivity of the membrane is another important dielectric parameter that can be sensitively monitored by DEP. This conductivity is negligibly small

for normal healthy cells, but can increase for diseased or dying cells[80].

Experiments have shown that DEP could distinguish viable from non-viable cells, making it a useful tool for monitoring malignancy progression before and after treatment[79]. It is believed that at specific electric field, distinguishable differences can be observed among different types of cancer cells derived from the same origin. For e.g., the specific membrane capacitance on breast cancer cells is over two times larger than that for Daudi cell line[79]. Studies also showed low membrane capacitance as a striking characteristic of malignant cell[79]. The differences observed in membrane capacitance lead to changes in cellular polarizability, which in turn result in varied DEP responses. Gascoyne *et al.* used a different set-up to retain human promyelocytic leukemic cells (HL-60) from peripheral blood, and to demonstrate that the dielectric properties of metastatic human breast cancer cell lines MDA-231 were significantly different from those of RBCs and T-lymphocytes. Thus, differences in dielectric properties were exploited to separate breast cancer cell lines from healthy cells[111].

In another recent study by Guido *et al.*, cellular mechanical properties and changes were evaluated for cancerous and non-cancerous cells by stretching the cells via DEP[116, 117]. Results showed that both kind of cells MCF-7 (human carcinoma cell line) and MCF-10A (epithelial cell line) were unambiguously distinguishable. Stretching experiments were conducted at 15 MHz and 6 V_{rms}. At this AC field condition, pDEP occurred, stretching the trapped cells between the two electrode edges. The strain response for non-cancerous cells was approximately 2.5 times stronger than the MCF-7 cells[117]. The non-cancerous cells appeared softer compared to the cancerous cells[117]. The differences in stretching behavior were attributed to the difference in the microtubule structures in the cytoskeleton[116]. For obtaining high throughput system for mechanical analysis of cells, the dielectrophoretic stretcher was further integrated into a microsystem which did not indicate any physical limitations[117].

3.4.3.3 Colorectal cancer

Colorectal cancer is the second most common cause of cancer death in U.S.[118]. Only 39% of the cases are diagnosed at a localized stage with the current screening methods compared to 61% for breast cancers[119]. Although, the current screening methods are effective to certain extent, compact microfluidic platforms could provide a new alternative for early detection.

One such microfluidic techniques, dielectrophoresis, was utilized to separate

human colorectal cancer cell line, HCT116 from human embryonic kidney 293 cells (HEK 293) and human *E. coli* bacterium[118]. Both HCT116 and HEK 293 are of 20 μm in diameter and are difficult to be distinguished under a microscope. Conventional AC DEP was utilized with two indium tin oxide (ITO) electrodes placed at the bottom of the channel. The cells experienced two different forces: (i) hydrodynamic forces, which drive the cells in the direction of flow and (ii) nDEP force that repels the cells in the direction perpendicular to the electrodes. The HCT116 cells experienced nDEP force in the frequency band of 1 Hz – 6 MHz and 31-75 MHz, whereas between 6-31 MHz, the cancer cells experienced pDEP force[118]. Maximum nDEP force was experienced by the cancer cells at 100 kHz. ~95% of the colorectal cancer cells were separated at an applied voltage of greater than 15 V. Approximately, 98% of the HCT116 cells were separated at a very low flow rate (<0.1μL/min) and the efficiency decreased at higher flow rates. This showed that DEP forces experienced by the cells are much larger than the hydrodynamic forces[118].

In another study by X. Xing *et al*., the cross over-frequency was first determined before a specific frequency range was adopted for the separation of colorectal cancer cells (HCT116) from blood lymphocyte using 3-D ring-array microelectrodes[120]. Employing the classical AC DEP technique, 300 sets of 40 μm-diameter rings, designed to be comparable in size to nucleated blood cells and fabricated through soft lithography and dry etching were self-aligned into a built-in flow chamber that cultivated a highly influential DEP force field. The crossover frequency was found near 25 kHz[120] . Above this frequency, between 35 and 100 kHz at 710 V_{pp}, the separation was carried out retaining the cancer cells under pDEP. Maximum recovery of the cancer cells was obtained at 100 kHz with average recovery of 81.86% at a flow rate of 0.1 mL/h. An average of 94.05% of the cancer cells were viable after separation[120].

3.4.3.4 Leukemia

Leukemia is a type of cancer of the blood or bone marrow characterized by abnormal increase of leukocytes. They are diagnosed visually by a blood test which involves more time [121]. An automatic blood cell counter to detect small density of leukemia cells in blood is required for early detection of leukemia.

Dielectrophoresis is an excellent technique that can be used to detect small density of leukemia cells in blood[121]. Human B-cell lymphotropic leukemia cell line (BALL-1) and human promyelocytic leukemia cell line (HL-60) were separated from healthy human

leukocytes. A creek-gap aluminum electrodes and AC electric field generated the required non-uniformity for separation of the cells. The cells were suspended in an isotonic medium containing 8.75% (w/v) sucrose solution with small amount of phosphate buffer saline salts. Leukemia cells experienced pDEP whereas healthy leukocytes exhibited nDEP. BALL-1 cells were separated from healthy leukocytes after 30 minutes of voltage application at 37 kHz and 14 V_{pp}. HL-60 cells and normal leukocytes were separated after 40 minutes of voltage application at 45 KHz and 14 V_{pp}[121]. An improvement in the microfluidic platform was desired due to some adherence of the cells on the glass surface in the microchannel[121].

In another study, HL-60 cells were successfully removed from peripheral blood by employing interdigitated electrode array[43]. Calculated cellular dielectric parameters showed that HL-60 cells experienced pDEP effects and healthy RBCs experienced nDEP effect which lead to trapping of HL-60 cells at 80 kHz[43]. Recent studies have allowed trapping of single K562 leukemia cells from healthy cells in novel structure based on microwells via nDEP for further manipulation, by forcing cell-cell interactions after capturing another cell in the same cage[63].

Human leukemia monocytes THP-1 were separated from MCF-7 breast cancer cells and MCF-10A healthy breast cells using a contactless DEP system[122]. A thin sheet of PDMS acts as an insulating barrier and separates the electrodes from the main channel. The insulating barrier exhibits a capacitive behavior and aids in generating an electric field in the main channel on applying AC voltage across them[122]. The electrodes are placed in the side channel in a highly conductive medium. At 85 kHz and 250 V_{rms}, both cancer cells were trapped experiencing pDEP. Translational velocity, rotational velocity, and pearl chaining were the DEP responses observed in this system. Pearl-chains were formed in both cancer cell lines at 85 kHz and 250 V_{rms}, whereas the rotational velocity was different for both types of cancer cell lines.

Human leukemia cells were trapped using a combination of DEP and environmental scanning electron microscopy (ESEM) to provide high-resolution analysis of individual non-adherent cells[123]. The microfluidic platform used consisted of a glass substrate that supports two independent sets of microelectrode arrays and a detachable PMMA chamber of height of approximately 2 mm. All leukemia cells were maintained in a full RPMI1640 medium at 37° C in a 5% CO_2 humidified atmosphere [123]. Cells were exposed to AC field for 90 to 110 minutes

at 12V, 20MHz in a low electrical conductivity (LEC) buffer. Using these techniques makes it more efficient for DEP-based immobilization of hematopoietic cells using ESEM imaging for better diagnosis of leukemia[123].

3.4.3.5 Melanoma

Melanoma, a type of skin cancer is the leading cause of skin disease death. Melanoma is currently detected by biopsy, which is painful and time involving. Sabuncu *et al.* successfully separated five B16F10 melanoma clones from blood based on the melanin content[124] via DEP. These melanoma cells were from the same origin but differed in their melanin content[124]. An increase in the percentage of melanin in cytoplasm may lead to a decrease in overall polarizability of the cell thus altering the DEP responses of the clones. This study can be further extended to separate malignant cells having different metastatic levels[124].

In another study, melanoma cell lines were manipulated by DEP gravitational field flow fractionation (FFF) technique[57]. Sorting of MDA-435 melanoma cells from RBCs was based on cell density, size, shape, and membrane electrical properties. Larger MDA-435 cells had higher membrane capacitance and dielectric polarization factors compared with healthy RBCs, thus yielding separation[57].

3.4.3.6 Oral cancer

Oral cancer, one of the ten most common cancers worldwide has seen a rise in the incidence over the past 40 years in young adults[125, 126]. Despite improved treatment methods, survival from OSCC remains poor as cancer is often detected at a later stage due to the lack of reliable tumor markers and morphological features of early stage cancer[125, 126]. It is mainly caused by tobacco and/or alcohol use, poor oral hygiene, poor diet, and possibly through sexually transmitted viral infection[16]. Treatment of oral cancers is ideally a multidisciplinary approach involving surgeons, radiation oncologists, chemotherapy oncologists, dental practitioners, nutritionists, and rehabilitation and restorative specialists[126]. Early detection of oral cancers may avoid other treatment procedures related to speech, facial prostheses, and chewing[126]. Currently, oral cancers are diagnosed through a combination of radiology, surgical biopsy, and pathological assessment of tissue samples based on the morphological and immunohistochemical characteristics[125].

Dielectrophoresis has been explored as a non-invasive technique for early detection

of oral cancer to distinguish or characterize human oral squamous cell carcinoma cell line H357 and human HPV-16 transformed keratinocyte cell line[16]. The mean radii of these cells were 9.1 µm and 7 µm respectively with a cytoplasmic conductivity of 0.3 and 0.45 S/m accordingly[16]. The normal HPV-16 cells were collected at a frequency range of 10 kHz-16 MHz whereas H357 carcinoma cells were collected at a frequency range of less than 5 kHz[16]. The collection of cells at different frequency ranges allows DEP to be used as an early-detection tool for oral cancer.

In another study by Mulhall *et al.*, cancerous, pre-cancerous, and normal cells were distinguished using cell electric properties[126]. Oral squamous cell carcinoma lines H357 and H157, along with pre-cancerous dysplastic oral keratinocyte cells and primary healthy oral keratinocyte cells were utilized to prove this proof-of-concept in a novel DEP-microwell electrode system. Cell's transition from healthy to diseased state is often associated with subsequent change in the electric properties of the cell, which can be used as a disease diagnostic electrophysiological markers[126]. The effective membrane capacitance (C_{EFF}) increases depending on the stage of the disease, which is a measure of membrane surface area, permittivity, and thickness. Higher values of C_{EFF} indicate more blebs, folds, ruffles, and microvilli in the cell membrane. This is consistent with the observations that increased membrane ruffling is characteristic of cancer cell phenotype and correlates with invasiveness. Cells with malignant phenotype have higher C_{EFF} and lower cytoplasmic conductivity compared to the cells with normal phenotype.

3.4.3.7 Prostate Cancer

Prostate cancer is the most common cancer among men (after skin cancer)[127]. More than 2 million men in the U.S. count themselves as prostate cancer survivors[127].
Detection of prostate cancer primarily relies on an abnormal digital rectal examination (DRE) and/or increased prostate specific antigen (PSA) levels. Measurement of PSA level helps in signaling the presence of prostate cancer and subsequent biopsy gives the extent of the disease[127].

However, this PSA test has not been reliable enough as 65–70% males with elevated PSA levels within 4–10 ng/ml generally reveal a negative biopsy result[128]. Sampling error and inefficiencies associated with trans-rectal ultrasound-guided biopsy of the prostate may also miss out some of the prostate cancer cells leading to false positive or negative result[128]. To

assist in the diagnosis of prostate cancer, DEP has been employed by several researchers. Huang's group, worked on the potency of DEP on the immunocapture of prostate cancer cell line (LNCaPs) from whole blood cell[127]. Immunocapture, the direct capture of an antibody spore on the surface of a small bead, has been a common method used in capturing cells with an efficiency of at least 62%[127]. The technique has the limitation or a tradeoff between high efficiency and high purity[127]. In the quest to improve the efficiency of the cell capture, Huang's group utilized a specially fabricated microdevice (Hele-Shaw flow-cell, Figure 3.5) to perform immunocapture of the LNCaPs.
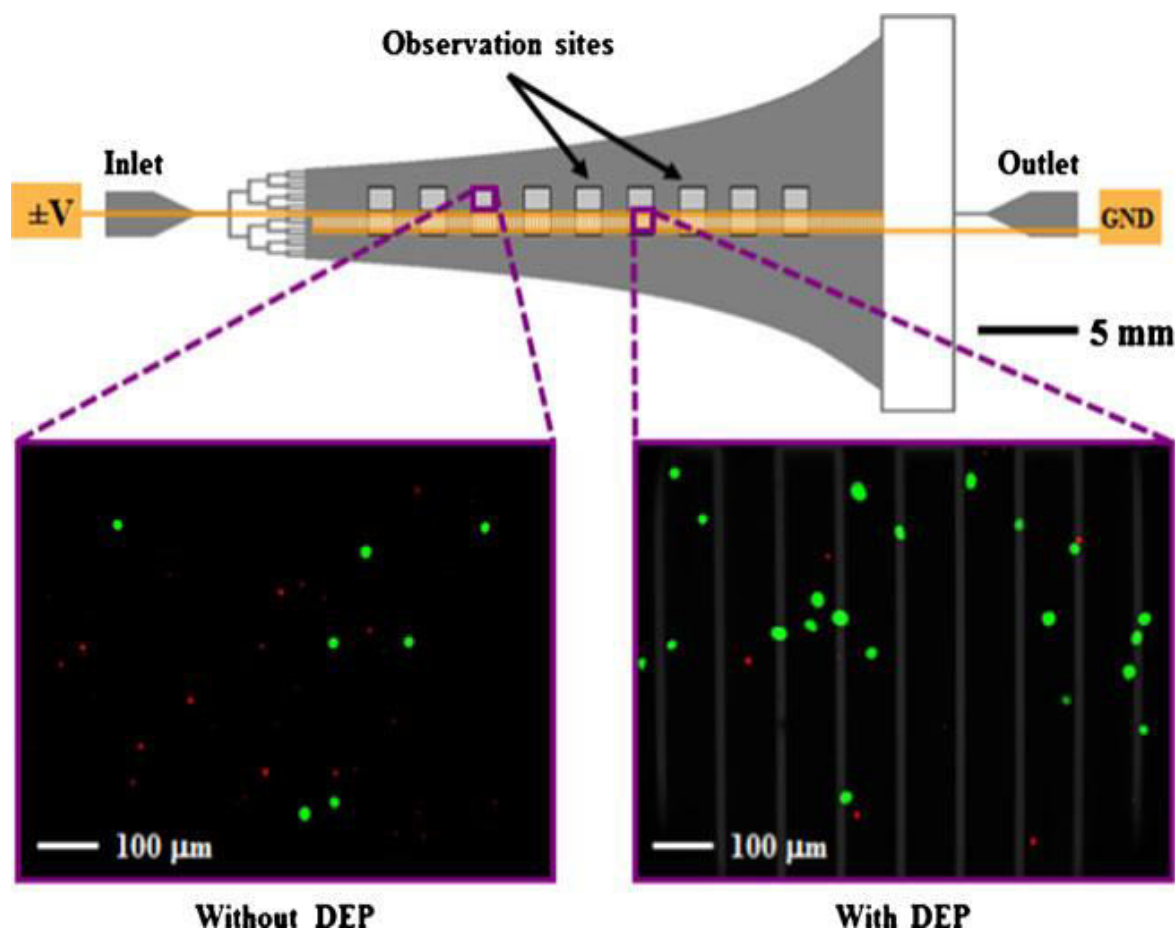
Figure 3.5.   Schematic of the Hele-Shaw flow cell and its interdigitated electrodes with lead connections to an applied voltage (±V) and ground (GND). Inset images show fluorescently labeled LNCaPs (*green*) and PBMCs (*red*) adhered to the antibody-functionalized surface with and without DEP effects[129] (Reprinted with permission from Springer).

The Hele-Shaw flow-cell is a device designed for characterizing cell adhesion as a function of shear stress: an important parameter used in optimizing microfluidic

immunocapture system. To compare the immunocapture performance with and without DEP, interdigitated array electrodes were fabricated along the length of the Hele-Shaw cell. When the electrodes were energized, both pDEP and nDEP responses of LNCaPs as a function of applied electric field frequency (10 kHz-10 MHz) were measured. Results showed that DEP can control capture performance by promoting or preventing cell interactions with immunocapture surfaces, depending on the sign and magnitude of the applied DEP force as well as on the local shear stress experienced by cells flowing in the device[127]. Using the same device, LNCaPs were also separated from peripheral blood mononuclear cells (PBMCs) at 6 Vpp, 350 KHz AC source where LNCaPs exhibited pDEP and PBMCs displayed nDEP characteristics[129].

In another study, contactless dielectrophoresis (cDEP) was used in studying the dielectrophoretic response of prostate tumor initiating cells (TICs)[130]. Using a 5 x 1 mm^2 microdevice fabricated through deep reactive ion etching (DRIE) process, the experiment was performed at 600 kHz, and 300 V$_{rms}$ AC conditions. At this electrical condition, the TICs were separated from non-TICs through pDEP[130].

Classical AC DEP application to prostate cancer was also studied by H. Jiang *et al* to separate prostate cancer (LNCaPs) cells from colorectal cancer (HCT116) cells[131]. The experiment was run using different conductivities of phosphate-buffered saline (PBS) solution. DEP spectra for the two cells were generated at a voltage range of 0-20 Vpp, 2.5 MHz. By comparing the spectra of LNCaP cell with that of HCT116 cell, the DEP force difference between LNCaP and HCT116 was largest at a medium conductivity of 300 μS/cm[131]. Between frequencies of 1 Hz - 20 MHz and 55 MHz - 70 MHz, LNCaP cells experienced nDEP, whereas between 20 MHz - 55 MHz and 70 MHz -100 MHz, they experienced pDEP force. HCT116 cells experienced nDEP force between 1 Hz – 2.5 MHz and 60 MHz – 100 MHz- 100 MHz, while pDEP was experienced between 2.5 MHz – 10 MHz. At 2.5 MHz, LNCaP cells experienced a stronger nDEP force while the DEP force acting on HCT116 cells was zero (i.e. 2.5 MHz was the cross-over frequency for HCT116 cells)[131]. Complete separation of both cells was observed at 12 V$_{pp}$ and 2.5 MHz.

3.4.3.8 Cervical Cancer

Cervical cancer has been one of the most common causes of cancer death for American women[15]. Risk factors for this disease have been identified as immunosuppression, chlamydia

infection, use of intrauterine device and diethylstilbestrol (DES). However, infection with Human papilloma virus (HPV) is considered the prime risk factor[15]. The American Cancer Society (ACS) estimated that, in 2015, about 12,900 new cases of invasive cervical cancer will be diagnosed and about 4,100 women will die from cervical cancer in U.S. alone[15]. But over the last 30 years, the cervical cancer death rate has gone down by more than 50% due to increased use of the Pap test: a simple, quick, and essentially painless screening test that involves the collection of cells from a woman's cervix and the subsequent evaluation for abnormalities (specifically for pre- cancerous and cancerous changes) under a high-tech microscope.

Even though pap test screening has contributed to sharp reductions in cervical cancer incidence and mortality throughout the developed world, it suffers from inadequate single-test sensitivity and frequent equivocal results have prompted searches for newer screening methods[132].
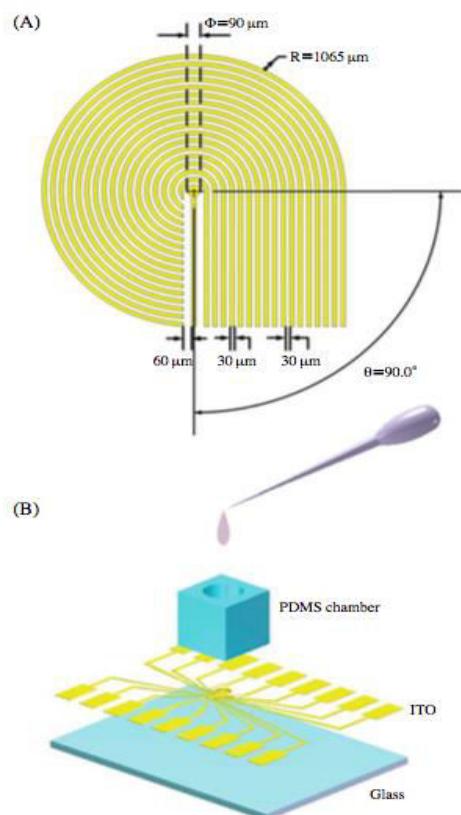
Figure 3.6   (A) Dimensions of the circular electrodes; (B) The schematic diagram of the microchip for concentrating cells utilizing dielectrophoresis in stepping electric fields[133] (Reproduced with permission from Springer)

With the advent of dielectrophoresis, human cervical carcinoma cells (HeLa cells) have been separated from normal RBCs by employing an open-top microdevice (Figure 3.6) fabricated through soft lithography and wet etching techniques[133]. Viable HeLa cells were suspended lysis buffer of electrical conductivity 10.66 μS/cm and permittivity, $\varepsilon_r = 78$. At 10 Vpp AC voltage and 1 MHz frequency, separation of HeLa cells from RBCs were noticed due to pDEP force experienced by the HeLa cells after a 20 second exposure to non-uniform field with recovery efficiency of 76 - 80%[133]. This area could be further explored especially now that the search for an alternative but smarter screening technique is ongoing.

3.3.3.9 Ovarian Cancer

Ovarian cancer is the sixth most common cancer worldwide[134]. The estimated annual incidence of epithelial ovarian cancer (EOC) is 225,500 with an estimated 140,200 deaths worldwide in 2008, consisting of 3.7% of all female cancers and 4.2% of cancer deaths[135]. In United States alone, it has been estimated that about 22, 280 women will receive a new diagnosis of ovarian cancer and about 14, 240 women will die from the disease in 2016[136]. Ovarian cancer causes more deaths than any other cancers of the female reproductive system[134]. Due to the inadequate screening tools and a lack of early clinical symptoms, ~70% of women with EOC are diagnosed with advanced stage of disease, which is associated with high morbidity and mortality[135].

A study by Salmanzadeh *et al.* investigated the DEP responses of mouse ovarian surface epithelial (MOSE) cells as they advance from benign to aggressive stages of ovarian cancer[137]. Four stages marked as early (MOSE-E), early intermediate (MOSE-E/I), intermediate (MOSE-I), and late (MOSE-L) were studied using contactless dielectrophoresis (cDEP).
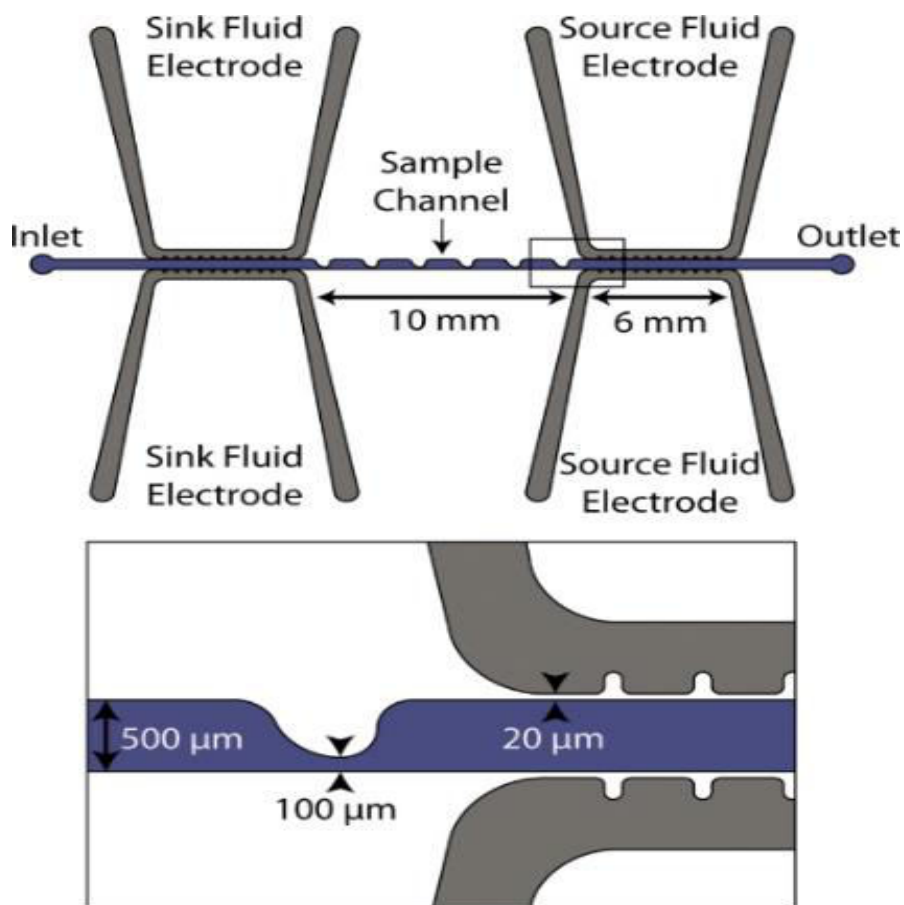
Figure 3.7   Schematic of a low frequency continuous sorting device. The sample channel runs left to right and is 500 μm wide with saw-tooth constrictions to 100 μm. The two pairs of fluidic electrode channels compose the source and sink electrodes, respectively, and are separated from the sample channels by a 20 μm think PDMS barrier[138] (Reproduced with permission from JoVE).

Using a mirrored groove-shaped microdevice (Figure 3.7), the ovarian cancer cells were isolated from peritoneal fluid [137] at frequency ranges 200-600 kHz and voltages between 50 and 250 V_{rms}. The electrical conductivity of sample was 10.56 μS/cm. Between 200 and 500 kHz, trapping of the cells was observed. The voltage required for complete trapping of MOSE-L was greater than that of MOSE-I but the reverse was noticed when the frequency was 600 KHz.

The same experimental procedure was repeated for sorting fibroblast (OP9) and macrophages (PC1)[137]. These two cells were believed to represent the normal and inflammatory cells found in the peritoneal fluid. Because these two cells displayed quite distinct DEP characteristics from MOSE cells, the authors believed that the ovarian cancer

cells would easily be separated from their surrounding peritoneal fluid if cDEP was employed. The average radii of MOSE-E, MOSE-E/I, MOSE-I, and MOSE-L cells were 7.19, 7.16, 7.29, and 7.05 μm respectively. The radii of PC1 macrophages and OP9 fibroblasts were 6.45 μm and 6.67 μm respectively[137, 138].

3.4.4 Dengue

Since 1950s, Dengue had been a worldwide problem[139]. Statistics reveals that as many as 400 million people are infected yearly with much prevalence in Puerto Rico, Latin America, Southeast Asia, and the Pacific Islands[139] .The disease, which is transmitted by the bite of a mosquito which in turn is infected with one of the four dengue virus serotypes, can be associated with life-threatening symptoms including bleeding and difficulty in breathing[140]. In Asia and Latin America, the disease is the leading cause of serious illness and death among children[140]. The absence of vaccine and specific medications for Dengue has left the world with no alternative but to prevent mosquito bite at all cost. This task is very herculean especially in tropical countries where mosquitoes usually breed as rapidly as possible. However, early diagnosis can forestall future complications and ensure the disease is well managed. However, the problem associated with current diagnostic methodologies may involve some laboratory-indeterminate cases[139]. For instance, a patient with suspected dengue infection at very late acute phase can be declared negative either by IgM Antibody Capture Enzyme-Linked Immunosorbent Assay (MAC-ELISA) or Reverse Transcription-Polymerase Chain Reaction (RT-PCR)[139] when the virus is at very low concentration.

Researchers in the dielectrophoresis arena have started looking into the application of DEP towards accurate diagnosis of Dengue even though reported research activities are still at the teething stage. Bashar Yafouz *et al*, recently reported the DEP spectra analyses and the associated determination of the crossover frequencies of normal and dengue-infected human hepatic fetal epithelial cells (WRL-68) using a microarray dot electrode[141]. The DEP forces applied to the cells were quantified by analyzing the light intensity shift within the electrode's dot region based on the cumulative modal intensity shift image analysis technique. The disparity between crossover frequencies of the healthy (220 kHz) and infected (140 kHz) WRL-68 cells in a suspending medium conductivity of 100 μS/cm, they believe, should allow direct characterization of these cell types by exploiting their electrophysiological properties[141]. This is a precursor to real-time separation of the healthy and dengue infected cells.

3.4.5   Anthrax

Anthrax is a serious infectious disease caused by soil-bound, gram positive, rod-shaped bacteria known as *Bacillus anthracis[140]*. The fact that the symptoms of this disease (pulmonary anthrax, for instance) largely intersect other common diseases like influenza, respiratory syncytial, diphtheria makes it more deadly if not diagnosed early and treated with an antibiotic. Current diagnostic activities depend on the type of anthrax suspected by the medical personnel[140]. While the observation of mediastinal widening or pleural effusion through CT scans can confirm the inhalation of anthrax, antibodies measurement, skin lesion swab, spinal fluid, and respiratory secretions can be obtained and tested for the form of anthrax i.e., cutaneous, gastrointestinal, or injection anthrax. However, a challenge might be posed in many areas of the world where these medical facilities might be unavailable. Having a portable and easy to use microelectromechanical device (MEMS) might help in the early and accurate diagnosis of these deadly pathogens.

The first work that attempted the use of dielectrophoresis for the sorting of Bacillus bacteria from their mixture in soil was reported by Fatoyinbo's group[142]. Therein, the dielectrophoretic isolation and concentration of a surrogate bacteria for *B. anthracis*, *B. globigii*, was studied[142]. *B. subtilis* has been known to simulate the behavior of *B. anthracis*, because they are able to resist desiccation, heat, and chemical treatment by forming tough spores[142]. Three different samples were used in the experiment: *B. subtilis* ATCC 9372, untreated *B. globigii* and treated *B. globigii* (lysophilized and pasteurized). Electrode geometry of a pin-type design was used for the determination of the crossover frequencies of the untreated (5 MHz) and treated (83 kHz) *B. globigii* variants at buffer conductivity of 0.3 mS/m. The crossover frequency for *B. subtilis* (ATCC 9372) in the same medium conductivity was found to be 1.4 MHz[142]. In the dielectrophoretic experimental phase, a mixture of $1.7 \, X \, 10^8$ particle per ml of diesel exhaust sample and $7.9 \, X \, 10^8$ spores per ml of treated B. globigii solution in 30ml ultra-pure water was used. Interdigitated microelectrodes were utilized for the isolation of the diesel particles from the mixture with the bacteria spores through positive dielectrophoresis. Percentage recovery was found to be a function of the flow rate of the inlet stream (99.25% and 98.70% for 0.51 ml/h and 4.08 ml/h respectively)[142]. These results are precursors for bio-sensing applications and further research is needed to explore the possibility of completely designing point-of-care diagnostic devices.

3.5   Conclusion

An extensive review of the latest medical diagnostic research findings utilizing dielectrophoresis has been done here. The application of DEP to disease diagnostics is a nascent field and has a lot of potentials to be employed in the development of point-of-care devices. DEP is completely label-free and non-destructive. Classical DEP relies on metal electrodes and AC field to create the spatial non-uniformity. Another recently developed DEP technique, called insulator dielectrophoresis (iDEP) utilizes DC field or DC biased AC field to create spatial non-uniformity employing insulated structures inside the microchannel. DEP has been used to separate live and dead cells, cancerous from healthy cells, and bacterial / viral infected cells from healthy cells. An early detection of some types of cancer and malaria has been possible as DEP depends on the dielectric and intrinsic properties of cells unlike electrophoresis, which depends on size to charge ratio of the cell. The cell's ability to conduct electric charges (conductivity) and to store electric charges (capacitance) can be measured by DEP.

Cells can be modeled mathematically using a single or double shell models depending on their structures. Ellipsoidal models are also available for cells like erythrocytes. Single shell models are based on a thin cell membrane, which can almost be neglected whereas double shell models do have a cell wall and cell interior.

So far, disease diagnostics using DEP was accomplished using cell lines. An improvement or a step-forward is the use of non-invasive samples like body fluids (e.g. human blood) in early disease detection remains unexplored. Using non-invasive samples would be safe, less harmful, and discomfort to the subject compared to the painful biopsies. Recent technological advancements have shown single cell analysis and cell fusion studies using dielectrophoresis, which can also be applied towards analyzing diseased cell interactions with healthy cells or single diseased cell analysis. Undoubtedly, dielectrophoretic microfluidic platform of disease diagnostics will generate a huge variety of new and exciting research for the betterment of human health.

DEP is dependent on the cell's morphology and physico-chemical properties, and the extent to which these subtle invisible differences can be distinguished by DEP is yet to be fully explored. Recent studies on studying the viscoelastic properties of the cells via dielectrophoresis has showed some promise in developing diagnostic tools for early detection

of diseases. However, the rewards for this effort to understand the complete power of DEP is valuable thus providing an opportunity to characterize the sub-populations of cellular phenotypes which is much needed in disease diagnostics.

The integration of dielectrophoretic elements into microfluidic or lab-on-a-chip system is becoming popular to perform complex cell processing and analysis tasks in a cost effective approach. This allows for minimal exposure of cells to personnel handling it, especially with the more sensitive cell types like the stem cells along with automatic operations and parallel processing of samples.

The next generation cell manipulation dielectrophoretic devices would possibly make use of a number of biochemical and biophysical properties unique to cancer cells that would be able to achieve high throughput and high capture rate, thus possibly detecting cancer at an early stage allowing sufficient time for diagnosis and treatment.

Most researchers utilize the single-shell dielectric model to describe erythrocytes while working towards obtaining their electrical properties either in their healthy states or parasitized forms. Exploring other shell models in erythrocytic characterizations might give a different insight into what is generally acclaimed at present. It is also commonplace to employ pDEP in an effort to obtain any unknown electrophysiological properties. AC-DEP is the most used DEP method for this purpose and this usually requires an initial fabrication of in-built electrode arrays. Future research efforts might need to look into the possibility of utilizing iDEP for the same purpose. This might not really require any complex fabrication. Coming up with simple designs that have adjustable electrode positions might be sufficient in generating the desired cell capture-frequency data. The limit of detection of DEP devices is a thing to consider during the design and fabrication processes.

If, truly, any DEP device would take its pride of place in disease diagnostics world, it would be essential for it to identify diseased conditions even at very low concentration of the particles of interest. Sample preparation is another factor that should be considered if DEP would be fully utilized in making diagnostic devices. For instance, malaria is caused by the disruption of red blood cells through Plasmodium falciparum, hence, a complete diagnostic device should incorporate a mechanism for separating the various components of the blood before the red blood cells are channeled to experience DEP force. The same goes for the Leukemia disease, which can be lymphocytic (affect only the lymphocytes) or myelogenous

(affecting myeloid cells). Myeloid cells give rise to red blood cells, white blood cells and platelet-producing cells. Diagnostic devices for Leukemia could be made to encompass pre-separator and micromixer. These are essential microfluidic components that assist in the preparation of the target particles for optimum DEP experience.

In coming up with novel point-of-care dielectrophoretic diagnostic devices, the incorporation of bio sensors might be essential. The optimal designs of these sensors would involve determining the required sensor metrics and achieving these metrics with minimum use of the available resources. While in certain applications, the best sensor performance in terms of signal-to-noise ratio (SNR) or dynamic range (DR) is desirable, in others, these metrics can be traded off with power, area and ease of design and implementation.

Most of the current applications of DEP to disease diagnostics seem to utilize AC-DEP. While this method has substantially paved way to the proof-of-concepts regarding the importance of DEP to disease diagnostics, it might be worthwhile to start considering other forms of DEP: iDEP, for instance. It is a known fact the level of sophistication in developed countries is far more advanced that the under-developed or the developing nations. Therefore, DEP experimentations in disease diagnostics should focus on low-voltage utilization so that end product (integrated portable diagnostic devices) could be easily powered by, say 9 V or 12V battery.

Another factor to consider is the operability of the end diagnostic devices when fully completed. Should the devices be disposable only (like testing strips) or be portable permanent instruments with disposable testing gadgets? Thorough consideration of the aforementioned suggestions might pave way for more attention to DEP applicability in disease diagnostics.

The list of diseases that have been tackled by DEP (Table 3.1) and those that are yet to be tackled by Dep (Table 2) are two important tables which should be thoroughly perused for some insights into future applications of DEP for disease diagnostics.

Table 3.1.   Selected diseases that have been tackled by DEP and the approaches used

Types of DEP	Electrode configuration	Target Particles	Buffer Conductivity	% Recovery	Voltage/Frequency
AC	Interdigitated	Malarial parasitized cells	20-55 mS/m	N/A	5Vpp,200kHz
AC	Spiral	Malarial parasitized cells	20-55 mS/m	N/A	3Vpp,2MHz
TWDEP	Spiral	Trypanosomes	16-60 mS/m,	N/A	2Vpp,140kHz
AC	Planar	Breast (MCF-7)	12.5 µS/cm	N/A	6Vrms, 15MHz
AC	3-D ring	Colorectal Cancer Cells (HCT-116)	100 µS/cm	81.86%	100 kHz,
iDEP	Planar	Leukemia Cells HL-60	N/A	N/A	85kHz, 250Vrms
AC	Interdigitated	Prostate cancer Cell line (LNCaPs)	300 µS/cm	N/A	12 Vpp, 2.5 MHz
cDEP	Planar	Ovarian surface epithelial cells (MOSE)	10.56 µS/cm	N/A	250 Vrms, 500 kHz (maximum)
AC	Planar	Human Cervical Carcinoma Cells (HeLa cells)	10.66 µS/cm	80%	10 Vpp, 1 MHz
AC	Pin-type	Bacillus globigii	10-60 mS/m	> 98%	10 Vpp, 1MHz
AC	Interdigitated	Circulating Tumor Cells (CTCs)	30 mS/m	90%(for small samples)	N/A, <60 kHz

Table 3.2.   Diseases of notifiable conditions to the world as at December 31st, 2015. Classification was based on Global Burden of Disease Regions used for

World Health Organization's CHOICE   N/A: Statistics not available

World Region	Tackled by DEP Diseases				Yet to be tackled by DEP Diseases			
	Communicable	Non-Communicable	Epidemic and Pandemic-prone	Tropical	Communicable	Non-Communicable	Epidemic and Pandemic-prone	Tropical
Africa	Malaria	Cancer (breast, cervical, colorectal, prostate)	N/A	Human African Trypanosomiasis	Tuberculosis HIV/AIDS	Cardiovascular diseases, Chronic Respiratory Diseases Noma	Cholera Ebola Marburg Influenza Lassa a fever	Buruli Ulcer Lymphatic filariasis Helminthiasis Trachoma Onchocerciasis
Eastern Mediterranean	Malaria	N/A	N/A/	N/A	Poliomyelitis Tuberculosis HIV/AIDS Hapatitis MERS	N/A	N/A	N/A
Europe	N/A	Cancer (prostate, breast, cervical ovarian)	N/A	N/A	Cholera,	Ischemic heart disease, Cerebrovascular disease, Chronic Obstructive Pulmonary Disease (COPD) Influenza Asthma Liver Cirrhosis Diabetes	N/A	N/A
Americas	Malaria, Anthrax Dengue	N/A	N/A	N/A	Cholera, Gonorrhea, Urinary Tract Infections, Tuberculosis, Syphilis, Hepatitis, HIV, Varicella, Botulism, Brucellosis, Pertusis, Small pox, Zika Babesiosis,	N/A	N/A	N/A
West Pacific	Malaria Dengue	Cancer(breast, cervical, colorectal, prostate)	N/A	N/A	Tuberculosis, HIV, Hepatitis	Diabetes Chronic Respiratory Dieseas	SARS, Avian Influenza	Schistosomiasis Filariasis Helminthiases Echinococcosis
South-East Asia	Malaria	N/A	N/A	N/A	HIV, Tuberculosis	N/A	Cholera, Influenza	N/A

References

1.   C. D. Chin, V. Linder and S. K. Sia, *Lab on a Chip*, 2007, **7**, 3-10.

2.   S. S. Saliterman, *Fundamentals of BioMEMS and Medical Microdevices*, SPIE- The International Society for Optical Engineering, 2006.

3.   A. J. Tüdos, G. A. J. Besselink and R. B. M. Schasfoort, *Lab on a Chip*, 2001, **1**, 83-95.

4.   P. R. C. Gascoyne and J. V. Vykoukal, *Proc. IEEE*, 2004, **92**, 22-42.

5.   S. K. Sia and L. J. Kricka, *Lab Chip*, 2008, **8**, 1982-1983.

6.   K. Ohno, K. Tachikawa and A. Manz, *Electrophoresis*, 2008, **29**, 4443-4453.

7.   G. M. Whitesides, *Journal*, 2006, **442**, 368-373.

8.   J. H. Kang and J.-K. Park, *Asia Pacific Biotech News*, 2005, **9**, 1135-1146.

9.   D. R. Walt, *Science*, 2005, **308**, 217-219.

10.   J. Voldman, *Annual Review of Biomedical Engineering*, 2006, **8**, 425-454.

11.   C. H. Kua, Y. C. Lam, C. Yang and K. Youcef-Toumi, *Review of bio-particle manipulation using dielectrophoresis*, Singapore-MIT Alliance, 2005.

12.   H. A. Pohl, *Dielectrophoresis the behavior of neutral matter in nonuniform electric fields*, Cambridge University Press, Cambridge, 1978.

13.   B. H. Lapizco-Encinas and M. Rito-Palomares, *Electrophoresis*, 2007, **28**, 4521-4538.

14.   G. A. N. Ulrich Zimmermann, 2006.

15.   I.-F. Cheng, H.-C. Chang, D. Hou and H.-C. Chang, *Biomicrofluidics*, 2007, **1**, 1-15.

16.   L. M. Broche, N. Bhadal, M. P. Lewis, S. Porter, M. P. Hughes and F. H. Labeed, *Oral Oncology*, 2007, **43**, 199-203.

17.   P. R. C. Gascoyne, X.-B. Wang, Y. Huang and F. F. Becker, *IEEE Trans. Ind. Appl.*, 1997, **33**, 670-678.

18.   F.-B. Hsiao, C.-P. Jen, H.-Y. Chen, H.-L. Hsu, Y.-C. Lee, C.-H. Chuang and C.-H. Wang, Sanya, China, 2008.

19.   P. Gascoyne, R. Pethig, J. Satayavivad, F. F. Becker and M. Ruchirawat, *Biochimica et Biophysica Acta (BBA) - Biomembranes*, 1997, **1323**, 240-252.

20.   H. Shafiee, M. B. Sano, E. A. Henslee, J. L. Caldwell and R. V. Davalos, *Lab Chip*, 2010, **10**, 438-445.

21.   S. K. Srivastava, P. R. Daggolu, S. Burgess and A. R. Minerick, *Electrophoresis*, 2008, **29**, 5033-5046.

22.   M. Borgatti, L. Altomare, M. Baruffa, E. Fabbri, G. Breveglieri, G. Feriotto, N. Manaresi, G. Medoro, A. Romani, M. Tartagni, R. Gambari and R. Guerrieri, *International journal of molecular medicine*, 2005, **15**, 913-920.

23.   Y.-K. Cho, S. Kim, K. Lee, C. Park, J.-G. Lee and C. Ko, *Electrophoresis*, 2009, **30**, 3153-3159.

24.   M. Koklu, S. Park, S. D. Pillai and A. Beskok, *Biomicrofluidics*, 2010, **4**, 1-15.

25.   B. H. Lapizco-Encinas, B. A. Simmons, E. B. Cummings and Y. Fintschenko, *Electrophoresis*, 2004, **25**, 1695-1704.

26.   B. H. Lapizco-Encinas, B. A. Simmons, E. B. Cummings and Y. Fintschenko, *Anal. Chem.*, 2004, **76**, 1571-1579.

27.   M. P. Hughes, *Electrophoresis*, 2002, **23**, 2569-2582.

28.   S. K. Srivastava, J. L. Baylon-Cardiel, B. H. Lapizco-Encinas and A. R. Minerick, *J. Chromatogr. A*, 2011, **1218**, 1780-1789.

29.   M. Washizu and O. Kurosawa, *IEEE Trans. Ind. Appl.*, 1990, **26**, 1165-1172.

30.   D. J. G. Bakewell, M. P. Hughes, J. J. Milner and H. Morgan, 1998.

31.   C. L. Asbury, A. H. Diercks and G. v. d. Engh, *Electrophoresis*, 2002, **23**, 2658-2666.

32.   H. Morgan and N. G. Green, *J. Electrostat.*, 1997, **42**, 279-293.

33.   M. P. Hughes, H. Morgan, F. J. Rixon, J. P. H. Burt and R. Pethig, *Biochim Biophys Acta.*, 1998, **1425**, 119-126.

34.   B. H. Lapizco-Encinas, B. A. Simmons, E. B. Cummings and Y. Fintschenko, California, USA, 2003.

35.   R. W. Clarke, S. S. White, D. Zhou, L. Ying and D. Klenerman, *Angew. Chem. Int. Ed.*, 2005, **44**, 3747-3750.

36.   B. H. Lapizco-Encinas, S. Ozuna-Chacon and M. Rito-Palomares, *J. Chromatogr. A*, 2008, **1206**, 45-51.

37.   R. Pethig, A. Menachery, S. Pells and P. D. Sousa, *Journal of Biomedicine and Biotechnology*, 2010, **2010**, 1-7.

38.   I. Turcu and C. M. Lucaciu, *Journal of Physics A: Mathematical and General*, 1989, **22**, 985.

39.   Y. Feldman, I. Ermolina and Y. Hayashi, *IEEE Transactions on Dielectrics and Electrical Insulation*, 2003, **10**, 728-753.

40.   E. Gheorghiu, *Annals of the New York Academy of Sciences*, 2006, **873**, 262-268.

41.   D. Vrinceanu and E. Gheorghiu, *Bioelectrochemistry and Bioenergetics* 1996, **40**, 167.

42.   E. Gheorghiu and K. Asami, *Bioelectrochemistry and Bioenergetics*, 1998, **45**, 139-143.

43.   F. F. Becker, X.-B. Wang, Y. Huang, R. Pethig, J. Vykoukal and P. R. C. Gascoyne, *Journal of Physics D: Applied Physics* 1994, **27**, 2659-2662.

44.   V. Raicu, G. Raicu and G. Turcu, *Biochimica et Biophysica Acta (BBA) - Bioenergetics*, 1996, **1274**, 143-148.

45.   Y. Hayashi and et al., *Journal of Physics D: Applied Physics*, 2003, **36**, 369.

46.   M. Sancho, G. Martínez and C. Martín, *Journal of Electrostatics*, 2003, **57**, 143-156.

47.   K. Asami, Y. Takahashi and S. Takashima, *Biochimica et Biophysica Acta (BBA) - Molecular Cell Research*, 1989, **1010**, 49-55.

48.   A. Irimajiri, T. Hanai and A. Inouye, *Journal of Theoretical Biology*, 1979, **78**, 251-269.

49.   B. J. Kirby, *Micro- and Nanoscale Fluid Mechanics: Transport in Microfluidic Devices*, Cambridge University Press, Cambridge, 2010.

50.   K. M. Leonard and A. R. Minerick, *Electrophoresis*, 2011, **32**, 2512-2522.

51.   R. D. Miller and T. B. Jones, *Biophysical Journal*, 1993, **64**, 1588-1595.

52.   R. Pethig, G.H. Markx, *Trends Biotechnol.*, 1997, **15**, 426-432.

53.   S. Srivastava, A. Gencoglu and A. Minerick, *Anal. Bioanal. Chem.*, 2011, **399**, 301-321.

54.   A. Gencoglu and A. R. Minerick, *Lab Chip*, 2009, **9**, 1866-1873.

55.   S. Choi and J.-K. Park, *Lab on a Chip*, 2005, **5**, 1161-1167.

56.   R. Pethig, Y. Huang, X.-B. Wang and J. P. H. Burt, *Journal of Physics D: Applied Physics*, 1992, **25**, 881-888.

57.   J. Yang, Y. Huang, X.-B. Wang, F. F. Becker and P. R. C. Gascoyne, *Anal Chem*, 1999, **71**, 911-918.

58.   P. Pham, I. Texier, A.-S. Larrea, R. Blanc, F. Revol-Cavalier, H. Grateau and F. Perraut, *Journal of Electrostatics*, 2007, **65**, 511-520.

59.   Y. Huang and R. Pethig, *Measurement Science and Technology journal*, 1991, **2**, 1142-1146.

60. F. F. Becker, X.-B. Wang, Y. Huang, R. Pethig, J. Vykoukal and P. R. C. Gascoyne, *Journal of Physics D: Applied Physics*, 1995, **27**, 2659-2662.

61. T. Sun, H. Morgan and N. G. Green, 2008.

62. C. Zhang, K. Khoshmanesh, A. Mitchell and K. Kalantar-zadeh, *Anal Bioanal Chem*, 2010, **396**, 401-420.

63. M. Bocchi, M. Lombardini, A. Faenza, L. Rambelli, L. Giulianelli, N. Pecorari and R. Guerrieri, *Biosensors and Bioelectronics*, 2009, **24**, 1177-1183.

64. C.-P. Jen, H.-H. Chang, C.-T. Huang and K.-H. Chen, *Microsyst Technol*, 2012, **18**, 1887-1896.

65. A. Menachery, C. Kremer, P. E. Wong, A. Carlsson, S. L. Neale, M. P. Barrett and J. M. Cooper, *Sci. Rep.*, 2012, **2**.

66. E. B. Cummings and A. K. Singh, *Anal. Chem.*, 2003, **75**, 4724-4731.

67. K. H. Kang, Y. Kang, X. Xuan and D. Li, *Electrophoresis*, 2006, **27**, 694-702.

68. S. K. Srivastava, K. M. Leonard, S. C. Burgess and A. R. Minerick, Boston, MA, 2008.

69. Y. Kang, D. Li, S. A. Kalams and J. E. Eid, *Biomed. Microdevices*, 2008, **10**, 243-249.

70. J. Zhu, T.-R. J. Tzeng and X. Xuan, *Electrophoresis*, 2010, **31**, 1382-1388.

71. I. Barbulovic-Nad, X. Xuan, J. S. H. Lee and D. Li, *Lab Chip*, 2006, **6**, 274-279.

72. K. P. Chen, J. R. Pacheco, M. A. Hayes and S. J. R. Staton, *Electrophoresis*, 2009, **30**, 1441-1448.

73. L. Zhang, J. Bastemeijer, J. Mollinger and A. Bossche, presented in part at the Proceedings of the 3rd IEEE Int. Conf. on Nano/Micro Engineered and Molecular Systems, Sanya, China, Jan 6-9, 2008.

74. J. Zhu and X. Xuan, *J. Colloid Interface Sci.*, 2009, **340**, 285-290.

75. B. H. Lapizco-Encinas, R. V. Davalos, B. A. Simmons, E. B. Cummings and Y. Fintschenko, *J. Microbiol. Meth.*, 2005, **62**, 317-326.

76. R. C. Gallo-Villanueva, C. E. R. g.-L. pez, R. I. Diaz-de-la-Garza, C. Reyes-Betanzo and B. H. Lapizco-Encinas, *Electrophoresis*, 2009, **30**, 4195-4205.

77. S. Mohr and C.-C. Liew, *Trends in Molecular Medicine*, 2007, **13**, 422-432.

78. P. Sharma, N. S. Sahni, R. Tibshirani, P. Skaane, P. Urdal, H. Berghagen, M. Jensen, L. Kristiansen, C. Moen, P. Sharma, A. Zaka, J. Arnes, T. Sauer, L. A. Akslen, E. Schlichting, A.-L. Børresen-Dale and A. Lönneborg, *Breast Cancer Research*, 2005, **7**, R634-R644.

79. E. G. Cen, C. Dalton, Y. Li, S. Adamia, L. M. Pilarski and K. V. I. S. Kaler, *Journal of Microbiological Methods*, 2004, **58**, 387-401.

80. R. Pethig, R. S. Lee and M. S. Talary, *Journal of the association for laboratory automation*, 2004, **9**, 324-330.

81. L. Wu, L.-Y. L. Yung and K.-M. Lim, *Biomicrofluidics*, 2012, **6**, 014113.

82. X. An and N. Mohandas, *Transfusion Clinique et Biologique*, 2010, **17**, 197-199.

83. Malaria: Fact Sheet, http://www.who.int/mediacentre/factsheets/fs094/en/).

84. X. A. Narla Mohandas, *Med Microbiol Immunol*, 2012, **201**, 593-598.

85. G. B. Nash, E. O. Brien, E.C. Gordon-Smith, J. A. Dormandy, *Blood*, 1989, **74**, 855-861.

86. R. Suwanarusk, Brian M. Cooke, Arjen M. Dondorp, Kamolrat Silamut, Jetsumon Sattabongkot, Nicholas J. White, Rachanee Udomsangpetch, *Journal of Infectious Diseases*, 2004, **189**, 190-194.

87. H. Kagiwada, Chikashi Nakamura, Takanori Kihara, Hideki Kamiishi, Keiko Kawano, Noriyuki Nakamura, Jum Miyake, *Cytoskeleton*, 2010, **67**, 496-503.

88. P. Gascoyne, J. Satayavivad and M. Ruchirawat, *Acta Tropica*, 2004, **89**, 357-369.

89.   P. Gascoyne, C. Mahidol, M. Ruchirawat, J. Satayavivad, P. Watcharasit and F. F. Becker, *Lab Chip*, 2002, **2**, 70-75.

90.   T. M. Madigan, J. M. Martinko and J. Parker, *Brock Biology of Microorganisms*, Prentice Hall, New Jersey, United Stated of America, Tenth edn., 2003.

91.   S. P. Aidley DJ, *Cambridge, UK*, 1996, **Cambridge University Press**.

92.   J. L. Oschman, *Energy Medicine: The Scientific Basis.*, 2000.

93.   R. A. Charman, *Clayton's Electrotherapy*, 1996, **London, UK: WB Saunders Companys Ltd**.

94.   G. Brown, 1999, **New York,** .

95.   J. P. Reilly, *Springer*, 1998.

96.   F. W. Cope, *Physiolo Chemic Phys*, 1978, **10**, 465-468.

97.   C. D. Cone, *Oncology*, 1970, 438-470.

98.   C. D. Cone, *CRC Press*, 1985, **Boca Raton, Florida**.

99.   J. C. Cure, *Resonant*, 1991, **1**.

100.   W. S. Seeger P. G., *Gesamtherstellung: Neuwieder Verlagsgesellschaft mbH*, 1990.

101.   S. G. Haltiwanger, *Second International Congress of BioEnergetic Medicine. Iinstitute of Quantum and Molecular MEdicine*, 1998.

102.   O. J. L., *Churchill Livingstone, Edinburgh, England.*, 2000.

103.   B. K. Soper S.A., Ellington A. Frazier B., Garcia-Manero G., Gau V. Gutman S. I., Hayes D. F., Korte B., Landers J. L. Larson D., Ligler F., Majumdar A., Mascini M., Nolte D., Rosenzweig Z, Wang J, Wilson D., *Biosensor and Bioelectornics*, 2006, **21**, 1932-1942.

104.   M. G. H. Pethig R., *Trends Biotechnol*, 1997, **15**, 426-432.

105. S. C. P. Williams, *Proceedings of the National Academy of Science of the United States of America*, 2013, **110**, 4861.

106. J. D. Toonder, *Lab on a Chip*, 2011, **11**, 375-377.

107. S.-B. Huang, W. Min-Hsien, Y.-H. Lin, C.-H. Hsieh, C.-L. Yang, H.-C. Lin, C.-P. Tseng and G.-B. Lee, *Lab on a chip*, 2013, **13**, 1371-1383.

108. N. M. Karabacak, P. S. Spuhler, F. Fachin, E. J. Lim, V. Pai, E. Ozkumur, J. M. MArtel, N. Kojic, K. SMith, P. Chen, J. Yang, H. Hwang, B. Morgan, J. Trautwein, T. A. Barber, S. L. Stott, S. Maheswaran, R. Kapur, D. A. Haber, M. Toner, *Nat Protoc.*, 2014, **9**, 496-710.

109. P. R. C. Gascoyne, J. Noshari, T. J. Anderson and F. F. Becker, *Electrophoresis*, 2009, **30**, 1388-1398.

110. D. M. Parkin, F. Bray, J. Ferlay and P. Pisani, *A Cancer Journal for Clinicians*, 2005, **55**, 74-108.

111. F. F. Becker, X.-B. Wang, Y. Huang, R. Pethig, J. Vykoukal and P. R. C. Gascoyne, *Proc. Natl. Acad. Sci.*, 1995, **92**, 860-864.

112. J. Rosenberg, Y. L. Chia, S. Plevritis, *Breast Cancer Research and Treatment*, 2005, **89**, 47-54.

113. R. Pethig, *Biomicrofluidics*, 2010, **4**, 1-35.

114. J. Kononen, L. Bubendorf, A. Kallionimeni, M. Bärlund, P. Schraml, S. Leighton, J. Torhorst, M. J. Mihatsch, G. Sauter and O.-P. Kallionimeni, *Nature Medicine*, 1998, **4**, 844-847.

115. R.-Z. Lin, C.-T. Ho, C.-H. Liu and H.-Y. Chang, *Biotechnology Journal*, 2006, **1**, 949-957.

116. I. Guido, M. Jaeger and C. Duschl, *European Biophysics Journal*, 2011, **40**, 281-288.

117. I. Guido, C. Xiong, M. S. Jaeger and C. Duschl, *Microelectronic Engineering*, 2012, **97**, 379-382.

118. F. Yang, X. Yang, H. Jiang, P. Bulkhaults, P. Wood, W. Hrushesky and G. Wang, *Biomicrofluidics*, 2010, **4**, 1-13.

119. M. Han, C. T. Liew, H. Zhang, S. Chao, R. Zheng, K. ThyeYip, Z.-Y. Song, H. Li, X. P. Geng, L. X. Zhu, J.-J. Lin, K. W. Marshall and C. C. Liew, *Clin. Cancer Res.*, 2008, **14**, 455-460.

120. R. Y. C. P. Xiaoxing Xing, Cesar S.C.Wong, Levent Yobas, *Biosensors and Bioelectronics*, 2014, **61**, 434-442.

121. H. Imasato and T. Yamakawa, 2010.

122. H. Shafiee, J. L. Caldwell, M. B. Sano and R. V. Davalos, *Biomed. Microdevices*, 2009, **11**, 997-1006.

123. A. J. Khoshmanesh K, Nahavandi S, Kalantar-sazdeh K, Baratchi S, Williams DE, Cooper JM, Wlodkowic D, *Anal Chem.*, 2011, **83**, 3217-3221.

124. A. C. Sabuncu, J. A. Liu, S. J. Beebe and A. Beskok, *Biomicrofluidics*, 2010, **4**, 1-7.

125. L. Yang, L. Arias, T. Lane, M. Yancey and J. Mamouni, *Analytical and Bioanalytical Chemistry*, 2011, **399**, 1823-1833.

126. H. Mulhall, F. Labeed, B. Kazmi, D. Costea, M. Hughes and M. Lewis, *Analytical and Bioanalytical Chemistry*, 2011, **401**, 2455-2463.

127. C. Huang, Steven M. Santana, He Liu, Neil H. Bander, Benjamin G. Hawkins, Brian J. Kirby, *Electrophoresis*, 2013, DOI: 10.1002/elps.201300242.

128. S. A. Yasushi Nakai, Masaomi Kuwada, Makito Mikaye, Yoshitomo Chihara, Nobumichi Tanaka, Akihide Hirayame, Katsunori Yoshida, Yoshihiko Hirao and Kiyohide Fujimoto, *Biomedical Central*, 2014, **14**, 1471-1490.

129. H. L. Chao Huang, Neil H. Bander, Brian J. Kirby, *Biomedical Microdevices*, 2013, **15**.

130. L. R. Alireza Salmanzadeh, Hadi Shafiee, Roberto C. Gallo-Villanueva, Mark A. Stremler, Scott D. Cramer, Rafael V. Davalos, *Lab on a chip*, 2012, **12**, 182-189.

131. X. Y. Fang Yang, Hong Jiang, William M. Butler, Guiren Wang, *Technology in Cancer Reserach and Treatment*, 2013, **12**.

132. M. Safaeian, Mark E. Sherman, *Journal of National Cancer Institute*, 2013, **105**, 1524-1529.

133. G.-H. Chen, Ching-Te Hunag, Hsin-Hui Wu, Tatyana N. Zamay, Anna S. Zamay, Chun-Ping Jen, *Biochip*, 2014, **8**, 67-74.

134. Y. Huang, S. Joo, M. Duhon, M. Heller, B. Wallace and X. Xu, *Analytical Chemistry*, 2002, **74**, 3362-3371.

135. C. C. Sun, Pedro T. Ramirez, Diane C. Bodurka, *Nature Clinical Practice Oncology*, 2007, **4**, 18-29.

136. Key Statistics about ovarian cancer, http://www.cancer.org/cancer/ovariancancer/detailedguide/ovarian-cancer-key-statistics).

137. H. K. Alreza Salmanzadeh, Michael B. Sano, Paul C. Roberts, Eva M. Schmelz, Rafael V. Davalos, *Biomicrofluidics*, 2012, **6**, 1932-.

138. A. S. Elizabeth S. Elvington, Mark A. Stremier, Fafael V. Davalos, *Journal of Visualized Experiments*, 2013, **79**.

139. Dengue, http://www.cdc.gov/dengue/).

140. Anthrax, http://www.cdc.gov/anthrax/).

141. B. Yafouz, Nahrizul Adib Kadri, Hussin Rothan, Fatimah Ibrahim, *Electrophoresis*, 2015, DOI: 10.1002/elps.201500282.

142. H. O. Fatoyinbo, Michael P. Hughes, Stacey P. MArtin, Paul PAshby, Fatima H. Labeed, *Journal of Environmental Monitoring*, 2007, DOI: 10.1039/b614556f, 87-90.

CHAPTER 4

APPLICATION OF DIELECTROPHORESIS FOR THE DIAGNOSTICS OF BABESIOSIS

The extensive review of the diseases that have been tackled by dielectrophoresis (as given in chapter three) enabled the identification of other deadly diseases that have not been tackled. One of these yet-to-be-tackled diseases is Babesiosis: a disease that affects the red blood cells through the internalization of the pathogen called *Babesia*. This chapter, therefore, presents the whole research efforts at identifying any red blood cell that has been infected with this pathogen. There are three major parts in the chapter: simulation of the dielectrophoretic separation using COMSOL Multiphysics software, fabrication of microdevice through soft lithography as well as experimentation and validation. Future works and directions on this project are given in the next chapter.

4.1   Introduction

Babesia species are tick-borne, tick-transmitted apicomplexan haemoprotozoan parasites that are the etiologic agents of Babesiosis, in animals and humans. *Babesia* species have recently emerged as a growing public health concern for humans, primarily in the United States. The initial U.S. case of human Babesiosis was first reported from California in 1966[1]. Since then, there has been a substantial growth in reported cases made to the Centre for Disease Control and Prevention (CDC). Babesiosis is now among the Nationally Notifiable Infectious Conditions. In 2013, the National Surveillance conducted in 27 States reported 1,762 cases[2] with the Northeast and Upper Midwest regions as the most endemic[3, 4]. *Babesia* species are naturally transmitted to humans and other mammals through the bite of infected ixodid ticks (Figure 4.1)[5]. The size of the ixodid tick can vary depending on the sex of the tick and feeding state. Approximately the size of a sesame seed, a female adult ixodid tick measures about 2.7 mm in length[6]. The males are smaller. These ticks are orange-brown in color but may change to be rust or brown-red in hue following feeding. The body becomes engorged after a meal and may expand considerably. Ixodid ticks are present throughout the majority of the eastern United States and tend to live in wooded areas and along trails in forests[6]. Ixodid ticks also reside on the tips of grass and leaves along these trails, enabling them to crawl directly onto the skin or fur of a passing host[6].

When the tick transfers *Babesia* pathogen into human, the infection produces a spectrum of diseases that can range from asymptomatic to severe, life-threatening illnesses[1]. In immunocompetent patients with their spleens intact, infection may be asymptomatic[1].

Figure 4.1   Image of ixodid tick: the vector that carries *Babesia* pathogen. The tick also carries *Borrelia*-the pathogen that causes Lyme diseases.

Symptoms like fever, headache, chills, drenching sweats, myalgia, malaise, and hemolytic anemia usually appear within one to nine weeks after infection[7]. In infants, elderly, asplenic and immunocompromised patients, infections can be life-threatening[8]. Usually, resultant complications in these populations include hemodynamic instability, acute respiratory distress, severe hemolysis, disseminated intravascular coagulation, renal dysfunction, hepatic compromise, myocardial infarction, and death[8]. Some patients who apparently resolve infections based on symptoms, via self-cure or chemotherapy, can permanently maintain low level parasitemia[9], which is often very difficult to detect, even by the state-of-art sensitive real-time PCR assays[10, 11].

These asymptomatic, chronically infected persons, therefore, are probably, the main source of secondary transmission of *Babesia* i.e. by blood transfusion[3]. Issues related to secondary transmission of *Babesia* are of major medical importance to blood collection organizations, test manufacturers, and the FDA[12]. As of today, a variety of interventions have been made to prevent the transmission of pathogenic agents by blood donation or transfusion. Some of the most common interventions adopted are discussed here. One such screening

technique is based on indirect immunofluorescent antibody (IFA) testing[12]; a method that detects both IgM (immunoglobulin M) and IgG antibodies in *Babesia*-infected RBCs[13, 14]. The presence of IgG antibodies is an indication of present or past infections, including those in which the infection may have cleared[13]. IFA requires microscopy skills, specific training, and access to a fluorescence microscope, which is practical for some reference laboratories but not a technique amenable to routine high-throughput use and practice by non-specialists, [15] although it displays high sensitivity, specificity, and reproducibility[13].

Another screening technique to prevent secondary transmission of the protozoan is by mere completing a set of questionnaires at blood donation centers to trace any history of Babesiosis. According to the standard issued by the American Association of Blood Banks (AABB), donors, who report any previous Babesia infection, are usually prevented from donating blood[16]. Unfortunately, querying donors about any previous *Babesia* infection has been shown to be largely ineffective at reducing transmission risk[17] owing to the fact that most donors who transmit infection are asymptomatic and unaware of any *Babesia* infection. Currently, there seems to be no licensed blood screening tests available or under development that could be employed to interdict the transfusion or donation of *Babesia*-infected blood[12].

In the detection of *Babesia* parasite, peripheral blood smear has been widely used[18]. This method is only useful at the acute stage of infection when the parasitemia levels are at their highest[2, 5]. At the chronic phase of infection, detection is rarely observed on blood smears due to the low percentage of parasitized erythrocytes (PPE). In contrast to peripheral blood smears, PCR assay is considered more sensitive for detecting the presence of the parasites in both acute infections[19, 20] and, to a lesser extent, chronic *Babesia* infections. However, parasitemia diminishes with time and detection by PCR is difficult after about 2 months[9]. EIA/enzyme-linked immunosorbent assay (ELISA), which uses recombinant antigens has also been developed[3, 21] but the time frame needed to obtain the results of the test is considerably substantial. The afore-mentioned shortcomings depict a dire need for better blood screening methodologies especially at donation centers.

A notable observation during the asexual growth cycle of *Babesia* parasites in a natural host, is the attachment, penetration, and internalization of the host RBCs by *Babesia's* extracellular merozoites[1, 7]. After internalizing the host RBC, they asexually multiply and come out of the RBC by rupturing it. The invasion causes ridge formation on the surface of the RBCs

as well as modification to the adhesive, mechanical, structural, and functional properties of the RBCs[22]. It is hypothesized that these invasions affect the electrophysiological properties of the infected RBCs. This is based on the reported fact that the invasion of RBCs by *Plasmodium falciparum* (a closely-related Apicomplexan-Aconoidasidaic protozoan pathogen) affected the electrophysiological properties of the Plasmodium-infected RBCs[23].

For this reason, the difference in the dielectric properties between the infected and healthy RBCs could be utilized to ensure their dielectrophoretic separation. Among many microfluidic techniques available to manipulate cells, dielectrophoresis (DEP) has been proven to sort cells based on the subtle differences observed in their electrical properties.

DEP, a non-destructive electrokinetic transport technique, manipulates cells by creating non-uniformity in the electric field in the microchannel. Aside manipulation, the tool has also been used for the separation and detection of bioparticles (particles of biological materials)[24-26]. Traditional (classical) DEP uses embedded microelectrodes positioned in a spatially non-uniform manner to achieve particle separation, trapping, and focusing by applying AC electric fields to induce motion[24-26]. However, challenges with bubble formation due to electrolysis, electrode fouling and delamination, sample contamination, and decaying electric field as the distance from the electrode surface progresses, were major factors that led to the introduction of insulator-based DEP (iDEP)[24].

In iDEP (also called DC-DEP or electrodeless DEP), electrodes are placed far outside the channel (in inlet and outlet ports, Fig. 4.5) in order to mitigate fouling and other disadvantages of classical DEP. Several researchers have applied iDEP to successfully achieve their set targets[25]. However, as of current state-of-art, this is the first research that is being reported to use iDEP in separating *Babesia*-infected RBCs within a homogenous sample containing healthy RBCs too.

In this novel work, it is demonstrated for the first time that when a mixture of *Babesia*-infected RBCs and healthy RBCs are subjected to non-uniform electric fields in a microchannel embedded with insulated saw-tooth shaped obstacles, they can be substantially concentrated and separated. The results obtained therefrom demonstrate the potency of iDEP microfluidic platform as an electrokinetic portable point-of-care tool for screening donors' blood for possible protozoan infections (i.e. Babesiosis in this research) at donation centers where there is a significant need. Utilizing iDEP technology in concentrating *Babesia* infected RBCs could

also generate the high parasitemia desired in preliminary research works on microbial attenuation; one of the steps in the development of vaccine.

4.2   Simulation of dielectrophoretic separation

Simulation of the trajectories or motion of both the healthy and infected RBCs was done using COMSOL Multiphysics 5.0 (COMSOL Inc. Burlington, M.A. USA) commercial software package. The essence of simulation was to optimize the geometry of the iDEP-based microdevice as well as the operating voltage that would be sufficient to generate the appropriate non-uniform electric field gradient such that the cells experience varying dielectrophoretic forces based on their electrophysiological properties. The data used for the infected RBCs in the simulation were obtained for Plasmodium falciparum (the etiologic agent for malaria in human) due to the fact that both *Babesia* and *Plasmodium* have been studied to show very similar characteristics with respect to pathogenesis and clinical course[27]. The boundary conditions were based on the non-uniformity caused by the electric field gradient within the channel and the channel wall was assumed as insulated.

Table 4.1   The electrophysiological properties used in simulating the trajectories of healthy and Babesia-infect RBCs. [*: calculated   ** source: [28]   *** source: [29]]

Zeta potential of cell**	-15.0 mV
Interior conductivity of uninfected cell***	0.31 S.m^{-1}
Interior conductivity of infected cell***	1.0 S.m^{-1}
Conductivity of medium	0.052 S.m^{-1}
Radius of RBC**	3.5 µm
Zeta potential of PDMS**	-50 mV
DEP mobility of uninfected cell*	$2.02e-17\ m^4/v^2.s$
DEP mobility of infected cell*	$2.80e-17\ m^4/v^2.s$
Viscosity of the suspending medium	0.001Pa.s
Dielectric constant	70
Permittivity of Vacuum	$8.854e-12\ A^2.s^4.kg^{-1}m^{-3}$

Flow dynamics of the suspended cells were modeled using the Navier-Stokes and continuity equations while assuming incompressible creeping flow and no slip boundary

conditions. The density of water (1000 kg/m^3) and viscosity (0.001 Pa*s) were also used because the buffer was assumed to have conditions similar to water (at ambient temperature) but for its pH and conductivity. Electric field regime combined the generalized Ohms law with the Gauss' law and continuity equation to handle the stationary electric current in conductive media. The transport of dilute species (healthy and infected RBCs) was also accounted for using the mass conversation equation. Fluid flow (Eq. 4.1-4.5), mass transport (Eq. 4.6) and electric flow fields (Eq. 4.7) were solved separately and the interface condition was matched up iteratively to get the solutions.

Below are the subdomain equations used in simulating the trajectories of the RBCs;

Momentum balance: $\qquad \nabla.\left[-pI + \eta(\nabla.u + (\nabla u)^T)\right] + F = 0$ $\qquad\qquad$ (4.1)

Continuity equation: $\qquad \rho\nabla.(u) = 0$ $\qquad\qquad\qquad\qquad\qquad\qquad\qquad$ (4.2)

Electro-osmotic velocity: $\quad u_{EO} = \mu_{EO}E = -\dfrac{\varepsilon_0\varepsilon_m\zeta_s}{\mu}E$ $\qquad\qquad\qquad$ (4.3)

Electrophoretic velocity: $\quad u_{EP} = \mu_{EP}E = \dfrac{\varepsilon_0\varepsilon_m\zeta_p}{\mu}E$ $\qquad\qquad\qquad$ (4.4)

Dielectrophoretic velocity: $\quad u_{DEP} = \mu_{DEP}\nabla E^2$ $\qquad\qquad\qquad\qquad$ (4.5)

Transport of dilute species: $\quad \nabla.(-D_i\nabla C_i + uC_i) = 0$ $\qquad\qquad\qquad$ (4.6)

Electric current: $\qquad\qquad \nabla.J = 0$ $\qquad\qquad\qquad\qquad\qquad\qquad\qquad$ (4.7)

where J is the current density (A/m^2), p is pressure (N/m^2), η is the viscosity (Pa.s) and F represents the body forces present in the channel; u is velocity (m/s), u_{EO}, u_{EP}, u_{DEP} are respectively electroosmotic, electrophoretic and dielectrophoretic mobilities. E is the electric field, D_i is the diffusion coefficient of species i, C_i is the concentration of species i, and $\varepsilon_0, \varepsilon_m, \zeta_p, \zeta_m$ are the permittivity of the vacuum, permittivity of the medium, zeta potentials of the particle and zeta potential of the medium respectively.

Based on the observation from the simulation, a new geometry for the microfluidic device was sequentially designed until the efficiency of continuous separation of the RBCs was observed.
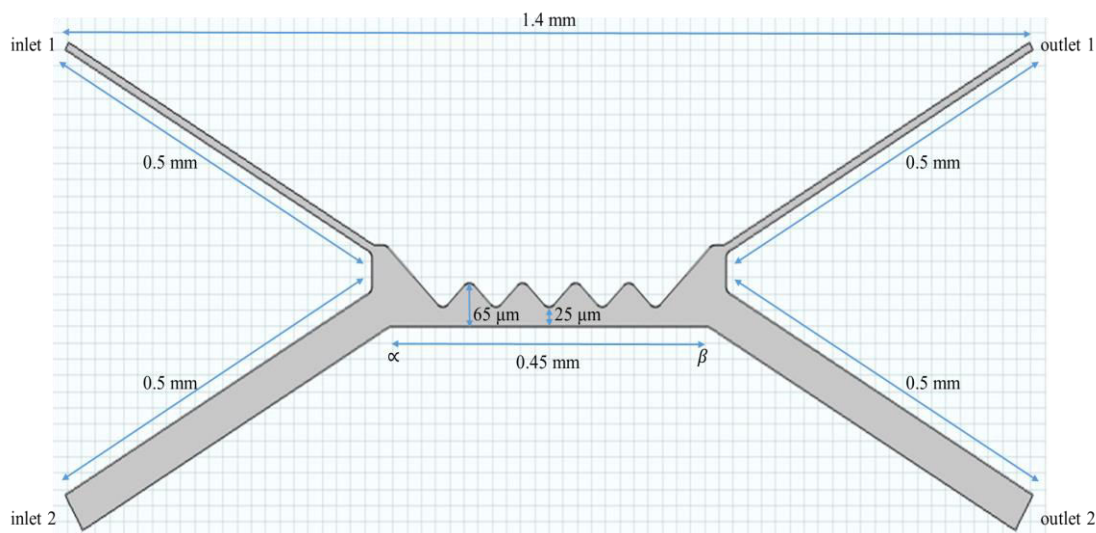
Figure 4.2 The schematic representation of the microdevice with two inlet and two-outlet ports. The entire device is about 1.4 mm long with embedded saw-tooth geometry to create non-uniformity in the electric field.

The geometry of the 1.4 mm microdevice is as shown in Figure 4.2. It consists of two inlet and two outlet arms each of which measures 0.5 mm long. The insulating region is made up of an array of hurdles, which are slightly trimmed at the tip to prevent complete cell trapping and as well provide the appropriate electric field strength for generating the negative dielectrophoretic force required for sorting the cells. The length $|\propto\beta|$ represents the length of the hurdle region. The distance 25 μm between the peak of the hurdle and surface of the length $|\propto\beta|$ was set to make the cells experience adequate dielectrophoretic force.

4.3   Experimental Materials and Methods
4.3.1   Fabrication of microdevice

A silicon wafer (fabricated by Trianja Technologies Inc., TX, USA) with a pattern made through wet etching was used to cast the Polydimethylsiloxane (PDMS) device platform. The etched silicon wafer referred here as the master had 35 identical designs per chip.
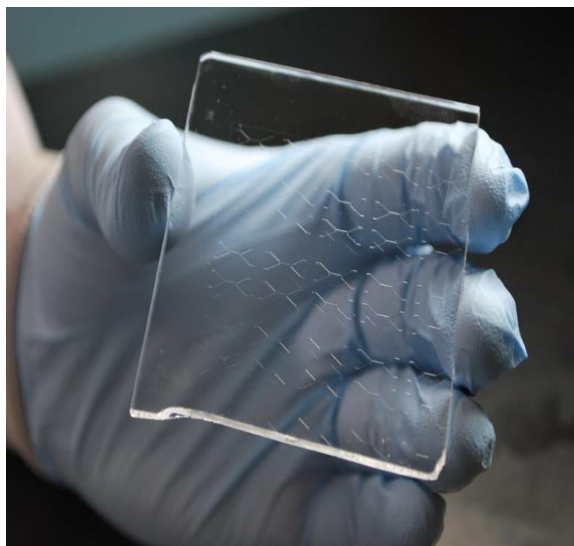
Figure 4.3   The image of the commercially fabricated master (mold) used in the rapid prototyping phase.

Rapid prototyping using the commercially fabricated master was initiated by mixing PDMS monomer (sylgard 184 silicon elastomer base) and a curing agent (sylgard 184 silicon elastomer curing agent) in 10:1 w/w ratio followed by degassing the mixture using Dekker Vacuum Pump/Degassing set-up for about 20 minutes. The air bubble-free PDMS slurry mixture was poured onto the master, which was contained in a 10 cm polystyrene Petri dish. The polymer was cured in (Blue M) automated oven at 80 °C for one hour, and then peeled off from the master. The master was leveled during the curing process so as to minimize any geometrical variations. Peeled PDMS devices with indented channels were punched with a 3 mm Miltex biopsy puncher to obtain the ports / reservoirs for the inlet and outlet channels. The device was then cut and fitted onto a 0.17 mm thick Corning borosilicate micro cover glass (size 24 mm X 40 mm). The PDMS was finally exposed to plasma treatment by the use of Harrick PDC-32G plasma cleaner/sterilizer at 300 mTorr for 1-minute to irreversible bonding of the PDMS to the clean cover slide and sealing the microchannel. The plasma treatment also ensured microdevice hydrophilicity generation, due to which external devices were not required to pump in the samples into the microchannel. The sealed device (i.e. PDMS together with the cover slip) was placed in a petri dish with channels filled with deionized water to maintain its hydrophilicity for certain period (usually 48 hours). Plasma-treated PDMS is usually kept is de-ionized water to avoid direct and rapid re-oxidation of the PDMS

microchannel surface. Re-oxidizing the PDMS treated surface would prevent fluid from fluid through the channel since the re-oxidized surface is hydrophobic in nature.

4.3.2 Cell Culturing and Preparation

4.3.2.1 Cell Culturing

The in vitro culturing technique for Mo7 strain of *Babesia bovis* involved cultivating *B. bovis* infected erythrocytes in a microaerophilous phase (MASP) using 24 well suspension plates, at 10 % (v/v) packed cell volume (PCV), and incubated at 37 °C in a 5% CO_2 in air humidified atmosphere. Cultures were maintained in M-199 culture medium (Gibco, 22340020) supplemented with 50 μg/ml gentamycin (Gibco, 15710-049), 1% (v/v) fungizone (Gibco, 15290-026), 20 mM N-Tris(Hydroxymethyl)Methyl-2-aminoethane sulfonic acid (Sigma-Aldrich, T5691) and 40 % (v/v) bovine serum. Subcultivation was performed by splitting/dilution with fresh normal bovine erythrocytes and M-199 medium when the achieved parasitemia levels were about 2-3%. Parasitemia was monitored by microscopic examination of Giemsa stained thin smears under a 100X microscope oil objective. The method described above was as specified by Michael G. Levy and Miodrag Ristic group [30] and the whole culturing was done at the United State Department of Agriculture Laboratory, Washington State University, Pullman, WA.

4.3.2.2 Experimental Cell-Sample Preparation

Fifty (50) g/ml dextrose buffer solution was prepared by dissolving 25 g of dextrose crystalline solids (weighed with 204 Mettler Electronic Weighing Balance) in 50 ml de-ionized water. The conductivity and pH of the medium (buffer) were measured to be 0.052 S/m and 7.04 respectively using Accumet XL 200 Ph/mV/conductivity meter. Within the confinement of a 1300 Series A2 Bio-Safety Cabinet, 1μL of the cell sample centrifuged at 1500 rpm for 5-minutes was measured and transferred into a 1 ml micro test-tube containing 600 μL low-conductivity freshly prepared buffer. The buffer was of low-conductivity to minimize any possible heat generation that could lyse the RBCs during their exposure to DC voltages.

4.3.3 Experimental Set up

The experimental set-up consists of an integration of the LabSmith HVS448 high voltage sequencer with an IX71 Olympus inverted microscope as shown in Figure 4.5. The

microdevice, mounted on the IX71 Olympus inverted microscope was entirely filled with the low conductivity dextrose medium and 0.008" diameter pure platinum electrodes were inserted into the inlet and outlet reservoirs as means of electrical connections. At the inlet channel 1 (Figure 4.2), the buffer solution was removed and replaced with a mixture of healthy and infected-RBCs (5.5 % PPE) suspended in the dextrose medium. Having ensured no pressure head (i.e. no cells were moving out of the inlet channel under the influence of pressure), DC voltages were applied using HVS448 high voltage sequencer. Inlet 1 and 2 (Figure 4.5) were connected to the same voltage source (10 V) while the outlet 2 was connected to the ground (0 V). The voltage at outlet 1 (Figure 4.4) was manual varied from 5.5-6.5 V to visualize the trajectories of the cells within the microchannel. Sequential sorting of the cells was observed and appropriate images captured.
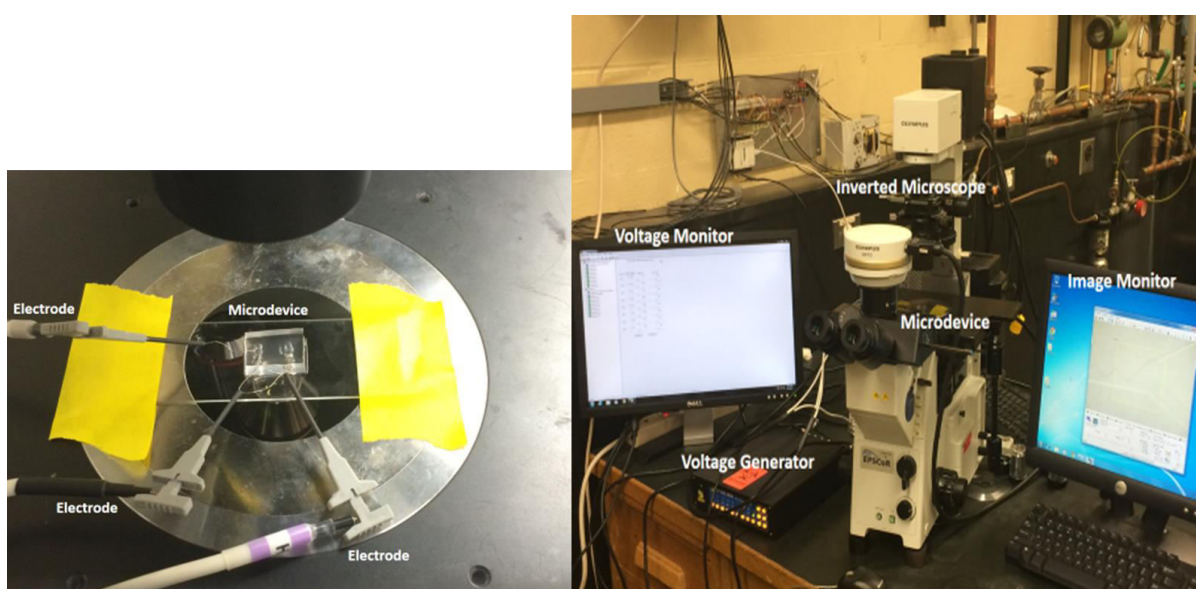
Figure 4.4   The photograph of the experimental set-up showing how the electrodes are connected to the inlet and outlet ports.

The experiment was conducted in two phases: pre-separation staining (before introducing the sample into microchannel) and post-separation staining stage (after the experimental run- at the outlet ports). The pre-separation staining was done in order to track the trajectory of the *Babesia*-infected RBCs while the post-separation experiments were done to aid the visualization of the *Babesia* pathogen inside the RBCs. In the first phase, cell samples were tagged to express green fluorescent protein (GFP) (only infected RBCs got tagged owing

to the presence of *Babesia* cells within the healthy RBCs) and experimented for optimal detection of the traditional fluorescein isothiocyanate (FITC). This pre-separation staining method enabled the visualization of the green-labeled *Babesia* nucleus as the infected RBCs migrated within the iDEP-based microchannel. In the second phase (post-separation staining phase), microscopic examinations were carried out under bright field by staining the separated cells at the outlet ports. Separated RBCs in each of the outlet ports were stained with 3-stage Siemens diff quik stain kit set to visualize the corresponding proportions of healthy and *Babesia*-infected RBCs. The stain set consists of three (3) solutions. Solution 1 (1.8 mg/L Triarylmethane Dye in methyl alcohol) is a fixative which stabilizes cellular components. Solution 2 (1g/L Xanthen Dye, buffer and sodium azide) and solution 3 [1.25g/liter Thiazine dye mixture; (0.625g/L Azure A, and 0.625 g/L Methylene blue), and buffer] are for cell staining. The resultant staining of nucleoli and cytoplasm is due to the methylene blue component of the mixture. The nuclei are stained purple by the azure component of the dye mixture because DNA is believed to be capable of functioning as a chromotrope for Azure A, B and methylene violet. After the staining process, the cells were visualized and counted under the microscope. The PPE were calculated at both outlet ports. The whole process was followed for each of the three samples (8.0 %, 6.0 %, and 5.5 %PPE).
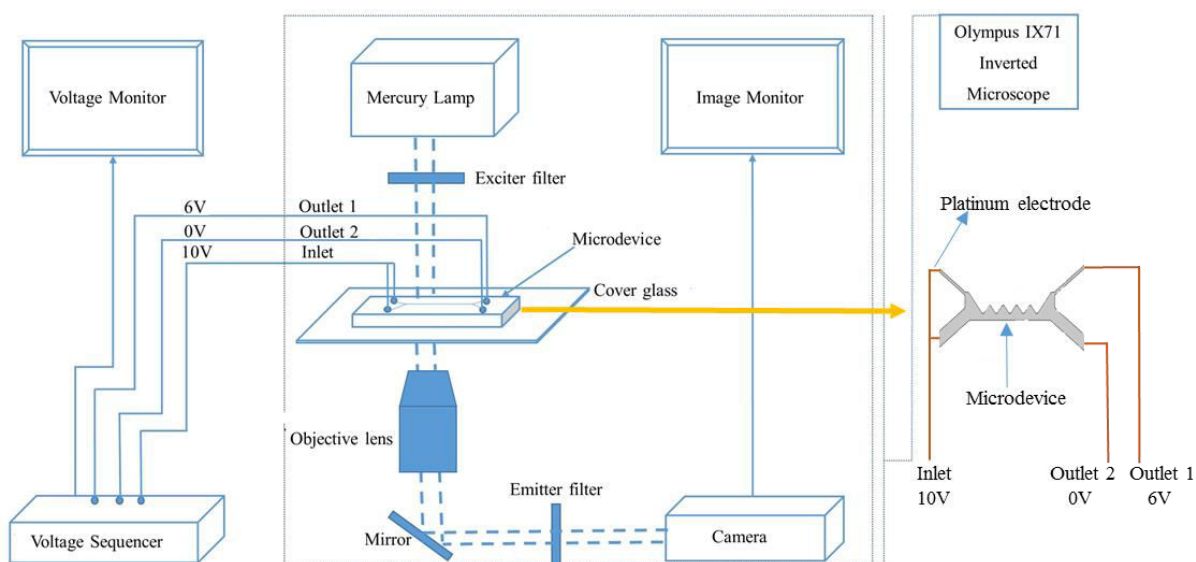

Figure 4.5   The schematic diagram of the experimental set-up showing the integration of the voltage sequencer with the Olympus IX71 Inverted Microscope.

4.4   Results and Discussion

The application of iDEP to concentrate and sort biological cells is not only about seeing the cells move to different destinations after experiencing DEP force. It goes further to observing and counting the cells at such destinations. This section shows the results obtained from both simulation and experiment and further provides insights as to how the two result streams compare.

4.4.1   Computational results

The governing equations (Eqs. 4.1-4.7) were solved for fluid flow, mass transport and electric field using COMSOL Multiphysics v5.1. In order to have an effective dielectrophoretic force, the simulation was made by considering both electrophoretic and electro-osmotic flows (electrokinetic flow). The balance between electrophoretic and electroosmotic flows moved the cells forwards to the hurdle regions where the dielectrophoretic force was acting. Figure 4.6A shows the surface velocity magnitude of the flow within the microchannel. The fluid velocity at the channel wall at a given period of time is sufficiently low. The fluid flow is, thus, at sufficient pace to enable the suspended erythrocytes to experience the dielectrophoretic force that separate them according to their inherent dielectric properties.

The applied potential difference between the inlet and the two separate outlet ports was swept to determine the optimum DC voltage range necessary for the dielectrophoretic separation. At low voltage (below 6.2 V) the generated electric field strength was not sufficient to effect the separation of the cells. As seen in Figure 4.6B, both healthy (red) and infected erythrocytes (blue) moved into the same port after passing through the insulating hurdles. In Figure 4.6C, the applied voltage, 6.2 V, was adequate to make the erythrocytes experience the desired DEP force. At voltage beyond this sorting voltage, the potential to move into the upper right-hand outlet channel was so high that all cells, healthy and infected, were drawn into it (Figure 4.6D).
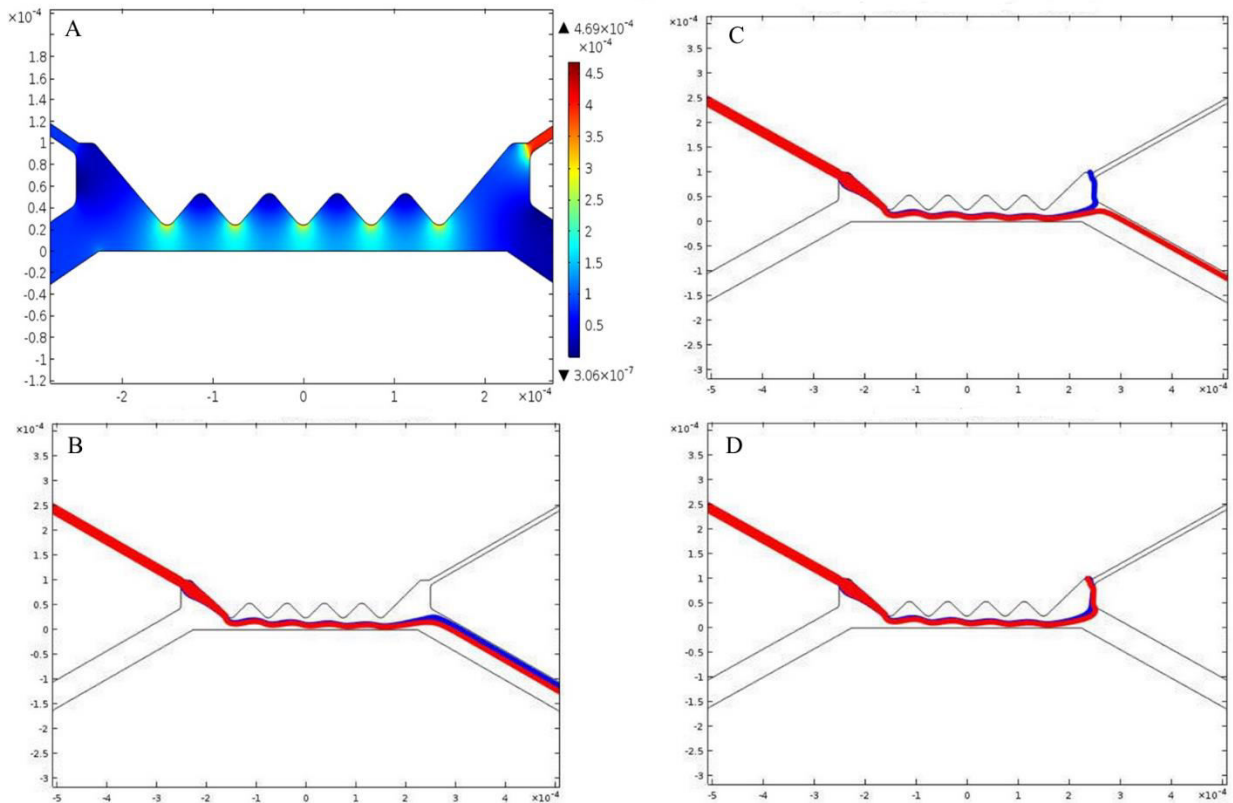
Figure 4.6 Computation velocity and particle flux due to the channel geometry and applied DC voltage. (A) Surface velocity magnitude within the microchannel. (B) Total flux of erythrocytes at the pre-separation stage (at voltage below 6.2 V) (C) Total flux of erythrocytes at the separation stage (at 6.2 V) (D) Total flux of erythrocytes at the post-separation stage (at voltage beyond 6.2 V). Red-color flux represents the healthy (normal) erythrocytes while the blue-color flux depicts the *Babesia*-infected erythrocytes.

4.4.2   Experimental validation of the sorting voltage

The dependence of iDEP force on cell size, field gradient, cell, and medium conductivities was leveraged by varying only the field gradient (since it is a function of the applied voltage). Manually changing the applied voltage, therefore, from 5.5 to 6.5 V enabled the identification of the exact range of non-uniform electric field gradient necessary for the separation between healthy and *Babesia*-infected RBCs population (Table 4.2). Before 5.9 V and after 6.1 V, it can be said that the associated field strength was not sufficient for the cells to experience the required iDEP force since other factors (cell size, cell and medium conductivities) on which the dielectrophoretic force depends, have been fixed. The application

of 5.9-6.1 V DC occasioned the desired separation even though, at this time, the number of infected RBCs in each port had not yet been ascertained. However, backflow, which might have resulted from dipole re-orientation, was observed at different periods. Therefore, experiment run time was fixed at 50 s with the inlet-outlet 10-6/0 V (Figure 4.5) configurations to ensure maximum separation of cells.

Table 4.2: Effects of voltage sweep (in volts) on the direction of flux using dextrose buffer of conductivity 0.052 s/m. (No separation indicates that both healthy and infected RBCs were moving to the same outlet port).

PPE of the inlet sample = 5%, inlet voltage = 10V and Outlet voltage 1 = 0V

Outlet 2 (volts)	Sorting	Backflow (sec)	Outlet 2 (volts)	Sorting	Backflow (sec)
5.5	No separation	0	6.1	Cells Separated	44
5.6	No separation	0	6.2	No separation	0
5.7	No separation	0	6.3	No separation	0
5.8	No separation	0	6.4	No separation	0
5.9	Cells Separated	41	6.5	No separation	0
6	Cells Separated	53			

4.4.3   Optical validation

The optical examination of the post separation outlet-ports contents at the inlet-outlet voltage configuration of 10-6/0V is presented here. The images were captured for both fluorescence and bright-field microscopic regimes.

4.4.3.1   Fluorescence

To ascertain the directional influx of the healthy and infected cells into their different ports (from the simulation results in Figure 4.6C), fluorescence microscopy with green-fluorescent-protein (GFP) pre-separation labeling, was employed (Section 4.3.3). It was easy to trace the direction of movement of the *Babesia*-infected erythrocytes from the color they emitted. The post-separation image examination from the pictures obtained during the experimental runs revealed that the labeled cell populations were indeed *Babesia*-infected erythrocytes due to the observed green colors, which were highly concentrated in the outlet

port 1 (Figure 4.7A). Some green-colored cells were seen in outlet-port 2 and this indicated that the separation was not total (Figure 4.7B).
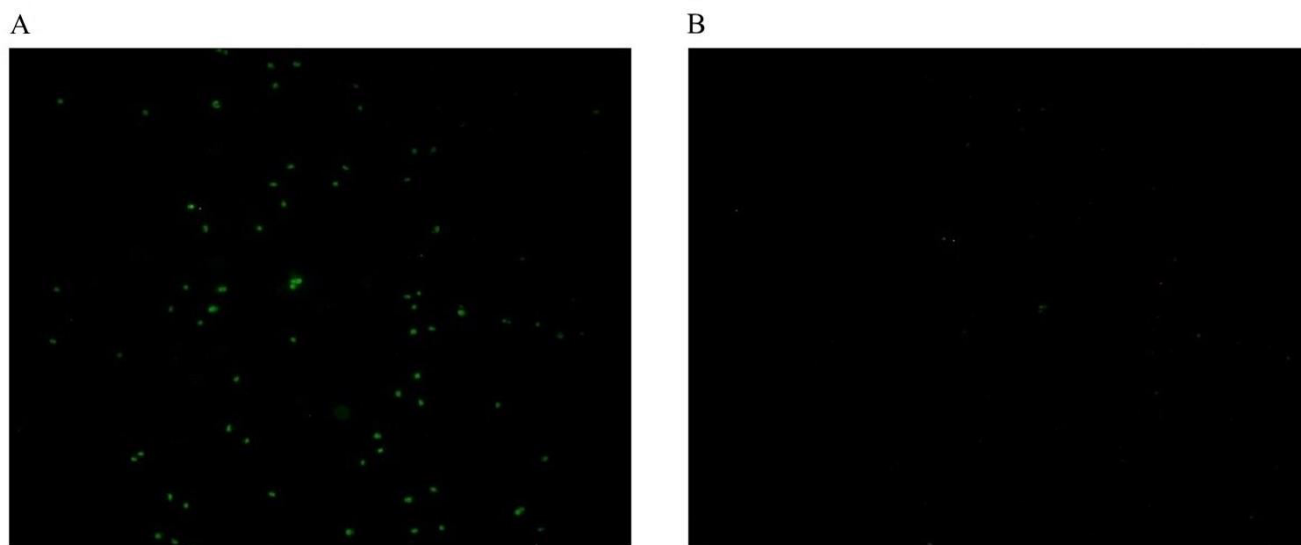
Figure 4.7 Images of the post-separation GFP-stained *Babesia*-infected and healthy erythrocytes. (A) Microdevice outlet port 1 (rich in *Babesia*-infected erythrocytes). (B) Microdevice outlet port 2 (lean in *Babesia*-infected erythrocytes). Magnification: 100X. The green spots indicate the *Babesia* parasites inside RBCs.

4.4.3.2 Bright field

Bright field imaging and quantification of the extent of separation was carried out using post-separation diff-quik cell staining technique (Section 4.3.3 for method details). This method enables the visualization of the *Babesia* parasite (B. Bovis) within the RBCs. *Babesia*-infected erythrocytes were enriched in one of the outlet ports in a similar manner as observed in the fluorescence microscopy. Figure 4.8 shows the images of each of the outlet ports obtained by the inverted microscope at 100X. Visualizing the *Babesia* parasites inside the RBCs (Figure 4.8) is an indication that the cells were not lysed and that the operating conditions were suitable for the sorting process. In essence, it can be said that there was no appreciable heat generation that would have lysed the cells during the application of voltages across the whole length of the microdevice.
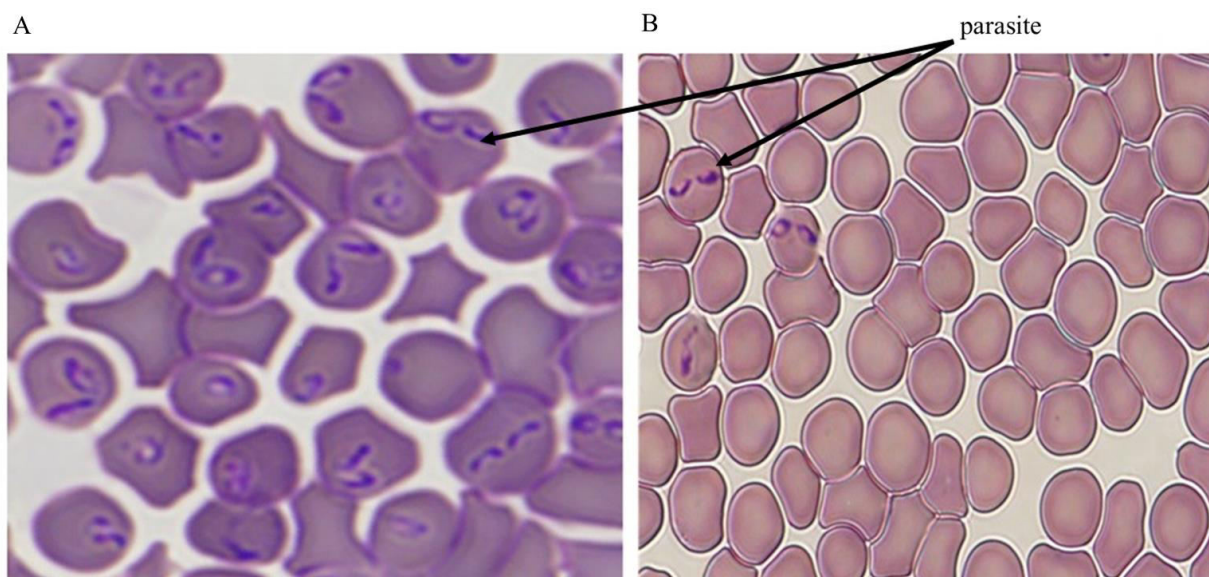
Figure 4.8   Images obtained at 100X magnification using post-separation diff-quik-stain kit showing *Babesia*-infected and healthy erythrocytes (Only the parasites were stained. Here, the cells were stained after they had been separated. (A) Microdevice outlet port 1 (rich in *Babesia*-infected erythrocytes). (B) Microdevice outlet port 2 (lean in *Babesia*-infected erythrocytes). The arrows show the parasite (nucleus-like structure) residing in the RBCs. Any RBC that contains the parasite is considered infected.

4.4.4   Quantitative analysis

Quantification of the proportion of parasitized RBCs in each of the ports is essential in determining the efficiency of the microdevice. As presented in Figure 4.9A, it is evident that iDEP-based microdevice concentrated the cell-mixture of 8.0%, 5.5% and 6.0% parasitized erythrocytes to 70%, 68% and 69% respectively in the outlet port 1. The range (68-72%) of the parasitized erythrocytes obtained from the post-separation analysis depicts that iDEP force had significant impact on the cell behavior and movement due to the non-uniformity in the electric field. In Figure 4.9B, the Percentage of Parasitized Erythrocytes (PPE) in the outlet port 2 was presented. 4-8 PPE obtained indicated that not all infected RBCs experienced sufficient dielectrophoretic force capable of streaming them into different ports.
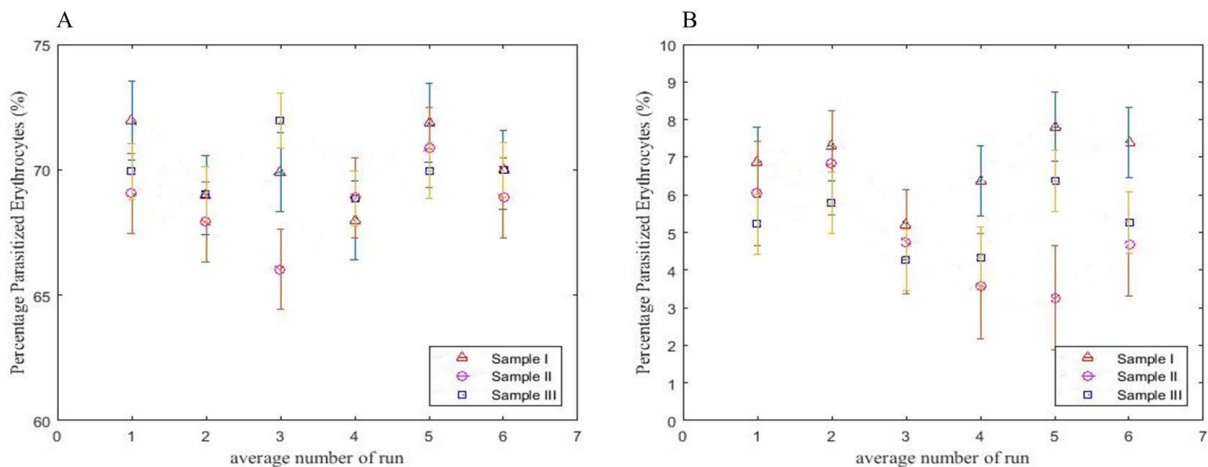
Figure 4.9 The graphical representation of the percentage parasitized erythrocytes (PPE) obtained after separation (A) The PPE in *Babesia*-rich port for samples I, II, III. (B) The PPE in *Babesia*-deficient port for samples I, II, III. The inlet concentration in samples I, II, III are 8.0%, 5.5%, and 6.0% PPE respectively.

Kuzman *et al.*[31] reported that a change in the elastic properties of the cell membrane would occur when the pH of the cell's suspending medium is changed. Changing the properties of the cell membrane could affect the DEP force that the cell would experience when passed through a non-uniform electric field. Therefore, throughout the experiment, the suspending medium pH of 7.04 was fixed not only to preserve the associated properties of the cell but also to provide a comparable pH for the RBCs (since the RBCs were previously in pH of ~ 7.0)
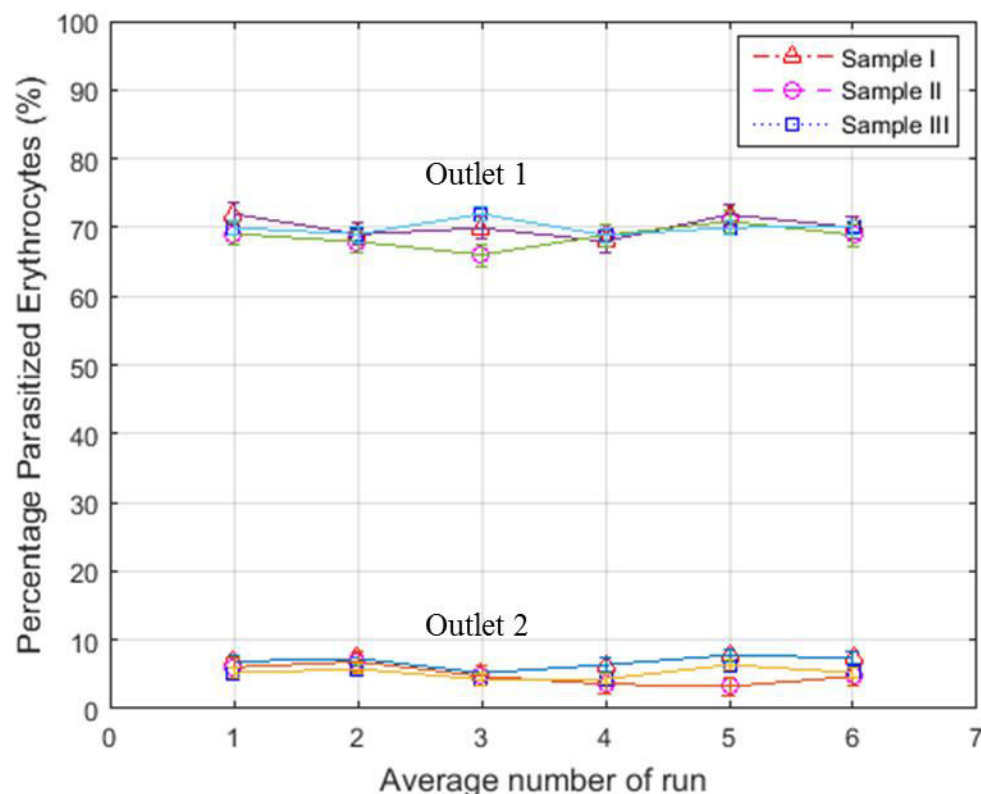
Figure 4.10　Comparison of the Percentage Parasitized Erythrocytes for various samples in outlet 1 and and outlet 2.

When a solution which has intracellular action mechanism is added to a suspension of viable cells, the change in the cells' dielectric properties is small [32]. In this work, we introduced pre-separation green fluorescent protein (gfp) staining of cells to aid the visualization of the green-labeled *Babesia* cells. The post-separation quantitative analyses revealed that the percentage-parasitized erythrocytes obtained from both pre-separation and post-separation staining sets were substantially similar.

This observation indicates that the degrees of sorting observed were pure functions of DEP effects and were, by no means, dependent on the employed stains. One point to note here is the variation in the percentage parasitemia. As reported[9], one of the defects of the current diagnostic tools for Babesiosis is the inability to detect *Babesia* in low-parasitemia sample. Our experiment revealed that at varied parasitemia content, cell differentiation would occur in as much as the right voltage configuration is used. Nevertheless, more research works need to be done regarding the range at which low or high parasitemia content should domicile.

4.5 Conclusion

This is the first study to have reported the application of insulator-based dielectrophoresis (iDEP) to separate or enrich *Babesia*-infected erythrocytes. The results presented here show that at voltage configuration of 10, 0, 6 V in the inlet and the two outlet reservoirs respectively (Figure 4.5), *Babesia*-infected RBCs could be isolated from their healthy counterparts. Studying the dielectrophoretic separation of *Babesia*-infected RBCs is the first of many steps required to develop a viable point-of-care diagnostic devices needed at blood donation centers to screen donors' blood for the notorious Babesiosis disease. As demonstrated, the required sorting voltage is 6 V with this configuration. This gives an indication that the point-of-care diagnostic device could be battery powered when completed. The entire separation process was completed within one minute; an indication that iDEP is a fast electrokinetic tool for identifying Babesiosis.

DEP has been a useful tool in cell sorting, especially for particles of biological materials such as RBCs. The properties associated with sorting are largely dependent on morphology, conductivity, size, and surface characteristics of the cells. Dielectric properties of the cells play a major role in determining the destination of the cells within a microfluidic channel experiencing a non-uniform electric field. Simulating this sorting process before the real-time experiment is a worthwhile practice since simulating gives the geometry of the microdevice as well as a guide on the operating voltage. This work used *Babesia Bovis* samples, which are assumed to be considerably similar to the *Babesia Microti*, the pathogen that infects humans. As observed from the sorting voltage values required to characterize the infected cells, we have close agreement between simulation (6.2 V) and experimental (6.0 V) measurements, which validates the simulation as a useful tool in determining the electric field strength that will be sufficient to achieve the desired sorting. Relative error analyses performed on the experimental data revealed an admissible confidence of > 95% and this gives credence to the entire dielectrophoretic process. It, therefore, becomes a hydra-headed endeavor to really determine where the course-effect representation of the simulation-experiment discrepancy should reside.

Worthy of note is the fact that the values of the electrophysiological properties used in the simulation were for Plasmodium falciparum-the pathogen that causes malaria. In malaria-endemic regions, however, the predisposition of misdiagnosing Babesiosis for malaria is very high. It might be worthwhile to determine the crossover frequencies of the hundreds of *Babesia*

strains and characterize them accordingly. This will be the focus of our research group in the future. The results of these proof-of-concept experiments have shown that the internalization of the *Babesia* cells within the RBCs actually affected the electrical properties of the RBCs. At the outset, it was only hypothesized that the electrical properties of the cells might have changed as a result of the *Babesia* attack. Dielectrophoresis has substantiated this claim because if the electrical properties had not changed as a result of the Babesia attack, there would not have been any separation.

Future works would require an automatic post-separation sensor to yield an integrated marketable device. If the separation efficiency is improved and sensor integration is achieved, then Babesiosis would be accurately screened just as HIV and other infectious diseases at blood donation centers.

References

1. A. Gorenflot, K. Moubri, E. Precigout, B. Carcy, T. P. Schetters *Ann. Trop. Med. Parasitol.*, 1998, **92**, 489-501.

2. http://www.cdc.gov/mmwr/preview/mmwrhtml/mm6127a2.htm, *United States Center for Disease Control and Prevention (Weekly Report: Babesiosis Surveillance)*, 2012, **61**, 505-509.

3. S. J. Kogut, C. D. Thill, M. A. Prusinski, J.-H. Lee, P. B. Backneson, J. L. Coleman, M. Anand , D. J. White *Emerg. Infect. Dis.*, 2005, **11**, 476-478.

4. S. C. Meldrum, G. S. Birkhead, D. J. White, J. L. Benach, D. L. Morse, *Clin. Infect. Dis.*, 1992, **15**, 1019-1023.

5. M. J. Homer, I. Aguilar-Delfin, S. R. Telford, P.J. Krause, D. H. Persing, *Clin. Microbiology. Rev.*, 2000, **13**, 451-469.

6. http://www.orkin.com/other/ticks/deer-ticks/, *Journal*, 2015.

7. K. P. Hunfeld, A. Hilderbrandt, J. S. Gray, *Int. J. Parasitol*, 2008, **38**, 1219-1237.

8. D. J. White, J. Talarico, H. G. Chang, G. S. Birkhead, T. Heimberger, D. L. Morse, *Arch. Intern. Med.*, 1998, **158**, 2149-2154.

9. P. J. Krause, A. Spielman, S. R. Telford, V. K. Sikand, K. McKay, D. Christianson, R. J. Pollack, P. Brassard, J. Magera, R. Ryan, D. H. Persing, *N. Engl. J. Med.* , 1998, **339**, 160-164.

10. D. A. Leiby, A. P. Chung, J. E. Gill, R. L. Houghton, D. H. Persing, S. Badon and R. G. Cable, *Transfusion*, 2005, **45**, 1804-1810.

11. E. Vannier, I. Borggraefe, S. R. Telford, S. Menon, T. Brauns, A. Spielman, J. A. Gelfand, H. H. Wortis, *J. Infect. Dis*, 2004, **189**, 1721-1728.

12. E. S. Chisholm, T. K. Ruebush, A. J. Sulzer, G. R. Healy, *American Journal of Tropical Medicine and Hygiene*, 1978, **27**, 14-19.

13. P. J. Krause, S. R. Telford, R. Ryna, P. A. Conrad, M. Wilson, *J. Infect. Dis, 1994, 169, 923-926*

14. P. J. Krause, R. Ryan, S. Telford, D. Persing and A. Spielman, *J. Clin. Microbiol.*, 1996, **34**, 2014-2016.

15. E. A. Levin, P. C. Williamsom, J. L. Erwin, S. Cyrus, E. M. Bloch, B. H. Shaz, D. Kessler, S. R. Telford III, P. J. Krause, G. P. Wormser, X. Ni, H. Wang, N. X. Krueger, S. Caglioti, M. P. Busch, *Transfusion*, 2014, **54**, 2237-2244.

16. R. G. Scholtens, E. H. Braff, G. R. Healy, N. N. Gleason, *The American Journal of Tropical Medicine and Hygiene*, 1968, **17**, 810-813.

17. L. Tonnetti, A. F. Eder, B. Dy, J. Kennedy, P. Pisciotto, R. J. Benjamin, D.A. Leiby, *Transfusion*, 2009, **49**, 2557-2563.

18. G. R. Healy, T. K. Ruebush, *Am. Soc. Clin . Pathol*, 1980, **73**, 107-109.

19. F. Brandt, G. R. Healy, M. Welch, *Journal of Parasitology*, 1977, **63**, 934-937.

20. N. N. Gleason, G. R. Healy, K. A. Western, G. D. Benson, M. G. Schultz, *The Journal of Parasitology*, 1970, **56**, 1256-1257.

21. R. L. Houghton, M. J. Homer, L. D. Reynolds, P. R. Sleath, M. J. Lodes, V. Berardi, D.A. Leiby, D. H. Persing, *Transfusion*, 2002, **42**, 1488-1496.

22. C. L. Hutchings, A. Li, K. M. Fernandez, T. Fletchet, L. A. Jackson, J. B. Molloy, W. K. Jorgensen, C. T. Lim, B. M. Cooke *Mol Microbiol*, 2007, **65**, 1092-1105.

23. P. Gascoyne, R. Pethig, J. Satayavivad, F. F. Becker, M. Ruchirawat, *Dielectrophoretic detection of changes in erythrocyte membranes floowing malarial infection*, 1997.

24. S. K. Srivastava, P. R. Daggolu, S. C. Burgess, A. R. Minerick, *Electrophoresis*, 2008, **29**, 5033-5046.

25. T. Z. Jubery, S. K. Srivastava, P. Dutta, *Electrophoresis*, 2014, **35**, 681-713.

26. C. F. Ivory, S. K. Srivastava, *Electrophoresis*, 2011, **32**, 2323-2330.

27. P. J. Krause, J. Daily, S. R. Telford, E. Vannier, P. Lantos, A. Spielman, *Trends in Parasitology*, 2007, **23**, 605-609.

28. A. Sze, D. Erickson, L. Ren, D. Li, *J Colloid Interface Sci*, 2003, **261**, 402-410.

29. P. Gascoyne, C. Mahidol, M. Ruchirawat, J. Satayavivad, P. Watcharasit and F. F. Becker, *Lab Chip*, 2002, **2**, 70-75.

30. M. G. Levy, M, Ristic, *Science*, 1980, **207**, 1218-1220.

31. D. Kuzman, T. Znidarcic, M. Gros, S. Vrhovec, S. Svetina, B. Zeks, *Pfligers Archiv*, 2000, **440**, R193-194.

32. P. M. Patel, A. Bhat, G. H. Markx, *Enyzme and Microbial Technology*, 2008, **43**, 523-530.

CHAPTER FIVE

CONCLUSIONS AND FUTURE WORK

5.1   Conclusion

This thesis gave a comprehensive analysis of particle motions in microchannels primarily by electrokinetics and how various techniques of dielectrophoresis have played important roles in the diagnostics of diseases. It is no more news that the advent of quick, cheap, and easy-to-use mobile medical devices is making diagnostic activities easier and faster. People, for instance, no longer need to visit the medical laboratory technologists to have their blood tested for sugar content. A simple mobile glucose-monitor medical device will give virtually the same result as the medical laboratory scientists'. In building some of these mobile diagnostics devices, various techniques have been used. Electrokinetics is one such technique, which seeks to account for the trajectories of particles flowing in microchannels.

Electrokinetics is known to encompass electro-osmosis and electrophoresis. The balance of these two forces (as in DC DEP) usually plays important role in dielectrophoretic manipulation of particles. Where electro-osmosis is not in use, micro-pumps are usually employed. Such is the case with AC DEP where electrodes are embedded within the confine of the microfluidic length.

At the moment, there are various diseases whose diagnostics inclinations are really challenging. A good example of such disease is Babesiosis, which seems difficult to accurately diagnose by virtue of the persistently low concentration of the etiologic pathogen: *Babesia*. Most sensitive PCR analysis sometimes fails to identify this dreaded pathogen (even after repeated run of the same sample) owing to the persistently low percentage of the infected RBCs in chronically infected people. This thesis, however, has been able to prove that when Babesia-infected RBCs in a mixture with healthy RBCs are passed through a microchannel creating non-uniform electric field (in an iDEP- based device), the infected cells can be identified and sorted based on their difference in the intrinsic electrical characterizations.

Even though the electrophysiological properties of *Plasmodium falciparum* were used in simulating the cell trajectories for identification of Babesia-laden RBCs, yet the numerical operating voltage of 6.2V closely matched the experimental value of 6.0V DC. This observation suggests that *Plasmodium* and *Babesia* might show similar manner with which

they change the electric characteristics of normal RBCs. Babesiosis as a disease seems to be unpopular in many developing countries owing to inadequate research activities. It might not be surprising if it was found that a percentage of the people who are diagnosed of malaria in some developing and under-developed countries might actually be suffering from Babesiosis since both diseases are caused by intra-erythrocytic protozoan pathogens.

5.2   Future work

Many opportunities for advancing this project abound. First, the device was able to concentrate infected RBCs (8.0, 5.5, and 6.0% PPE) to an average of 70%. There is a need to improve this capture rate. Not only would this improved capture rate enhance post separation sensing, it will also increase the number of Babesia pathogen that can be extracted from the infected RBCs after separation. The extracted pathogen can be used for experiments on Babesiosis vaccine formulation. In Figure 4.2, the gap between the tip of the hurdle and the opposite site of the microchannel is 25μm. RBCs are known to have a diameter of 7 μm. This indicates that at a time, about three (3) RBCs might find their ways into this 25 μm-space. The result of this is some form of shielding in which one RBC experiences maximum available DEP force at the hurdle while other RBCs are presumably shielded from maximum dielectrophoretic impact. Therefore, future work will look into the possibility of reducing this 25 μm space. Toward the realization of this plan, there will be a need to re-simulate the dielectrophoretic separation through device optimization methodology. This is a very complex but achievable feat. Sequel to this is the probability of getting the micro-scaled device fabricated without encroaching into the already low 10 μm depth of the channel. In essence, there will be a need to strike a balance between the numerically optimized microdevice and the feasibility of fabricating the simulated microdevice. More so, changing the Zeta potential values of the microchannel has been established as a function of the change in the pH of the polar electrolyte. Therefore, while trying to modify the pH of the electrolyte, caution should be exercised in order not to compromise the integrity of the RBCs.

Another plausible approach towards improving the dielectrophoretic capability of the microdevice is to employ dielectrophoretic spectra analyses of both Babesia-infected and healthy RBCs. From these extrapolative analyses, the intrinsic electrical characterisitcs of healthy and infected RBCs will be obtained. The procedure will involve the construction of microwell from where DEP cell capture- frequency data will be obtained. Then, curve fitting

analyses will be performed to back calculate the interior and shell dielectric properties of both healthy and infected RBCs. These values will then be fed into COMSOL Multiphysics software to obtain a new device geometry and possibly a new operating voltage. Since, the main aim of this Babesiosis project is to come up with a battery-powered portable medical device for screening donors for Babesiosis, simulation endeavors will reside within the domain of low voltage. Whether the current device is optimized to give higher separation efficiency or a new device is made through the DEP-spectra route, there will still be a need to incorporate a biosensor into the device. Research is still ongoing regarding the best type of biosensor to use for this device.

In the work done so far, the red blood cells were mechanically separated from the other blood components before they were diluted in ratio 1:600 (cell: medium) in mini-test-tubes for dielectrophoretic experimentation. Using the proposed device on site would mean that there should be a means of getting the initial blood components separated before the RBCs are channeled for dielectrophoretic experience. Therefore, the inlet to the dielectrophoretic chamber may need modification. Whole blood would be in the inlet and this will be channeled to a dielectrophoretic separating chamber from where the RBCs can then be sent to the iDEP zone. More so, with the use of whole blood for onsite testing of the device, there would be need to consider particle-particle interactions within the microchannel.

What has been done so far is a measure of specificity. i.e. infected cells are directed to a specific port. It is necessary to move further to check the sensitivity of the device. Device sensitivity is a measure of the number of parasite the device can detect per million or billion number of healthy RBCs. In the current device, the least inlet PPE of the sample is 5.5 %. Quantitatively, this represents 55000 infected RBCs per one million homogenous cell population. On site, the circulating parasite can be as low as 0.01% (100 infected RBCs per one million homogenous cell population). Therefore, serial dilution of this (or lower PPE) sample will be attempted until a concentration of approximately 0.005% is reached. The microdevice will be proven sensitive if the parasite is identified at this extremely low PPE. Once all these are tried out, the capability and credence of the microdevice will be put to test through other diagnostics approaches. There are two proposed methods for this. First, infected samples will be tested using FISH, PCR, and many antibody-measurement techniques to confirm the disease no matter how long it takes to obtain the result. Then, the same samples

will be fed into the microdevice to confirm the results of various other tests even though it is clear that some other tests might give false negative results. The second phase will be to carry out the concentration of the infected cells in the microdevice and test the outlet collections using other diagnostics methods.

It has been reported that ixodid ticks are the vector for both *Borrelia burgdorferi* (the parasite that causes lyme disease) and *Babesia* species (the parasite that causes Babesiosis). Epidemiological evidence reveals that when this ixodid tick bites humans, it leaves a mark on the skin if it transfers *Borrelia burgdorferi* to human as a result of the bite. However, no mark is seen on the skin if *Babesia* is the pathogen transferred as a result of the tick bite. This makes Babesiosis more deadly as patients do not have any clue about the tick bite. Therefore, in patients diagnosed with Lyme disease, there is a very high proclivity of co-infection with Babesiosis. It might be a worthwhile endeavor to look into the co-infection possibility of Babesiosis with Lyme disease. Also, Plasmodium has been found to be closely related to Babesia. In fact, the observed simulation (using Plasmodium electrical properties) and experimental (using Babesia-infected RBCs) separating voltages of 6.0 V and 6.2 V respectively underscores this relationship. Hence, attempting the dielectrophoretic separation of Plasmodium-infected and Babesia-infected RBCs might initiate some novel ideas that would prevent clinical misjudgement of one parasite for the other.

Since one of the major challenges facing the application of PCR for the diagnosis of Babesiosis is the persistently low parasitaemia content of the sample, this proposed iDEP-based microfluidic system could be used to pre-concentrate samples before they are fed into PCR. Exploring this option might be a worthwhile exercise.